THESIS FOR THE DEGREE OF DOCTOR OF PHILOSOPHY

Synthesis and Photochemical Characterization of Photoactive Compounds for Molecular Electronics

Behabitu E. Tebikachew

Department of Chemistry and Chemical Engineering

CHALMERS UNIVERSITY OF TECHNOLOGY

Gothenburg, Sweden 2018

Synthesis and Photochemical Characterization of Photoactive Compounds for Molecular Electronics

Behabitu E. Tebikachew
ISBN 978-91-7597-784-3

Doktorsavhandlingar vid Chalmers tekniska högskola
Ny serie nr 4465
ISSN 0346-718X

Department of Chemistry and Chemical Engineering
Division of Applied Chemistry
Chalmers University of Technology
SE-412 96 Gothenburg
Sweden
Telephone + 46 (0)31-772 1000

Cover:
[Artistic drawing by Mariza Mone illustrating the concept of creating molecular electronics devices based on the norbornadiene-quadricyclane photoswitch system.]

Chalmers Reproservice
Gothenburg, Sweden 2018

Synthesis and Photochemical Characterization of Photoactive Compounds for Molecular Electronics

BEHABITU TEBIKACHEW

Department of Chemistry and Chemical Engineering
Chalmers University of Technology

ABSTRACT

In this modern age of technology, communication is highly reliant on computing devices such as mobile phones and computers. The advent of artificial intelligence (AI) and internet of things (IoT) as well as the widespread use of user-generated contents (UGC) are demanding more computing power and large data storage. However, traditional silicon based semiconductor technology is struggling to fulfill the required infrastructure due to fundamental physics and fabrication challenges. To overcome these challenges, molecular electronics has been proposed as potentially viable solution. With judicious design, organic molecules can be synthesized with tailored properties that can emulate the functions of conventional electronics devices such as diodes, switches and transistors.

To this end, photochromic molecules attract significant attention since they can be switched with light/voltage between a less conducting and highly conducting forms. This property can be exploited to perform logic operations similar to transistors. This thesis explore the potential of norbornadiene-quadricyclane (NBD-QC)-based photochromic system, to serve as a switch for molecular electronics application. Four NBD derivatives, terminated with a thiol and thiophene groups, to enable tethering between gold electrodes, were synthesized. The compounds photochemical and photophysical properties were investigated using absorption and fluorescence spectroscopy. The results showed the compounds ability to switch between the NBD form and QC form upon photoirradiation. Moreover, the compounds were found to exhibit intrinsic emission. In particular, the long conjugated NBD form were found to be highly emissive, Φ_F = 49%. Moreover, it was discussed that the emission can be tuned by the use of light, this makes them a potential candidate for optical memory device application. To test the robustness of the switching, more than 100 switching cycles were performed in solution and little or no degradation was observed, particularly under inert atmosphere. Additionally, the charge transport through the molecules were studied as well, using Scanning Tunneling Microscope-Break Junction (STM-BJ) technique. The results showed higher conductance values for the NBD forms and lower conductance values for the QC forms.

Furthermore, we tested the potential of 2-nitrobenzyl-based photocleavable protection group (PPG) to release terminal alkynes on plasmonic surfaces by selective light activation. The terminal alkynes may then react, for example, with azido groups embedded on nanoparticles to create a dimer linked by a single molecule. By using the tools of template self-assembly the dimers can be aligned and placed on electrodes made by lithography. Initial findings showed promising result moving us closer to create single molecule devices based on parallel fabrication.

Keywords: Molecular electronics, norbornadiene, photoswitch, photocleavable protection

Abbreviations

BDT - Benezene-1,4-dithiol

CP-AFM - Conducting Probe-Atomic Force Microscopy

DAE - Diarylethene

DHA-VHF- Dihydroazulene-Vinylheptafulvene

DSC - Differential Scanning Calorimeter.

G_o - Quantum of Conductance

HOMO - Highest Occupied Molecular Orbital

LUMO - Lowest Unoccupied Molecular Orbital

MCBJ- Mechanically Controllable-Break Junction

MOSFET - Metal oxide-Field Effect Transistor

MOST - Molecular Solar Thermal Energy storage

NBD - 2,5-Norbornadiene

OPE - Oligo(phenyleneethynylene)

OPV - Oligo(phenylenevinylene)

PPG - Photocleavable Protecting Group

pH - power of Hydrogen

QC - Quadricyclane

SPM - Scanning Probe Microscopy

STM-BJ - Scanning Tunneling Microscopy-Break Junction

UV-vis - Ultraviolet visible

THF - Tetrahydrofuran

TTF - Tetrathiafulvalene

TCNQ-Tetracyanoquinodimethane

List of Publications

This thesis is based on the following scientific papers, referred to by Roman numerals in the text. The papers are appended at the end of the thesis.

Paper I **Effect of Ring Strain on the Charge Transport of a Robust Norbornadiene-Quadricyclane-Based Molecular Photoswitch**
Behabitu E. Tebikachew, Haipeng B. Li, Alessandro Pirrotta, Karl Börjesson, Gemma C. Solomon, Joshua Hihath and Kasper Moth-Poulsen, *J. Phys. Chem. C*, **2017**, 121 (13), pp 7094–7100. **DOI**: 10.1021/acs.jpcc.7b00319

Paper II **Turn-off Mode Fluorescent Norbornadiene-Based Photoswitches**
Behabitu E. Tebikachew, Fredrik Edhborg, Nina Kann, Bo Albinsson, and Kasper Moth-Poulsen
*Phys. Chem. Chem. Phys.*2018, 20, pp 23195- 23201. **DOI**: 10.1039/c8cp04329a

Paper III **Heteroaryl-linked Norbornadiene Dimers with Redshifted Absorptions**
Mads Mansø, Behabitu E. Tebikachew, Kasper Moth-Poulsen and Mogens Brøndsted, *Org. Biomol. Chem.* **2018**, 16, pp 5585-5590. **DOI**: 10.1039/c8ob01470a

Paper IV **Release of Terminal Alkynes *via* Tandem Photodeprotection and Decarboxylation of *o*-Nitrobenzyl Arylpropiolates in a Flow Microchannel Reactor**
Behabitu E. Tebikachew, Karl Börjesson, Nina Kann and Kasper Moth-Poulsen, *Bioconjugate Chem.* **2018**, 29 (4), pp 1178–1185. **DOI**: 10.1021/acs.bioconjchem.7b00812

CONTRIBUTION REPORT

Paper I Performed the synthesis and spectroscopic characterization of the compound except the quantum yield and kinetics measurement. The STM-break junction and theoretical simulation were also conducted by co-authors. Wrote the paper together with the other co-authors.

Paper II Conceived the idea, performed all the synthesis and spectroscopic characterization of the compound except the time-resolved spectroscopy and fluorescence quantum yield measurements. Analysed the data and wrote most of the paper together with the other co-authors.

Paper III Participated in the design and synthesis of part of the compounds, and their full spectroscopic characterization. Wrote the experimental part that I carried out. Participated in the data analysis with inputs towards the paper.

Paper IV Performed the synthesis of all the compounds and their full characterization. Wrote the manuscript with inputs from the other co-authors.

List of Publications that are not included in this thesis

1. Johnas Eklöf, Alicija Stolas, M. Herzberg, Anna Pekkari, Behabitu E. Tebikachew, Tina Gschneidtner, Samuel Lara-Avila, Tue Hassenkam and Kasper Moth-Poulsen " Guided selective deposition of nanoparticles by tuning of the surface potential." *Europhys. Lett.* **2017**, 119, 18004.

2. Johnas Eklöf-Österberg, Tina Gschneidtner, Behabiu Tebikachew, Samuel Lara-Avila, and Kasper Moth-Poulsen. "Paralllel fabrication of self-assembled nanogaps for molecular electronic devices." *Small* **2018** (accepted).

3. Ambra Dreos, Zhihang Wang, Behabitu Ergette Tebikachew, Kasper Moth-Poulsen, and Joakim Andréasson. "A three-input molecular keypad lock based on a norbornadiene-quadricyclane photoswitch." *J. Phys. Chem. Lett.* **2018**, 9, 6174.

Table of Contents

ABSTRACT ..... **III**

Abbreviations ..... **iv**

List of publications and contribution reports ..... **v**

List of publications not included in this thesis ..... **vi**

Table of contents ..... **vii**

CHAPTER 1 INTRODUCTION **1**

1.1. The genesis of molecular electronics: General background 3
1.2. Challenges in single molecule electronics 5
1.3. Motivation and aims 5

CHAPTER 2 ORGANIC PHOTOCHROMISM **9**

2.1. Brief introduction to photochromism 9
2.1.1. Positive photochromism *10*
2.1.2. Negative photochromism *11*
2.1.3. Typical organic photochromic molecules *12*
2.2. Photochromic compounds for molecular electronics 15
2.3. Design considerations of photochromic compounds for single molecule electronics 16
2.3.1. The Electrode *16*
2.3.2. The active molecular switching unit *16*
2.3.3. The anchoring unit *17*
2.4. Break junction techniques for measuring molecular conductance 18
2.4.1. The Mechanically Controllable Break-Junction technique (MCBJ) *18*
2.4.2. The Scanning Tunnelling Microscopy Break-Junction technique (STM-BJ) *19*

CHAPTER 3 THE NORBORNADIENE-QUADRICYCLANE PHOTOSWITCH PAIR **21**

3.1. Brief introduction to norbornadiene-quadricyclane 21
3.2. Molecular solar-thermal energy storage application 22

CHAPTER 4 NBD-QC FOR MOLECULAR ELECTRONICS APPLICATIONS **33**

4.1. Charge transport in NBD-QC 33
4.2. The synthesis of 2,3-dibromonorbornadiene 35
4.3. 2,3-Disubstituted NBD derivatives via the Sonogashira reaction 36
4.3.1. Spectroscopic and photoisomerization study of the NBD derivatives (Paper II) *38*
4.3.2 Fluorescence in the NBD derivatives (Paper II) *40*
4.3.3. Charge transport in the NBD derivatives (Paper I) *44*

CHAPTER 5 PHOTOCLEAVABLE PROTECTION TOWARDS PARALLEL FABRICATION **49**

5.1. Brief introduction to Photocleavable Protecting Groups (PPG) 49
5.2. The 2-nitrobenzyl PPG 50
5.3. Terminal alkyne protection strategy 51

CHAPTER 6 CONCLUSIONS AND OUTLOOKS **57**

CHAPTER 7 METHODS **59**

CHAPTER 8 ACKNOWLEDGMENTS **67**

CHAPTER 9 REFERENCES **69**

Chapter 1 Introduction

Since the prehistoric times of mankind, the ability to share information has played a vital role in our evolution as human beings, and in shaping our modern civilization. The advent of written languages enabled the sharing of knowledge for generations, and the invention of printing technologies laid the foundation for mass distribution of information. Likewise, in this modern age of technology, the use of digital communication devices such as computers, and mobile phones, linked through the Internet, have enabled near instant sharing of information. In particular, due to the widespread use of social media platforms for accessing and sharing information, never before in human history has such a large amount of data been generated at the rate we do today.

The main driving force of this digital revolution has been the discovery of the transistor, a device that regulates the flow of current acting as a switch. Silicon based transistors were discovered in 1947, by Shockley and co-workers.[1] In the 1960s, many transistors could be interconnected on a silicon wafer, leading to integrated circuits (ICs).[2] Due to significant advancement in fabrication technology, the size of transistors have become smaller over the years. This reduction in size made it possible to fit twice as many transistors onto a chip, approximately every two years, following the empirical law of Gordon Moore.[3] The current state of the art chips contain tens of billions of transistors on a chip as small as a finger nail. Nowadays, nanometre scale transistors and ICs are carved out of a bulk silicon wafer in what is known as the top-down approach, making them cheaper, smaller in size, easier to mass produce and able to perform complex operations.

Prior to the miniaturization of transistors and ICs, the use of computing devices were initially restricted to government agencies due to their sheer size and high cost. However, significant advancement in the miniaturization of ICs and their mass production have made electronic devices commodity items in all parts of the world. Now, they are found in home appliances, vehicles, personal mobile phones and computers. Moreover, these devices have become “smart” in such a way that they can be interconnected and exchange information through the Internet, exclusively by themselves. This phenomena is coined “the Internet of Things” (IoT). The future of computation will be tasked with handling enormous amounts of data created by cloud computing, IoT and artificial intelligence[4] in addition to the large data created by users in social media.

Recently, however, the process of miniaturization using the top-down approach is facing serious technological setbacks due to physical and technological limitations (Figure 1-1).[5–7] The main challenges are high cost of fabrication, current leakage, and more importantly heat dissipation.[8,9] Some of the challenges, such as current leakage have been addressed partially, by using advanced microarchitecture in the chip design. Heat dissipation however, still remains to be a serious issue. Hence, building powerful electronic devices based on a radically new technology to store and process large data, beyond the current limits of miniaturization, is indispensable.

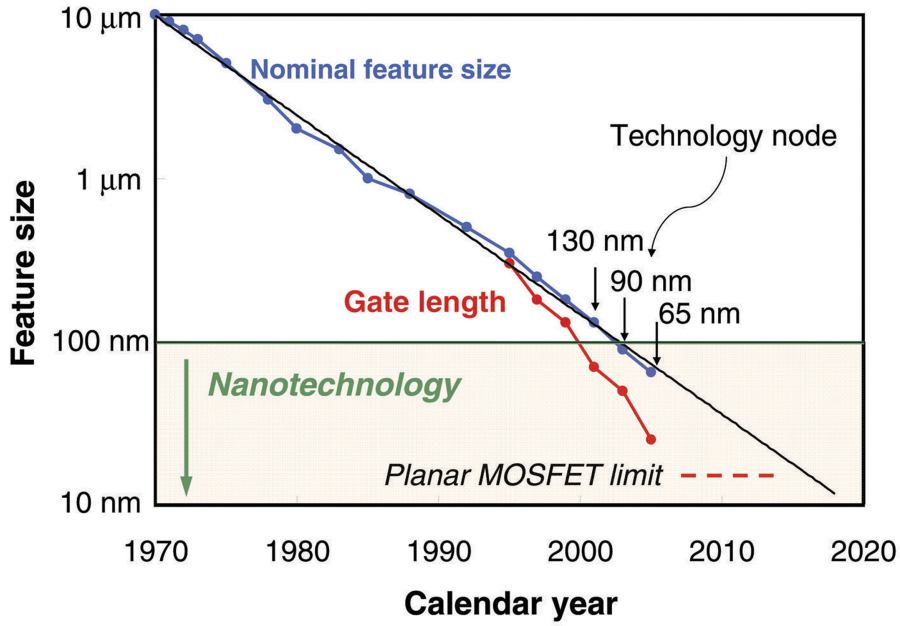

Figure 1-1: Progressive reduction in the feature size of transistors over the years for the most common transistor type metal-oxide-semiconductor field-effect transistor (MOSFET)[10]. Reprinted with permissions © 2006 Elsevier Ltd.

One such radical idea to address the miniaturization problem has been quantum computing.[11,12] Quantum computing uses quantum phenomena such as entanglement and superposition that are observed in particles as small as electrons and even molecules to perform computation, while some other researchers have suggested an all-optical computation based on photons instead of electrons and holes.[13] However, there are many other research groups, including our research group, who are trying to develop molecular electronics into a viable alternative.[14–20] Molecular electronics involves the use of organic molecules as functional units to aid the miniaturization process by complementing the current silicon-based computing devices.

Even though the argument to reduce the size of electronic components using organic molecules has waned over the years, due to advances in microelectronic fabrication, organic molecules have certain inherent advantages compared to silicon-based bulk design. Most small organic molecules dimensions are in the range of 0.5 – 5 nm. Despite their minuscule size, it has already been shown that a molecules can act as a wire,[17,21] transporting charge between metal junctions.

It has even been shown that molecules can perform basic electronic functions such as conductance switching.[22–25] Moreover, if designed judiciously, an isolated molecule may act as a rectifier,[26–30] a device that lets electrical current flow in only one direction. Certain photoswitchable molecules, that reversibly switch between a more conductive and less conducting forms, can serve as single transistors by using light as a gate.[31–33]

In principle, these functional molecules can be synthesized in the lab without the need for costly clean-room setups. Moreover, the synthetic method is scalable to large quantities. Mind that there are about 6.02×10^{20} molecules in a mere 350 mg (1 mmol) of the molecule, shown in Figure 1-2, which can be used as a molecular wire. Hypothetically, this represents about 20 billion times more units than the number of transistors in the current state of the art chips. Also, the ability of molecules to recognize each other and self-assemble may be used as an advantage to create large surface areas without the need for advanced technology. More importantly, the intrinsic quantum properties exhibited by molecules, for instance quantum interference[34–36] and quantum spin effects,[37] can perhaps be exploited to develop electronic devices in unconventional ways.

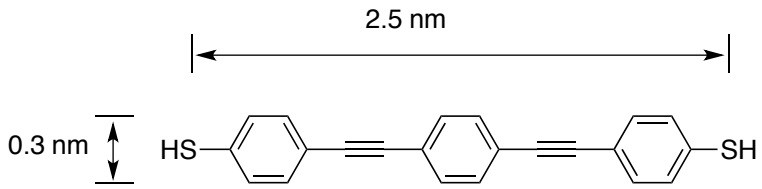

Figure 1-2: A typical example of molecular wire based on oligophenylene ethynylene (OPE) end-capped with thiols for anchoring to electrodes.

1.1. The genesis of molecular electronics: General background

The history of molecular electronics can be traced back to the 1950s. The idea was born out of a desire to bring a radical change to circuit integration and miniaturization through bottom-up molecular engineering, using atoms and molecules.[38] In particular, molecules are considered to be the ultimate limit of miniaturization for functional computing devices. After a period of stagnation in the 1960s, the field was revived in the late 1970s by a group of chemists. In 1974, Aviram and Ratner published the widely recognized theoretical paper on Molecular Rectifiers[14] based on the electron-donor (D) tetrathiafulvalene (TTF) and the electron-acceptor (A) tetracyanoquinodimethane (TCNQ) moieties conjoined by a saturated hydrocarbon unit (σ), **1** (Figure 2-1). The idea was to generate a large current when a voltage is applied across the D-σ-A molecule, from the TTF to the TCNQ unit. Little current will be created when the voltage is reversed, and hence, **1** can act as a traditional p-n junction-type diode. Unfortunately, the proposed molecule was not synthesized at that time to test the hypothesis and the paper failed to incite interest for over a decade.

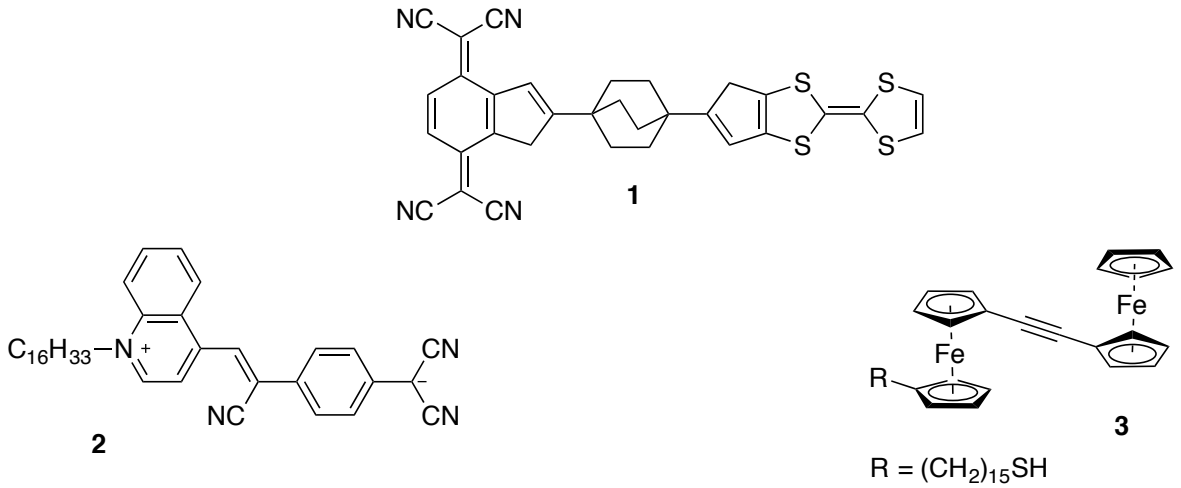

*Figure 1-3: Earliest examples of molecular diodes by Aviram-Ratner, **1**, and Metzger, **2**, as well as a more recent example by Nijhuis group, **3**, a diode based on ferrocenyl units, which has a ON/OFF comparable ratio to conventional diodes based on silicon.*[14,39,40]

In the early 1980s, Carter put forward the use of conductive polymers and oligomers as components such as wires and switches for molecular electronic devices.[41,42] In contrast to the Aviram and Ratner molecule, most of his molecules were designed to be anchored to surfaces such as silicon for ease of integration. In parallel to Aviram, Carter successfully organized interdisciplinary community-building activities, such as symposia, to popularize the field.

Despite the fact that most of the initial work in molecular electronics was dominated by theory and speculation, promising experimental results were obtained afterwards. For instance, the first molecular rectifier was demonstrated by Metzger et al. in 1997,[39] from the Langmuir-Blodgett films of γ-hexadecylquinolinium tricyanoquinomethanide, **2** (Figure 1-3) and subsequently by many other research groups.[27,29,43,44] Self-assembled monolayers of certain organic molecules with redox-active ferrocenyl end-groups were also found to have a large current rectification (ON-OFF) ratio.[28] In the case of compound **3**, (Figure 2-1) the rectification ratio was found to be comparable to those of conventional diodes ($R \geq 10^5$).[40]

Molecular electronics has evolved to become a truly interdisciplinary research field, by bringing together various academic disciplines since the 1990s. For instance, synthetic organic chemists have made tremendous contributions by synthesizing a variety of functional molecules for molecular electronics applications. Tour and co-workers have synthesized an extensive list of thiol-terminated conjugated molecules based on oligophenyleneethynylene (OPE) and oligothiopheneethynylene.[17,21,45] In collaboration with Reed (an engineer and experimental physicist), Tour has also reported the first example of molecular conductance on benzene-1,4-dithiol using a mechanically controllable break junction (MCBJ) technique,[46] which will be discussed in detail in Chapter 2. This breakthrough heralded a new era in molecular electronics,

where a “single” or a few molecules can be tethered between metal electrodes to study their electrical conductance.

Similarly, advancement in scanning probe microscopy (SPM), such as scanning tunnelling microscopy (STM)[47] and conducting probe-atomic force microscopy (CP-AFM),[48] further unlocked an additional set of tools to manipulate molecules in the nanometre scale. SPM and MCBJ techniques have since become a basis to establish nanometre scale metal-molecule-metal junctions. Subsequently, these junctions have enabled a direct way of studying electronic transport properties of molecules that are tethered between metal electrodes. Since the inception of molecular electronics, many candidate molecules have been proposed, synthesized, studied and reviewed for the purpose of creating electronic devices based on a single or ensemble of organic molecules.[33,49–54] These molecules range from structurally simple entities such as molecular wires to more intricate types of molecular switches that can be controlled using light, such as azobenzenes,[55] diarylethenes,[56] and mechanically-interlocked architectures such as rotaxanes[18] and catenanes.[57]

1.2. Challenges in single molecule electronics

Almost any imaginable molecule can be synthesized using the tools of synthetic chemistry. However, so far there is no molecular electronics device that breaks into the consumer market, except for a few niche examples.[58] One of the biggest challenges is that molecules are tailored to emulate traditional silicon based electronics architecture without the tools that can address a single molecule at a time. Nonetheless, despite the sheer challenge of connecting them to bulk electrodes while being addressed individually, molecular wires and molecular switches are synthesized to substitute the role of interconnecting metal wires and to perform logic operations. Therefore, to create a molecular junction that is stable at various working temperature ranges, as well as to create individually addressable junctions at the molecular level, has become a formidable challenge.

1.3. Motivation and aims

Although some genuine efforts have been put into the synthesis of molecules to study charge transport while tethered between metal electrodes, there is still an ongoing effort to make new compounds that may exhibit unique and unforeseen quantum phenomena.[59–61] Since the inception of the field, theoretical calculations have played and are still playing a significant role in the design of various molecules for molecular electronics. Synthetic chemists have also synthesized most of the molecules predicted to be suitable for molecular electronics applications, as well as a plethora of molecules out of wisdom and curiosity. There are also cases where

molecules targeted for other types of applications, e.g. organic photovoltaics[62] and solar energy storage,[63] have become interesting for molecular electronics.

This thesis, basing its foundation in synthetic organic chemistry, has aimed at answering the following research question.

Is it possible to synthesize functional molecules that can lead to stable "single" molecule metal-molecule-metal junctions?

This question is based on the assumption that stable metal-molecule-metal junctions can lead to stable devices, one of the areas molecular electronics has been struggling to address so far. In the first approach, this thesis aims to address this question by using the norbornadiene-quadricyclane system (NBD-QC). The NBD-QC pair is known to undergo structural isomerization from relatively stable NBD to the strained QC upon photoisomerization (*vide infra* Scheme 1-1). The strain energy in QC has been exploited for storing solar energy. Solar energy storage in the NBD-QC system is discussed in detail in Chapter 3, in relation to Paper III.

What is interesting for molecular electronics application, however, is that the reversible change in the bond order between C2 and C3 (or C5 and C6) from two to one when isomerized from NBD to QC. This change in bond order can be used to control charge transport between the two R groups via the C2-C3 connection (Scheme 1-1). The change in the bond order is also accompanied by a small change in the overall structure of the molecule, which can potentially be exploited to create a molecular photoswitch system that leads to stable junctions. Our target is to synthesize a NBD/QC photoswitch molecule with thiol end groups for anchoring to gold electrodes. Gold is the most common electrode materials for molecular junctions due to its inertness, resulting in consistent and reproducible conductance values.[50] Since thiols are prone to oxidative dimerization, they will further be protected, for example, as thioacetates. This is discussed in detail in Chapter 4, based on the results in Paper I and II.

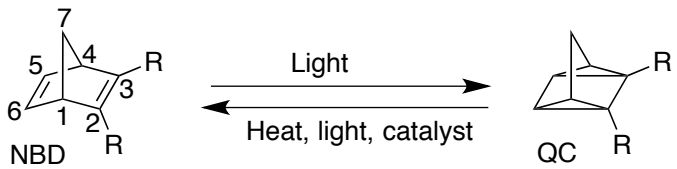

Scheme 1-1: Light induced isomerization of norbornadiene (NBD) to quadricyclane (QC).

The second approach to create a stable junction is, by using a photocleavable protection-deprotection chemistry. In this approach, selective photodeprotection of a photocleavable protecting group is envisaged to release a reactive functional group that can undergo specific

chemical transformations to create a robust functional molecular wire. For this purpose, we targeted anchoring group-bearing terminal alkynes, protected with the known photocleavable protecting group (PPG), 2-nitrobenzyl moiety.[64] Similar to approach one, the anchoring group can aid the immobilization of the PPG-protected terminal alkynes onto gold nanoparticles or electrodes. After light-induced release of the terminal alkyne, selective "click chemistry" with an azido compound for instance, can be pursued to prepare nanoparticle dimers (Figure 1-4). Furthermore, since the efficiency of photodeprotection 2-nitrobenzyl group is reported to proceed with poor yields,[65] we will explore benzylic substitution of the 2-nitrobenzyl group to increase the efficiency of photodeprotection. This second approach can potentially lead to dimers with a single or a few robust functional molecules in between two nanoparticles, which has proven to be challenging to prepare.[66] Our effort to realize the second approach is presented in Chapter 5, based on the results in Paper IV.

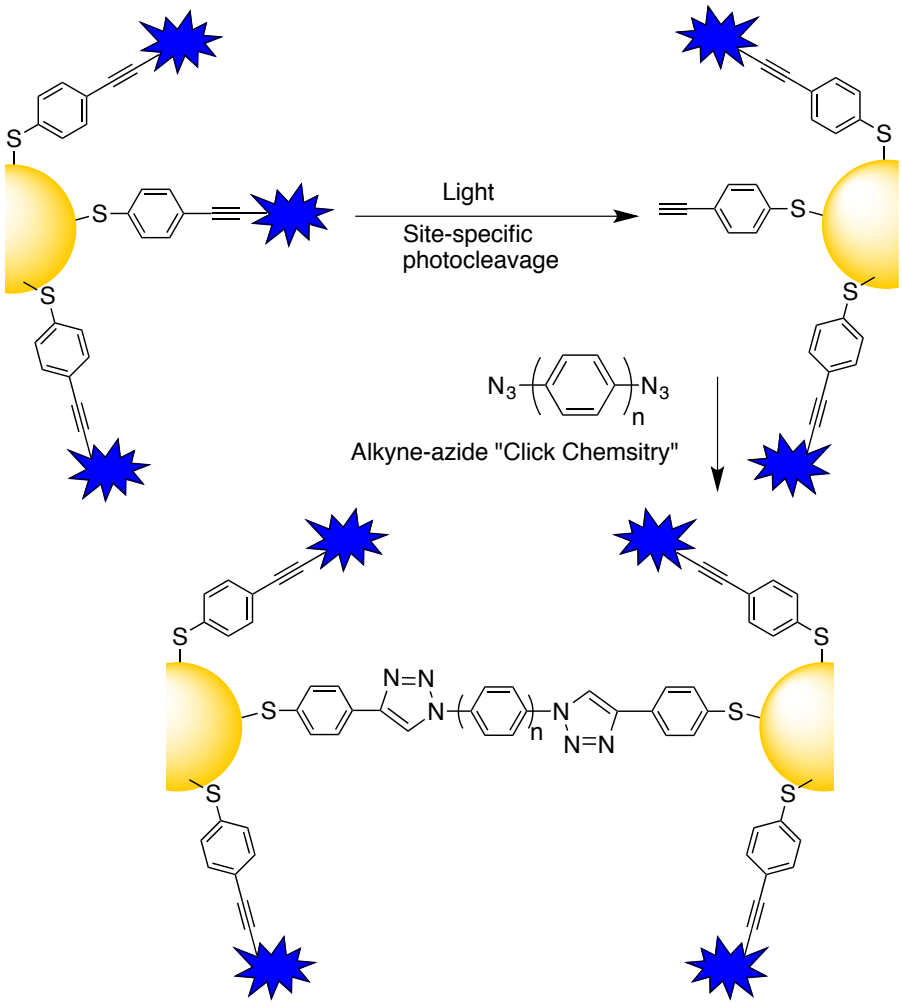

Figure 1-4: Site-selective photocleavage of a photocleavable group (PPG) for the selective "click" reaction of terminal alkynes with para-diazidobenzene derivatives to form a "single" molecular wire between gold nanoparticle dimer. n ≥3 for safe-handling of azides.[67]

The outline for the rest of the thesis is as follows: In the upcoming chapter, Chapter 2, a general introduction to organic photochromism, design criteria for photochromic molecules intended for molecular electronics applications as well as typical photochromic compounds are presented. In addition, break junction techniques that are commonly used to study charge transport in organic molecules are summarized in this chapter. In Chapter 3, the norbornadiene-quadricyclane (NBD-QC) photochromic system in the context of solar energy storage, as described in Paper III, is discussed. In Chapter 4, the NBD-QC system, devised for molecular electronics applications is disclosed. Moreover, details on the spectroscopic properties and how the NBD-QC photoswitch pair behaved between metal electrodes in STM break-junction experiments are discussed, based on the original work described in Paper I. Moreover, based on Paper II, the cause for unique emission properties observed in the NBD-QC system, which can potentially be exploited for optical data storage applications, is elaborated. Chapter 5 expands our effort in making PPG protection chemistry to prepare "single" molecule junctions, based on the worked described in Paper IV. In Chapter 6, I will summarize the thesis based on the aim presented in Chapter 1 and will highlight future work to be done towards individually addressable "single" molecule based devices.

Chapter 2 Organic Photochromism

This chapter describes the origin of photochromism and the types therein. Furthermore, it describes the criteria for photochromic molecules that are targeted for use between metal junctions, followed by a description on how charge transport is measured using break junction techniques.

2.1. Brief introduction to photochromism

Certain compounds undergo a reversible structural isomerization in the presence of light, which results in a colour change (Figure 3-1). The first observation was reported by Fritzsche in 1867 on tetracene molecules.[68] Upon exposure to sunlight, an orange tetracene solution was reported to bleach, while in the dark, the parent colour was recovered. Later, in 1950, Hirshberg coined the term photochromism, after the Greek words "*phos*"-light and "*chroma*"-colour.[69] The reverse reaction from **B** to **A** can occur either thermally or photochemically. Thermally back-converting photochromic compounds are known as T-type photochromes. In most cases, the thermal back-reaction occurs when the energy barrier from **B** to **A** is low. In this case, the photoisomer **B** is metastable and relaxes back spontaneously to the thermodynamically stable parent **A**. Intriguingly, some T-type photochromic systems can be driven back to the parent **A**, both by light as well as heat.[70,71] On the other hand, when the back-reaction is driven only by photons, these photochromic compounds are known as P-type photochromes. Although initially, the term photochromism was used to describe processes that show visible colour changes upon photoirradiation, it has now been expanded to include systems that have different absorption spectra in the UV, visible or IR region of the electromagnetic spectrum.[68]

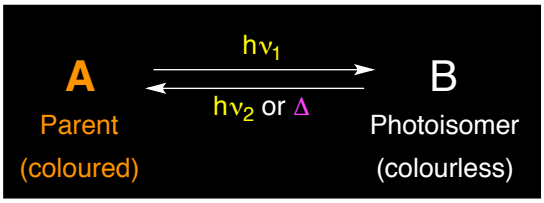

*Figure 2-1: General scheme of photoinduced reversible colour change in a photochromic compound **A** to **B**.*

Photochromism is observed in both organic and inorganic materials. Certain transition and alkaline-earth metal halides, oxides and sulphides can be mentioned as examples of inorganic photochromic molecules. The naturally occurring mineral hackmanite is also known to fade from violet to colourless when exposed to visible light. In the dark, the original violet colour is restored slowly.[72] Perhaps the most well-known examples in this category are silver halides, widely used in photochromic eye glasses, that darken when the sun is shining and becomes

transparent when the sun sets. Most inorganic photochromic systems absorb in the UV region and display low sensitivity, which limits their areas of application.[73]

Similarly, there are several examples of organic photochromic molecules reported in the literature which will be highlighted in this thesis. Anthracenes, azo-compounds, stilbenes, diarylethenes, dihydropyrans, dihydroazulenes, fulgides and fulgimides, spiropyrans, chromenes and spiroxazines are some examples of organic photochromic molecules. The capabilities that come with modern organic synthesis enables tailoring of specific physical properties for the desired applications, such as absorption at a desired wavelength from the electromagnetic spectrum. For instance, the absorption spectrum can be tuned by incorporating electron donating/withdrawing groups while designing the photochromic molecule. Upon photoirradiation, some of these photochromic compounds may transform from a *cis* to a *trans* isomer while some others may undergo pericyclic or ring closing reactions. Although most organic photochromic compounds are prone to degradation upon light-induced interconversion between the photochromic pairs, some are quite stable and resistant to fatigue, e.g. certain diarylethene derivatives.[56] In the following sections, different types of organic photochromic molecules will be classified based on the their absorption profile, and common examples found in the literature will be discussed.

2.1.1. Positive photochromism

Positive photochromism is a term used to describe photochromic systems that absorb higher energy photons (e.g. UV) and are converted to photoisomers that can absorb a longer wavelength of light. More simply, positive photochromism describes systems that interconvert from a colourless to a coloured form upon photoisomerization (See Figure 2-2 for the positive photochromic DHA-VHF system). For such systems, the absorption maximum is located at a shorter wavelength in the parent form, whereas the photoisomer has a redshifted absorption maximum. It is worth noting that most organic photochromic molecules are positive photochromes. Typical examples in this category includes fulgides, diarylethenes, azobenzenes, spiropyrans, and dihydroazulene derivatives. Positive photochromes have found applications in ophthalmic glasses,[74] replacing silver halides as well as other applications such as optical memory storage devices,[75] and single molecule imaging and sensing.[76,77]

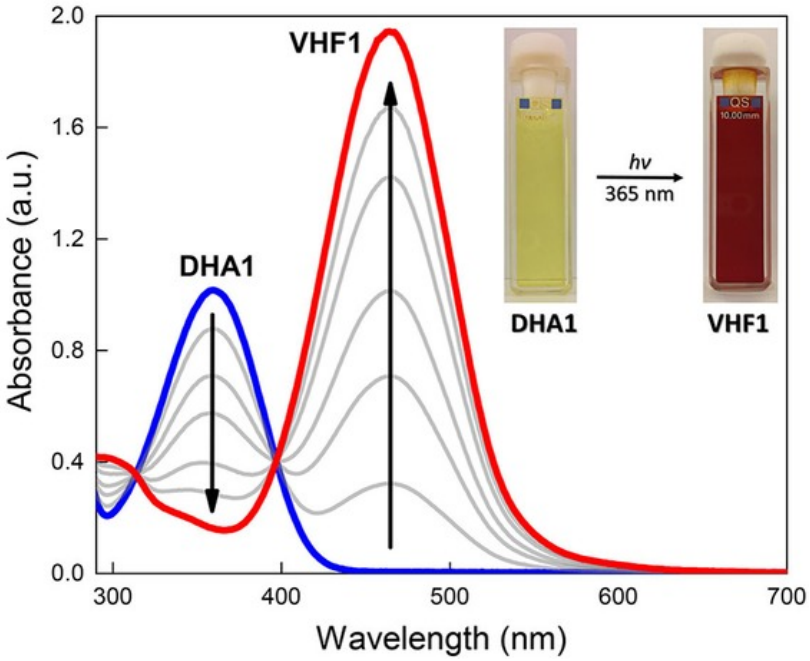

Figure 2-2: Dihydroazulene-Vinylheptafulvene (DHA-VHF); an example of positive photochromic molecule[78]. Reprinted with permission ©2018, John Wiley and Sons.

2.1.2. Negative photochromism

In negative (inverse) photochromism, the parent molecule becomes decolorized upon photoirradiation, resulting in a blue-shifted absorption spectrum for the photoisomer (Figure 2-3). Such types of systems are not as common as the positive photochromic compounds. Negative photochromes have seen a rise in interest due to possible applications as memory elements, as camouflage coatings and in biological labels.[79,80] Typical examples in this category include certain spiropyran derivatives,[81] as well as dihydropyrene[82] and norbornadiene derivatives.[83] The latter will be the main focus of this thesis and will be described in more detail in the next chapters, Chapter 3 and Chapter 4.

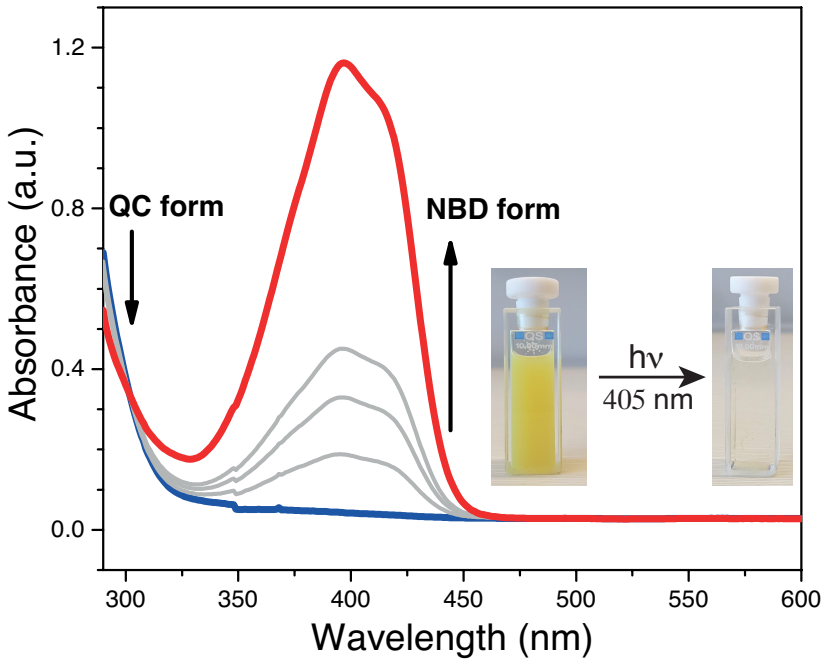

*Figure 2-3: Norbornadiene-quadricyclane (NBD-QC); typical example of negative photochromic NBD compound **3-3**, presented in Chapter 3.*

2.1.3. Typical organic photochromic molecules

Under this subsection, some common organic photochromic molecules (both negative and positive photochromes) are listed based on the type of photochemical reactions they undergo, and discussed briefly:

a. Photochromism based on *trans-cis* photoisomerization

A molecule containing two atoms connected by a double bond and substituted unsymmetrically around the double bond can exist in two isomeric forms, *trans* or *cis* (Figure 3-4). Thermodynamically, the *trans* isomer is more stable for stereoelectronic reasons. Upon photoirradiation, the *trans* isomer converts to the *cis* isomer. Likewise, the *cis* isomer can be converted back to the *trans* isomer by a thermal process. The lifetime for the thermal back-conversion ranges from a few seconds to months, depending on the type of solvent, temperature, pH as well as the nature of the substituents around the double bond.[84] The *cis* and *trans* isomers have different absorption spectra, where the *trans* isomer absorbs at a longer wavelength and has a higher extinction coefficient than the *cis* isomer. Depending on where the absorption lies in the electromagnetic spectrum, the isomers can exhibit visible colour changes as well. *Trans-cis* isomerization in retinal is responsible for the vision in humans. In this class of photochromic compounds, typical examples are stilbenes and azobenzenes,[85] which are widely studied for their photochemical properties.[86] In addition, they undergo large structural changes during the photoisomerization process. This property has been exploited to control biological functions,[87,88] in surface relief patterning[89] and molecular electronic devices.[90,91]

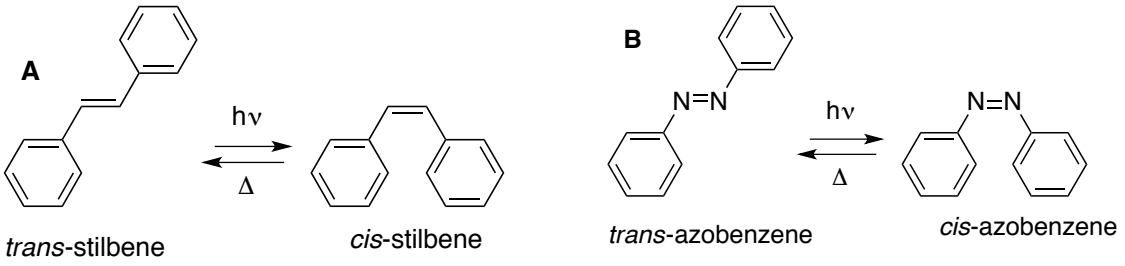

*Scheme 2-1: Photochromic molecules with trans-cis isomerization: Stilbenes (**A**) and azobenzenes (**B**).*[85]

b. Photochromism based on photocyclization reactions

Photoinduced 6π-electron delocalization over six different atoms, akin to the textbook example 1,3,5-hexatriene, is one of the most commonly encountered photochromic reactions. Fulgides, diarylethenes, spirooxazines, spiropyran as well as dihydroazulenes can be categorized under this example.

Fulgides

Fulgides are derivatives of succinic anhydrides with two exomethylene groups, in general containing at least one aromatic unit. The first examples of fulgides, with phenyl substituents, were T-type photochromes.[85] Later, replacing phenyl rings with heterocyclic aromatic units increased the thermal stability of fulgides, making them essentially P-type photochromic compounds (Scheme 2-2).[92] Fulgides have been used in rewritable optical storage devices and as chemical actinometers.[93]

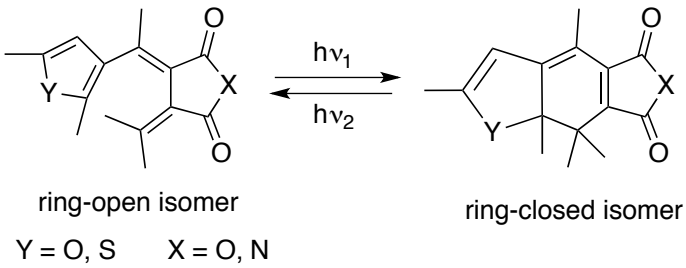

Scheme 2-2: Photoisomerization in a fulgide-based photochromic system.[93]

Diarylethenes

Diarylethenes (DAE) are derivatives of stilbenes where the phenyl rings in stilbene are replaced with five-membered heterocyclic aromatic rings such as thiophenes or furans. Unlike stilbenes, DAEs undergo light-assisted 6π electrocyclization. Upon photoisomerization, the ring-open isomer (colourless) converts to the ring closed, dimethylphenanthrene-type isomer (coloured), making them typical examples of positive photochromic molecules (Scheme 2-3). Since, the reverse reaction is facilitated using visible light, they are P-type photochromes. Due to their

superior photochemical properties, DAEs are the most extensively studied photochromic system since their discovery by Irie et al. in 1988.[94] They have been exploited as optical memory storage devices, actuators and in single-molecule imaging techniques.[22,33,56,76] The small structural change between the two isomers also made them ideal candidates for molecular switch applications.[95–97]

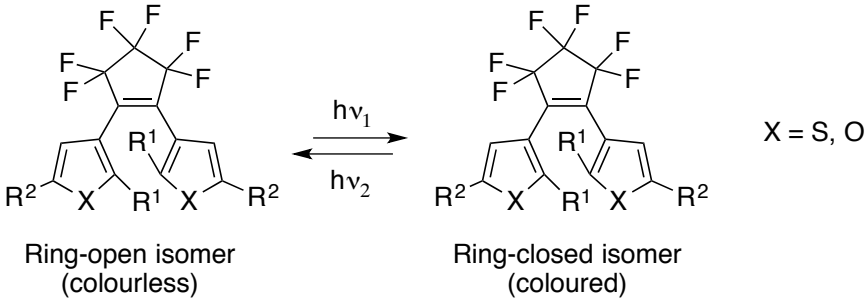

Scheme 2-3: Photoisomerization in a diarylethene (DAE)-based photochromic system.[33]

Spiropyrans and spirooxazines

The photochromic properties of spiropyrans and spirooxazines are based on the reversible photochemical cleavage of C–O bonds in the pyran and oxazine rings, respectively. The ring-closed spiro forms are often colourless. Upon light induced photoisomerization, the ring opens up to the coloured merocyanine forms (Scheme 2-4).[98,99] In most spiropyrans, the closed form is the more stable isomer. However, there are examples of stable merocyanine forms, representing negative photochromic systems.[80] The reverse reaction is induced thermally or with light. However, most spiropyrans and spirooxazines are T-type photochromic systems. Spiropyrans are one of the first types of molecules which were nominated for use in photochemically erasable memories by Hirshberg,[100] and spirooxazines have been utilized in commercial ophthalmic glasses due to their superior resistance towards photodegradation.[81]

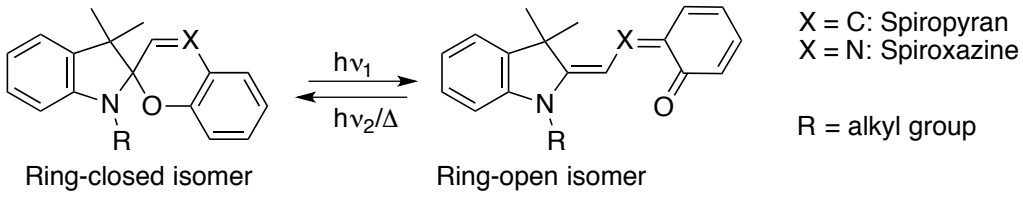

Scheme 2-4: Photoisomerization in spiropyran and spiroxazine-based photochromic sytems.[81]

Dihydroazulene derivatives

1,8a-dihydroazulene-1,1-dicarbonitrile (DHA) is a T-type photochromic molecule.[101] Upon photoirradiation, DHA undergoes a ring-opening photoreaction to the coloured vinylheptafulvene (VHF), while the open VHF-form is converted to DHA thermally, as shown

in Scheme 2-5. Nielsen and co-workers have explored different synthetic chemistries to elaborate the DHA system to make it suitable for anchoring between metal electrodes for use in memory devices,[102,103] as well as for solar energy storage applications.[78]

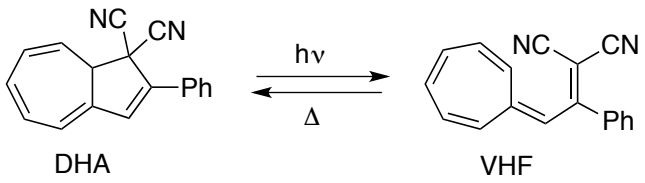

Scheme 2-5: Photoisomerization of dihydroazulene-vinylheptafulvene (DHA-VHF)-based photoswitch system.[102]

2.2. Photochromic compounds for molecular electronics

The ultimate goal of molecular electronics is to create operational logic circuits such as wires and transistors using organic molecules. Since the 1960s, it has been established that certain types of organic materials can carry current.[104] In particular, those molecules with an alternating single and double bond (conjugated) systems are found to be more conductive than the non-conjugated counterparts. For an infinitely conjugated system, the highest occupied molecular orbitals (HOMO) will be completely filled with π-electrons relative to the lowest unoccupied molecular orbitals (LUMO), converging the band gap, in theory, close to zero electron volt. This leads to metallic conduction in such types of organic molecules. If the conjugation is broken by intentionally placing a saturated unit in one or more locations in the chain using an external stimuli, the metallic conduction can be attenuated. The stimuli can be light,[31] heat,[102] pH,[105] electrochemical[106] or mechanical forces.[107] For photochromic compounds, light (in certain cases, heat) is usually used as an external stimuli.

Most organic photochromic molecules, including those summarized in Subsection 2.1.3., are designed rationally in such a way that the bond conjugation is longer in the coloured form, which upon photoisomerization becomes shorter. Needless to say, this change in bond conjugation also brings about a change in conductance among other chemical and physical changes. However, it is also important to recognize that the photochromic switching ability of a photochromic molecule in solution may not translate directly to conductance switching in solid state devices. When photochromic molecules are tethered between electrodes, the activation barrier between their isomeric forms could alter significantly. This can result in random switching even at low temperatures, in the solid state, due to hybridization of molecular orbitals of the molecules with the electrode.[108] More importantly, strong molecule-electrode coupling can result in charge transfer from the photoexcited state to the electrode instead of photoisomerization. Consequently, reversible conductance switching operations becomes challenging, even though no significant structural change occurs between the isomeric forms, e.g. diarylethenes.[97,109] This

issue can be alleviated by decoupling the photoswitch unit from the electrode using saturated units.[23,110] Hence, certain photochromic molecules that can switch reversibly between high- and low-conducting states in the presence of light acting as a "gate", can play a similar role as conventional transistors. This process can pave the way for logic operations and data storage at the molecular level.

2.3. Design considerations of photochromic compounds for single molecule electronics

Ultimately, if photochromic molecules are to replace conventional transistors, the following three design considerations need to be implemented.

2.3.1. The Electrode

For charge transport measurements, gold is mostly widely used due to its inertness towards oxidation.[50] However, other metals such as silver,[111] palladium[112] and platinum[113] have also been explored. More recently, graphene and carbon nanotube electrodes are becoming more attractive due to their unique advantages. Particularly, electron beam lithography, followed by selective oxygen plasma etching, yields a carboxy modification, which makes it easier to attach a photochromic unit with amino side groups via a peptide linkage.[114,115] Thus, while designing a photochromic molecule, the target electrode must be taken into consideration since the strength of the coupling between the molecule and the electrodes will control electron transport properties.[116]

2.3.2. The active molecular switching unit

Any organic photochromic molecules can potentially be considered for conductance switching applications. However, some are better suited than others when placed between electrode materials for various reasons. For instance, *trans-cis* photoisomerizable photochromic molecules do not operate efficiently if placed between fixed-distance electrodes. Usually, such types of photochromic systems are assembled on one electrode, keeping the other side free for structural flexibility during photoisomerization. In general, while designing a photochromic compound, emphasis needs to be given both to the main chain as well as side chains, if present. The main chain is the backbone of the molecule comprised of alternating single and double bonds, which facilitates charge transport. In the tunnelling transport regime, the conductance (G) through a molecule has an exponential correlation to the length (L) of the molecule and its conductance decay constant (β) given by the following Equation 2-1.[117]

$$G = Ae^{-\beta L} \qquad (2\text{-}1)$$

where A is the pre-exponential factor.

In general, smaller β and L values results in higher conductance. L is straightforward to determine from the bond length. However, β is dependent on the intrinsic electronic behaviour of the repeating units in the main chain. Depending on the type of anchoring group employed, chains that are strongly conjugated (or quinoid structures) are efficient charge transporters and hence have smaller β-values. Conjugated molecules such as OPVs, i.e. oligo(phenylenevinylene) and OPEs have β-values of 2.0 - 3.4 nm^{-1} and 1.7 – 1.8 nm^{-1}, respectively.[118] On the other hand, alkanes with no bond-conjugation have the highest β-values, 8.4 nm^{-1}.[119] It is also worth noting that conjugated molecules that consist of aromatic unit(s) with strong resonance stabilization energy, have higher β-values than those with less aromatic or with no aromatic units in the main chain due to aromatic stabilization.

Similarly, side chains can also fine-tune the charge transport through a molecule by altering its electronic structure and conformation. Excluding other factors, the general trend is that electron-donating side chains increase electron density on the main chain, raising the HOMO toward the Fermi energy (E_f) of the electrode resulting in higher conductance. On the contrary, electron-withdrawing groups bring about the opposite effect.[120]

2.3.3. The anchoring unit

Anchoring groups are used to tether a photochromic compound between electrodes, where the type of anchoring unit used depends on the type of electrode material. Since gold is the most common electrode material employed, the anchoring units needs to be aurophilic, making use of lone electron pairs for dative interactions. Thiols, amines and pyridyl groups are typical examples of aurophilic linkers. The type of anchoring group used, as well as the nature of the anchoring group, play a crucial role on the charge conductance efficiency of a photochromic molecule. For instance, thiols are robust anchoring groups that can withstand harsh conditions, however, they are prone to dimerization.[50] Hence, the thiol groups are protected with a thioacetate protecting group, which can be readily removed on the surface of gold electrodes. Moreover, despite the strong binding, S-Au linkages show broad conductance features due to variable contact geometry.[121] Pyridyl and amine groups have also found widespread use as anchoring groups due to their well-defined contact geometry, resulting in narrowly spread conductance values.[122,123] Pyridyl groups are reported to give slightly higher conductance values compared to amines due to stronger binding interaction with gold electrodes.[124] Amines are becoming a popular choice as anchoring group when carbon based electrodes are used due to the their facile coupling via a peptide linkage.[115] Direct tethering of carbon end-groups to gold

has also proved to be another good strategy. Direct Au-C conductance values are reported to be up to 100-fold higher than amine-based anchoring groups.[125] Transmetallation of trialkyltin,[125] desilylation of TMS,[126] and electroreduction of diazonium salts,[127] have been implemented to yield direct C-Au linkages. Unfortunately, these anchoring strategies cannot be used universally due to their toxicity, explosive nature or limited substrate scope.

2.4. Break junction techniques for measuring molecular conductance

Measuring molecular conductance is not an easy undertaking. It requires constructing junctions based on molecules on the nanoscale level with mesoscopic electrodes. The tiny dimensions of the molecules also makes it challenging to manipulate them directly and place them between the electrode materials. Moreover, to make molecularly scaled devices, stable and individually addressable nanoscale junctions need to be formed. So far, such a feat has not been achieved. However, there are several experimental techniques that allow gauging the electrical conductance in nanoscale molecular interconnections. Here, the so-called break-junction techniques for single molecule conductance measurements will be introduced.

2.4.1. The Mechanically Controllable Break-Junction technique (MCBJ)

The MCBJ technique involves the breaking of a metal wire (usually gold) fixed on top of a flexible solid substrate. The solid substrate is arranged in a three point mechanism, which upon bending stretches the wire and eventually breaks it (Figure 2-4). The gap between the newly formed electrode surfaces can be tuned with picometer precision to accommodate a molecule of interest containing an anchoring unit. Molecules in solution form are applied between the gap either before or after the breaking process to form an electrode-molecule-electrode junction.

The MCBJ technique was introduced in the 1980s to study tunnelling in superconductors.[128] Later, in 1997, it was used by Reed et al. to measure the conductance of benzene-1,4-dithiol (BDT).[46] In their experiment, the gold electrode was broken in a 1 mM tetrahydrofuran (THF) solution of BDT under argon, forming a self-assembled monolayer. After evaporation of the THF, the electrode tips were brought together until characteristic current-voltage and conductance features were acquired with high reproducibility. This method enables direct observation of charge transport through organic molecules under vacuum. Subsequently, the conductance of various molecules ranging from simple hydrogen molecules to more advanced functional molecules has been investigated using MCBJ. This technique has also been used to measure molecular conductances in solution, despite a strong solvent effect compared to vacuum measurements. For instance, Huber et al. determined electrical conductance of various oligo(phenylene ethynylene, OPEs) and oligo(phenylene vinylenes, OPVs) in mesitylene.[129]

One of the advantages of conductance measurements in solution is the ability to use electrochemical gating to manipulate the energy alignment based on redox processes.[130] Moreover, MCBJ has additional advantages, such as excellent device stability, precisely tuneable gap size and minimum electrode contamination.[131] However, MCBJ is only capable of testing a single sample at a time, which limits mass fabrication. It is also challenging to obtain surface topography using scanning probe techniques before and after conductance measurements.

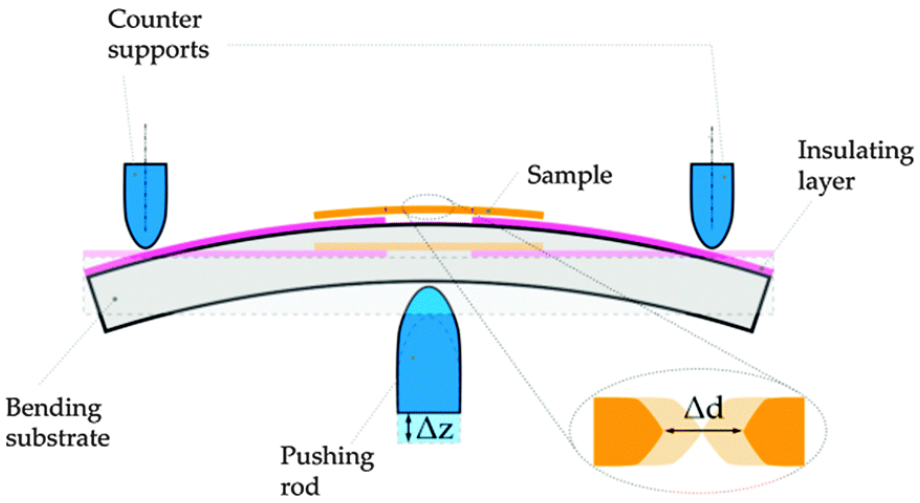

Figure 2-4: Schematic illustration of mechanically controllable break-junction (MCBJ) technique for measuring molecular conductance[130]. Reproduced with permission of the Royal Society of Chemistry.

2.4.2. The Scanning Tunnelling Microscopy Break-Junction technique (STM-BJ)

The STM-BJ technique involves the creation of electrode-molecule-electrode junctions between a STM tip electrode and a substrate electrode. The junctions can be broken and formed many times in a solution of the desired molecule provided with an anchoring unit. The movement of the STM tip is controlled by piezoelectric transducer. During the measurement, the tip is brought close to the surface of the substrate containing the anchored molecules. At this point, one or more molecules may bind to the STM tip using the second anchoring group, forming junction(s). Then the tip is pulled away from the surface of the substrate until the molecular junctions breaks. During this process, molecular conductance is recorded as a function of tip displacement. The resulting traces show conductance values of 1 G_o for single Au-Au contact followed by plateaus of conductance values below G_o until no plateau is observed depending on the number of molecules anchored between the tip and the substrate.[51]

This method was developed and demonstrated by Tao and co-workers to study the conductance of 4,4'-bipyridine and alkanedithiols.[47] About a thousand experiments were conducted by repeatedly forming the junctions in a relatively short time. Conductance histograms were constructed from the thousand experiments, revealing well-defined peaks at integer multiples of the G_o values. Since conductance values are measured until all the junctions are completely

broken, this method is suitable to identify the conductance of a "single" molecule junction. The STM-BJ technique has also been used to form a molecular junction without touching the substrate. Instead, the tip was approached close enough until a tunnelling current was observed indicating spontaneous junction formation.[132]

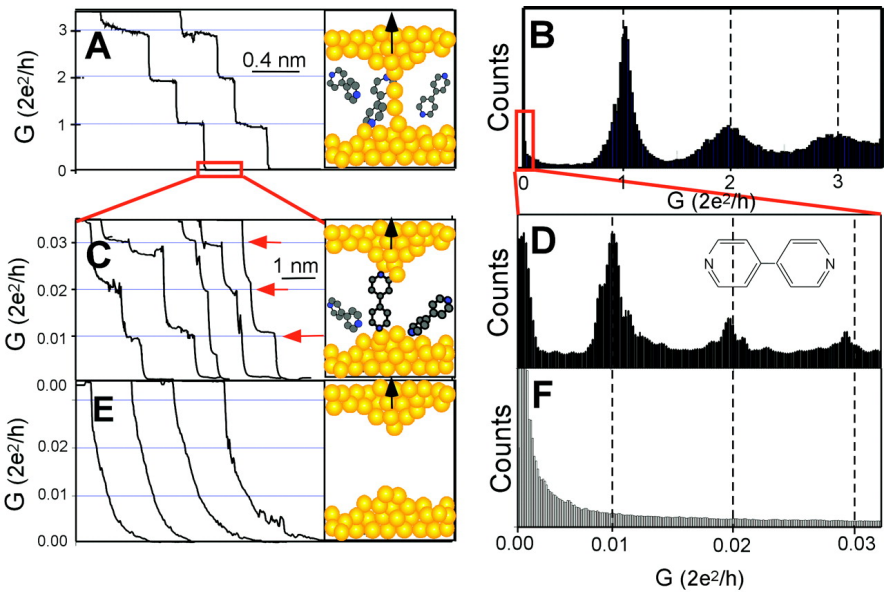

Figure 2-5: Schematic illustration of scanning tunnelling microscopy-break junction technique along with conductance traces and histograms of 4,4'-bipyridine.[47] Reproduced with permission ©2003, American Association for the Advancement of Science.

Many researchers have used this platform to investigate molecular conductance with a similar outcome as for MCBJ.[123133134] Venkataraman et al. have used this technique extensively to investigate the effect of different anchoring units such as amines (NH_2), dimethyl phosphines (PMe_2), and methyl sulphides,[135] as well as to identify the type of charge carriers.[136] One of the advantages of STM-BJ is its ability to image the substrate and movement of the STM tip to any area on the substrate for a thorough investigation. The downside is that it has lower mechanical and thermal stability compared to MCBJ.

Another scanning probe microscopy technique related to STM-BJ is Conducting Probe-Atomic Force Microscopy (CP-AFM). In this technique, the tip positioning on the surface is controlled by force feedbacks instead of current as in STM-BJ. The conducting AFM-tip also helps in measuring both conductance and intermolecular forces simultaneously during junction elongation until rupture.[48,137]

Chapter 3 The Norbornadiene-Quadricyclane Photoswitch Pair

In the previous chapter, the definition of photochromism and typical examples of photochromic systems were described. In this chapter, another example of a T-type photochromic system based on the norbornadiene-quadricyclane photoswitch pair is introduced in the context of solar energy storage. Some basic criteria that need to be kept in mind while choosing molecular energy solar energy storage (MOST) systems, along with some examples reported in the past using NBD-QC are presented. Moreover, our contribution to the MOST system using NBD-QC based on the original work presented in Paper III, is summarized.

3.1. Brief introduction to norbornadiene-quadricyclane

Bicyclo[2.2.1]hepta-2,5-diene, commonly known as norbornadiene (NBD), is a strained, unsaturated bicyclic compound with a ring strain energy of about 145 kJ/mol.[138] The strain arises due to restrictions brought about by a bridging methylene unit compared to the non-bridged cyclohexane derivatives as shown in Scheme 3-1.

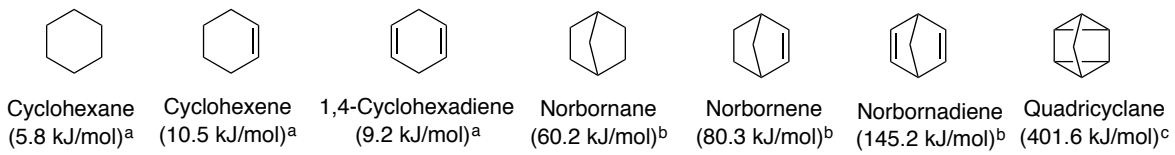

Scheme 3-1: Strain energies in some cyclic and bicyclic derivatives of hexane. a[138]b[139]c[140]

The bridgehead carbons at the 1 and 4 positions on norbornadiene are allylic and the double bonds are isolated as well (Chapter 1, Section 1.4, Scheme 1-4,). However, such types of double bonds are known to interact through space, resulting in homoconjugation.[141] Upon photoactivation, the homoconjugated double bonds undergo a [2+2] intramolecular cycloaddition reaction to yield a fully saturated analogue, tetracyclo[3.2.0.0.0]heptane, also known as quadricyclane (QC). The photoisomer QC is metastable and has a significantly higher strain energy of about 400 kJ/mol, which is over two times higher than NBD. However, it is thermally stable with a half-life of >14 h at 140 °C.[142]

The unique stability of QC can be explained based on the Woodward-Hoffmann rules.[143] These rules states that for a system with 4n π-electrons, under thermal reaction conditions, bonding interactions are formed via a *conrotatory* process since the terminal orbital envelopes overlap on opposite faces of the system (Scheme 3-1). On the other hand, these bonding interactions are formed via a *disrotatory* process under light-induced reaction conditions, since the promotion of an electron to the first excited state brings about a change in symmetry of the orbitals at the terminals. However, in both NBD and QC, *conrotatory* processes are not favoured due to

geometrical restrictions. This means that the thermal *conrotatory* NBD-QC interconversion is "forbidden", while the light induced *disrotatory* process for the interconversion between NBD and QC is "allowed". Interestingly, the thermal back conversion of QC to NBD is often observed, albeit at higher temperatures (140 °C).

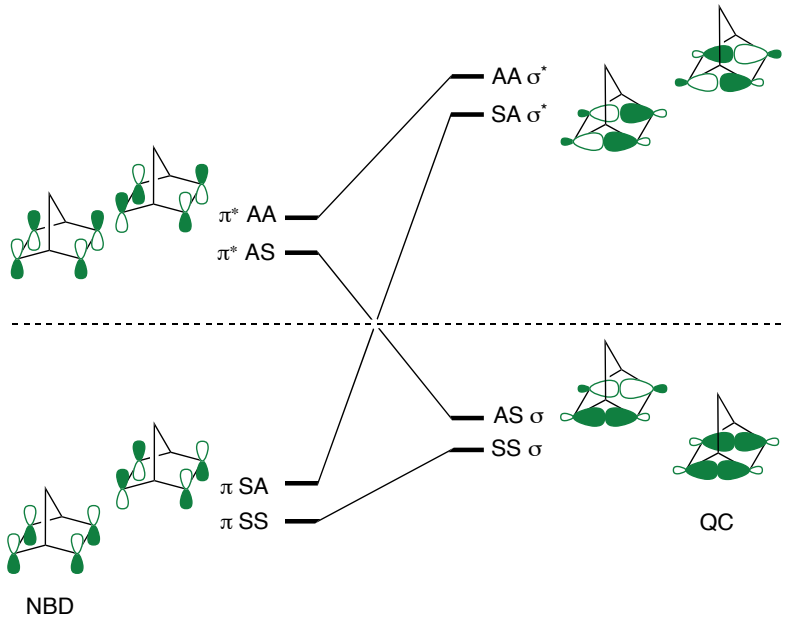

Figure 3-1 Correlation diagrams for norbornadiene-quadricyclane (NBD-QC) [2+2] photoisomerization based on the Woodward-Hofmann rule. Adapted from ref. 136 ©2003, John Wiley and Sons.

Consequently, the rigid structure, the stability due to unique geometry, and the high ring strain in NBD-QC systems have made the NBD-QC pair a primary candidate for studying reactivities in strained structures,[144] as well as for exploring its potential to store energy photochemically.[63,83,145,146] Moreover, the back-isomerization from QC to NBD can be induced electrochemically or by using a catalyst in addition to the thermal and light-induced methods elaborated earlier. The back reaction from QC to NBD releases about 92 kJ/mol of energy.[147] To put this in context, the energy required to evaporate liquid water is about 41.8 kJ/mol, commonly called the enthalpy of vaporization of water. That means, the energy stored in NBD-QC system is more than enough to boil water.

3.2. Molecular solar-thermal energy storage application

According to the U.S Energy Information administration, the world energy consumption is predicted to increase by 28% in 2040. The main reasons for such a rise is attributed to strong economic growth in Asia and Africa.[148] Traditionally, the energy demands are met by finite and unsustainable energy sources such as fossil fuels. Consequently, many countries are shifting their attention progressively towards sustainable energy sources. Energy production from renewable sources is becoming more affordable due to research and development in the field. However,

the energy production from sustainable resources often does not match the demand. For instance, the sun does not shine in the evening when the demand is higher and the wind does not blow all the time. Hence, it is important to develop efficient energy storage methods to store the energy produced during peak production times and utilize it later when energy demand is high. There are various ways of storing energy, such as using batteries or a capacitors, thermal energy storage using molten salts and many more.[149] Recently, however, solar fuels from biologically inspired techniques such as artificial photosynthesis are attracting considerable attention.[150] In these techniques, solar energy is used to facilitate the catalytic reduction of carbon dioxide into various hydrocarbon products, as well as in the generation of hydrogen from water splitting.

In the past, storing solar energy in the form of strain energy in certain organic molecules has also been researched.[63,145] This technique is now known as *mo*lecular *s*olar *t*hermal (MOST) energy storage. Practical challenges to turn this system into a commercial product has hampered its widespread use. More recently, however, the MOST system has seen a renewed interest due to significant improvement in molecular design, synthesis and outdoor testing.[151–155]

Next, a brief discussion about the criteria a molecule is required to fulfil for use in a MOST energy storage system will be presented. I will also describe our efforts towards the design, synthesis, and practical challenges faced in using NBD-QC pairs as a MOST systems.

In principle, any molecule A that can be isomerized in the presence of light to a high energy photoisomer B can be considered for MOST applications. However, there are a number of criteria that need to be fulfilled for efficient energy storage and practical applications. The important criteria are listed here.

a. The first molecule A must absorb in the range of 350-700 nm for efficient solar energy harvesting.
b. The photochemical conversion of A to B must proceed with high quantum efficiency (ideally 100%), and B should be stable over a long period of time to allow storing the energy absorbed and release the stored energy when triggered externally.
c. The photoisomer should be colourless to avoid competing absorption that minimizes the full conversion of A.
d. To be able to store considerable amounts of energy ($\Delta H_{storage}$), the ground state energy of B must be high compared to A while maintaining the activation barrier sufficiently high to ensure the stability of B.
e. A and B should be inexpensive, non-toxic, easy to synthesize, scalable, have long-shelf lives and low molecular weights to maximize energy density.

Various molecular systems that fulfil some of these requirements have been reported and reviewed in the past.[83,156,157] However, the NBD-QC pair is found to be potentially most promising.[158] The photoisomerization of unsubstituted NBD to the metastable isomer QC offers many advantages compared to other MOST systems. NBD is commercially available and fairly cheap. Both NBD and QC are liquid at room temperature, which make them ideal candidates for operations in a continuous flow system. Even though NBD has an absorption maximum in the UV region, it can be photoisomerized to the QC isomers using sunlight in the presence of sensitizers such as acetone, acetophenone or benzophenone.[142] Besides requiring a high activation energy, the QC-NBD thermal back-conversion is thermally forbidden by Woodward-Hoffmann rules, making it quite stable even at high temperatures.[159] When triggered using a catalyst,[160,161] QC releases about 89 kJ/mol of heat, which is equivalent to 966 kJ/kg,[147] a more practical way used to express the energy density of materials. This value is the highest obtained so far, not only for MOST systems but also compared to typical Lithium ion batteries.[162]

On the other hand, unsubstituted NBD-QC systems have some limitations. While QC is more stable, NBD is volatile and prone to oxidation and polymerization. Triplet sensitization of NBD also causes reagent contamination and the formation of unwanted side products, compromising cyclability. Although, this problem has been partially mitigated by using polymer bound triplet sensitizers,[163] it comes at the expense of reduced quantum yield. Direct photoisomerization of unsubstituted NBD to QC also suffers from a poor solar spectrum mismatch, hence affecting the ability to store solar energy. Therefore, there has been a lot of effort in the scientific community to maintain the inherent qualities of unsubstituted NBDs while redshifting its absorption spectra. This can be achieved by attaching one or more substituents on any of the 7-carbon frameworks.

The first examples were characterized by symmetrical substitution of NBDs with electron withdrawing groups (EWG) across the double bonds at the C-2 and C-3 positions (Scheme 3-2A).[160,164,165] Substituting the bridging C-7 carbon was also pursued as a viable option (Scheme 3-2B).[146,166] The C-7 substitution method has shown significant improvement, with absorption onsets reaching up to 360 nm, compared to 267 nm for the unsubstituted NBD, and photoisomerization quantum yield values (Φ_{NBD-QC}) reaching up to 50%. To further redshift the absorption onset, unsymmetrical substitutions across the double bonds were pursued. In particular, substituents such as aryl carbamoyl and carboxy moieties attached to the C-2 and C-3 positions on NBD were reported to provide absorption onsets over 400 nm (Scheme 3-2C).[167] However, the quantum yields ($\Phi_{NBD-QC} < 12\%$) for these derivatives were found to be too low to be of any practical use. Aroyl and aryl substituents at the C-2 and C-3 positions red-shifted

the onset of absorption (λ_{onset} > 400 nm), and quantum yields ranging from 30% to 60%, were achieved (Scheme 3-2D).[168] The general observation is that NBDs with carbonyl substituents exhibit a considerable redshift in their absorption spectra, while the QC can be triggered to revert to NBD by using acid as a catalyst.

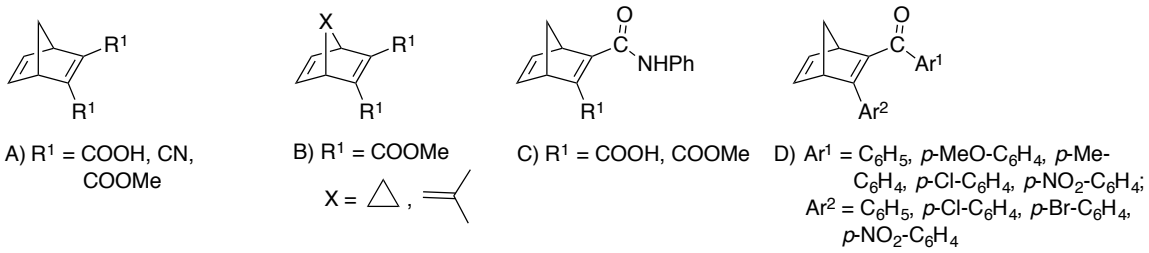

Scheme 3-2: Substituted NBD derivatives (A), symmetrically substituted (B), symmetrically substituted with additional substitution on the bridging C-7, as well as unsymmetrically substituted (C). and (D).

Another approach that was found to be promising was the systematic unsymmetrical substitution of NBDs with various donor (D) and acceptor (A) units across the double bonds. In the past, Yoshida and co-workers utilized this approach to synthesize NBDs substituted with D-units on one side of the two double bonds and A-units on the other side.[146] In spite of the fact that the double bonds of NBD are isolated and formally non-conjugated, they interact through space via homoconjugation,[169] which is possible due to the presence of the bridging methylene unit, as pointed out earlier in Section 3.1. Consequently, NBD absorption spectra are reported to be redshifted up to 50 nm compared to the non-bridged 1,4-cyclohexadiene (Scheme 3-1).

Specifically, for the DA NBD shown in Scheme 3-4, the absorption onsets are found to be well above 400 nm, due to the charge transfer transition from the HOMO of the D units to the LUMO of the A units (Scheme 3-3A). Moreover, for some of the derivatives, the quantum yields, $\Phi_{NBD\text{-}QC,}$ were unity, even at ambient condition and the half-lives for some of the QC photoisomers were close to 38 years.[146] By combining C-7 substitution with the DA approach, Jorner et al. have reported NBD-derivatives with absorption onsets around 400 nm and quantum yield, $\Phi_{NBD\text{-}QC,}$ over 70%.[170] Furthermore, the effect C-7 substitution on the half-lives was examined. Sterically bulky groups, such as isopropyl, were found to increase the half-life significantly due to negative activation entropy. Similarly, Hirao et al. have reported NBD-derivatives with absorption onsets well over 550 nm, covering a reasonably wide range of the visible light.[171] Certain derivatives were found to be stable with quantum yield, $\Phi_{NBD\text{-}QC,}$ values as high as 75%. With the aim of improving thermal stability, Nagai et al. have synthesized NBD derivatives with trifluoromethyl groups as acceptors with various donor groups (Scheme 3-3B). Strongly donating groups redshifted the onset of absorption up to 580 nm. Moreover these fluorinated NBD derivatives were characterized by high molar absorptivity (ε_{max} = 0.5 - 2.0 × 10^4 $M^{-1}cm^{-1}$)

and excellent thermal stability with very high fatigue resistance (1000 number of cycles with little degradation).[172]

In general, the DA and C7 substitution strategies produced NBD derivatives, with relatively good absorption onsets, ideal photoisomerization quantum yields and long half-lives, make them potentially promising molecules for commercial MOST applications.[173] However, multi-step synthetic procedures, scalability as well as lower energy storage capabilities due to their large molecular mass, limited their practical use. The examples given above demonstrates how intricate the challenges are in making ideal substituted NBDs that maintain a balance between good solar spectrum match, high photoisomerization quantum yields and molar absorptivity (ε) while keeping the molecular mass as low as possible to maximize solar energy storage density.

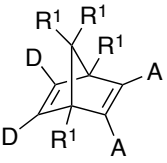

A) D = H, Me, Ph, *p*-$MeOC_6H_4$, *p*-$Me_2NC_6H_4$
A = CN, COMe, CF_3, CONHPh
R^1 = H, Me

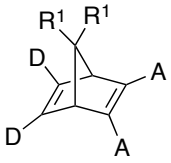

B) D = Me, Ph, *p*-$MeOC_6H_4$, *p*-$Me_2NC_6H_4$
A = CO_2Me, CF_3
R^1 = H, Me, isopropyl

Scheme 3-3: Examples of substituted NBDs based on the donor (D) and acceptor (A) strategy.

More recently, the effect of C-2 and C-3 D-A substitution on the absorption spectra of 2, 3-disubstitued NBD derivatives have been explored, aiming at reducing the molecular mass.[63,151,154,174] It has already been shown that DA substitution on one of the double bonds can lead to NBD derivatives with a good solar spectral match ($\lambda_{onset} \approx 620$ nm), fairly high quantum yield ($\Phi \approx 75\%$), fast and quantitative photoisomerization, and more importantly a lower molecular weight.[63] In our research group, this DA approach was further explored to obtain NBD derivatives with good spectral match ($\lambda_{onset} > 450$ nm) and high molar absorptivity by using an alkyne spacer ($\varepsilon = 30000\ M^{-1}cm^{-1}$),[154] as well as high photoisomerization quantum yields ($\Phi >$ 70%) with extremely stable QC (half-lives over 18 years), enabled by ortho substitution on the aromatic ring.[174] More importantly, low molecular weight derivatives, compared to previous reports,[63,146] with solar energy storage densities over 600 kJ/Kg were achieved, making them practical for real outdoor testing.[155,175] Some C-7 substituted derivatives were even found to be liquid, which make them ideal for use under neat conditions and minimizing dilution of the thermal properties.[176]

With the aim of increasing the energy storage density while redshifting the absorption onsets, dimers and trimers of NBD derivatives were also targeted for synthesis. This idea has been demonstrated in the past, showing promising results with absorption onsets approaching 500 nm,

and an interesting stepwise photoreaction for the dimers were reported.[177,178] In our group, Mansø et al. conjoined two molecules of 2-cyano NBD derivatives at the C3 positions of the respective NBD units, with a central electron rich benzene ring (Scheme 3-5).[153] In some of the derivatives, ethynyl spacer units between the two NBDs and the aromatic moiety were included in the design to obtain high molar absorptivity, as well as to redshift the absorption spectra.[154] As expected, the dimers showed a fairly good absorption onset, > 410 nm, for the para-linked derivatives and very high molar absorptivity (up to $\varepsilon = 53000\ M^{-1}cm^{-1}$) for the trimer. Moreover, the dimers with an ethynyl spacer units, were found to be redshifted by greater than 10 nm compared to those without ethynyl linkers, at the expense of reduced half-lives. This could be explained by the extra degree of freedom furnished by the ethynyl linker. The most significant improvement was observed on the photoisomerization quantum yields ($\Phi_{NBD\text{-}QC}$ = 52 - 94%) compared to previous works.[177,178]

Another unique feature with these derivatives is that upon photoisomerization, the NBD converts instantaneously to QC, with a significant blue shift in the absorption profile, with a spectral window above 50 nm between the NBD and QC absorption spectra. In addition, the para derivatives were also found to exhibit sequential switching in agreement with previous works.[177] In summary, the para-dimer with an ethynyl linker has an energy density above 500 kJ/kg, a redshifted absorption spectrum with very large molar absorptivity ($\lambda_{onset} > 400$ nm; $\varepsilon = 40000\ M^{-1}cm^{-1}$), an improved half-life ($t_{1/2} > 4$ h) as well as a high quantum yield ($\Phi_{NBD\text{-}QC} > 85\%$), making it a highly promising candidate for MOST applications.

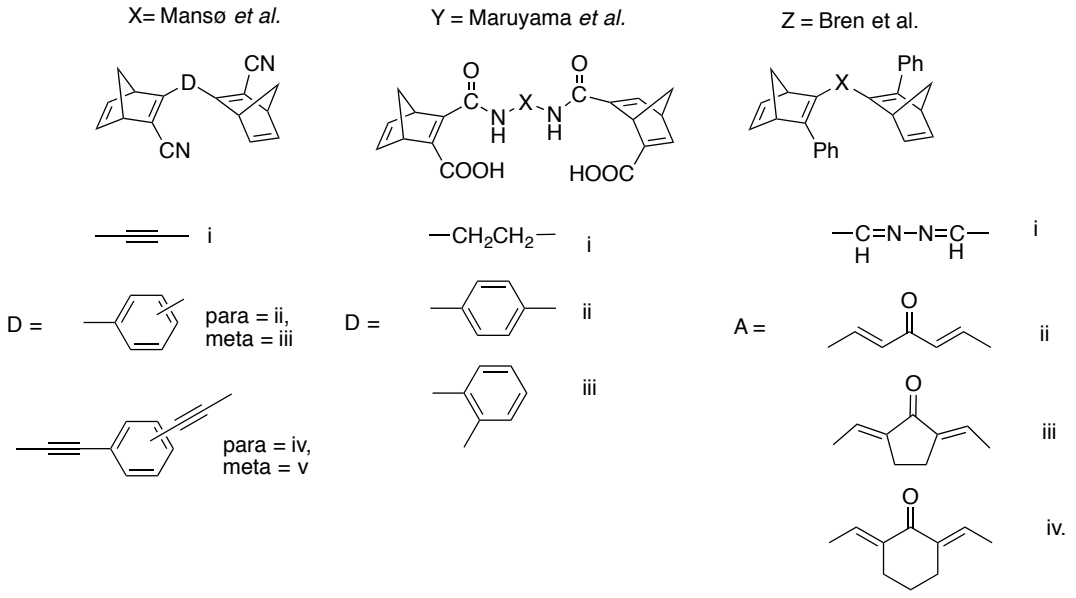

Scheme 3-4: Some examples of NBD dimers reported in the past.[153,177,178]

Encouraged by the outcome of the dimer strategy, we wanted to explore new bridging units beyond benzene in order to redshift the absorption spectra further in the visible region. Hence, in Paper III, we explored the utility of thiophene and carbazole groups appended with ethynyl units as linkers to bridge a 2-cyano NBD derivatives (Scheme 3-5). These groups are chosen for their strong donor ability compared to benzene while keeping the molecular weight as low as possible to increase the energy storage density.[151,179] Moreover, maximum solar energy conversion efficiency is reported to be obtained for MOST systems with absorption onsets of at least 590 nm.[180] Two sets of NBD dimers, i.e. 2,5-disubstituted (**3-2**) and 3,4-disubstituted (**3-3**) on the thiophene, and 2,7-disubstituted (**3-4**) and 3,6-disubstituted (**3-5**) on the carbazole, both with an ethynyl spacer, were prepared. Ethynyl units were included in the design to enhance the molar absorptivity of the molecules, as it is reported to create a favourable HOMO-LUMO state across the entire molecule.[154] Another NBD dimer molecule (**3-1**) with 2,5-disubstitution on the thiophene without an ethynyl unit was also synthesized for comparison.

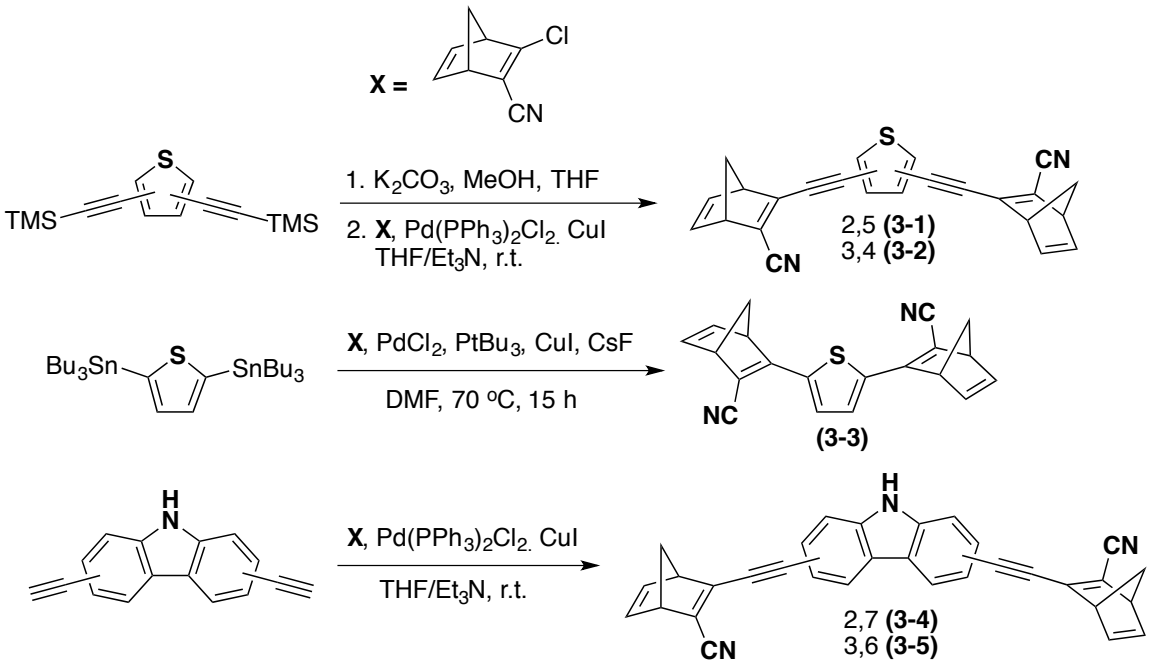

Scheme 3-5: NBD dimers, disclosed in Paper III, based on (a) 2,5-thiophene di-substitution; as well as (b) thiophene and (c) carbazole donors appended with ethynyl linkers.

Compound **3-1** was synthesized by reacting 2,5-bis(tributyltin)thiophene and the previously reported 2-chloro-3-cyanonorbornadiene[181] via a Stille coupling in one step. Compounds **3-2** and **3-3** were synthesized by reacting 2,5- or 3,4-diethynylthiophene, which were prepared according to literature procedures,[182] with 2-chloro-3-cyanonorbornadiene via a Sonogashira reaction in good yields. Similarly, Compound **3-4** and **3-5** were synthesized by reacting 2,7- or 3,6-diethynylcarbazole, also prepared according to literature procedure from the corresponding dibromo analogues,[183] with 2-chloro-3-cyanonorbornadiene. To reduce the molecular weight

imposed by the carbazole bridge, a pyrrole group was also targeted. However, due to stability issues in the intermediate steps, the synthesis was abandoned. Likewise, the attempt to synthesize tetramer NBD derivatives, i.e. involving 2,3,4,5-*tetra*NBD substitution on the thiophene to maximize the energy storage density, was also abandoned for similar reasons.

The UV-vis absorption spectra of all the dimers were redshifted compared to the benzene[153] analogues with appended ethynylene as a bridge (see Figure 3-2). The results are summarized in Table 3-1. In particular, the linearly conjugated 2,5-disubstituted dimers exhibit the most redshifted absorption onsets, approaching 470 nm, which is redshifted by about 60 nm. Besides being a good donor, the low aromatic resonance stabilization of thiophene compared to benzene could be responsible for the redshifted absorption spectra for the NBD dimers with a thiophene bridge.[184] For the carbazole dimers, the molar absorptivity was found to be almost twice as high compared to the thiophene bridged NBD dimers owing to the large chromophore carbazole unit, which was also found to have a similar effect on the molar absorptivity of the QC photoisomer. The large molar absorptivity of the QC isomer is not a desired effect, since it may compete with the absorption of light by the parent NBD, compromising the efficiency of the system. For compound **3-1**, a peculiar feature was observed. Despite significantly lower molar absorptivity due to lack of an ethynyl linker, it is almost as redshifted as the one with the ethynyl linker, **3-2**. The QC isomer for this compound has an absorption onset of around 320 nm, which provides this compound with a 170 nm wide spectral window of operation.

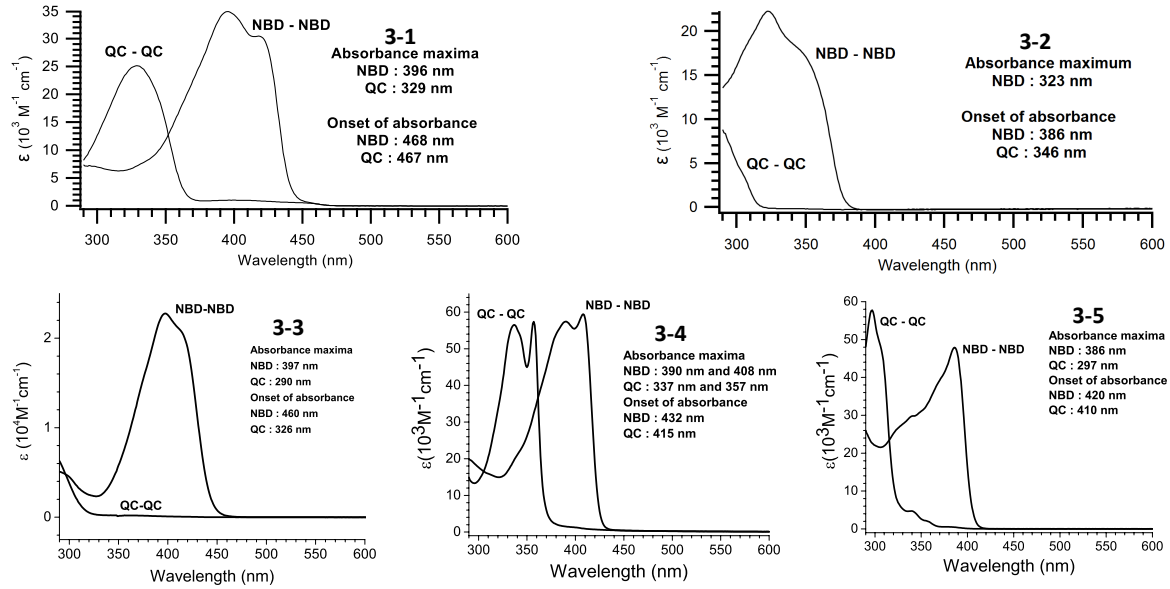

Figure 3-2:UV-vis absorption spectra of the dimer NBD derivatives in toluene: NBD and QC absorption spectra are shown.

Photoisomerization quantum yields were also measured based on the ferrioxalate actinometer[185] for all the compounds following the procedure described in the Methods, Chapter 7, Section 7.3.

The quantum yields were calculated taking into account the presence of two NBD subunits per molecule. The average values from two measurements are displayed in Table 3-1. The quantum yield values are significantly improved compared to the parent NBD/QC system, but slightly lower compared to the dimers reported previously.[153] Photoisomerization quantum yields for two of the dimers, **3-1** and **3-3**, were not measured due to the non-linearity of change in concentration against wavelength during the measurement.

Table 3-1: Photophysical properties of dimers of NBD/QC in toluene summarized from Paper III as well as values reported for previous literature examples.[153154174]

Compound	λ_{max} (nm); ε (M^{-1} cm^{-1})		λ_{onset} [b] (nm)	$\Phi_{NBD \rightarrow QC}$ (%)	$t_{1/2,\ 25\ ^oC}$	E_a (kJ/mol)	$\Delta H_{calculated}$ [f] (kJ/mol)
	NBD	QC	NBD		QC to NBD	QC to NBD	QC to NBD
Parent **NBD-QC**[a]	205; 2100	-	267	5	14 h	141	93
Xv (Scheme 3-4)[153]	334; 28131	258; 24191	381	83[e]	14.2	101.5	99
Xiv (Scheme 3-4)[153]	359; 41005	300; 34014	411	94[e]	4.33 h	93.3	90.8
2-Cyano-3-(1-naphthyl) NBD (NaphNBD)[174]	321; 7600	-	373	59[e]	6729 h	144.4	142.4
3-1	396; 34900	329; 25100	468	-	1.32 h	97.0	94.4
3-2	323; 22300	-	381	50[d]	16.1 h	104.2	101.7
3-3	397; 22800	326;	460	-	43.8 s	92.0	89.5
3-4	408; 59400	357; 57400	432	70[e]	22.0 min	148.6	146.1
3-5	386; 47900	297; 57800	420	44[e]	10.7 min	99.5	97.0

[a]Values are given for solution in ethanol. [b]Absorption onset is defined as the wavelength where log(e) = 2. [c]Half-life is given at 140 °C. [d]Measured at 340 nm on non-degassed samples. [e]Measured at 340 nm on non-degassed samples. [f]Calculated from the Eyring plot.

To determine the half-lives and the Arrhenius parameters, the dimers were irradiated with light and allowed to relax at different temperatures (Methods, Chapter 7, Section 7.3). The half-lives, the time required for the photoisomer QC concentration to decrease by one-half of its initial concentration, were determined at the corresponding temperatures rate constants, considering

first order reaction rate. The dimers NBDs (**3-1 – 3-2**) exhibit a significant loss in their half-lives compared to both the parent NBD/QC and the previously reported dimers. Particularly, the dimers with a carbazole bridge and the dimer compound **3-3** without the alkyne linkers suffered the most, with the latter having the shortest of all with half-life of 44 seconds. The short half-life for the 2,7-carbazole bridged dimer was surprising, since its activation energy was higher than even the parent QC to NBD barrier of activation (141 kJ/mol) (Table 3-1).

The rate of the back reactions was then plotted against the inverse of the temperatures to determine the activation energy (E_a) based on the Arrhenius equation. The activation energy at 25 °C was determined by extrapolation. Using the Eyring equation, the enthalpy of activation (ΔH^*) and change in entropy (ΔS^*) were determined. The results are summarized in Table 3-1. Then the Gibbs energy of activation (ΔG^*) was calculated from ΔH^* and ΔS^*, to see if there is any trend in the back reaction kinetics. It turns out that four of the compounds we synthesized have similar values to the parent NBD-QC, the outlier being compound **3-3** with a small ΔG^* value accounting for the short half-life (Figure 3-3). Compound **D**, with the highest ΔG^*, is recently reported to have a half-life over 18 years.[174]

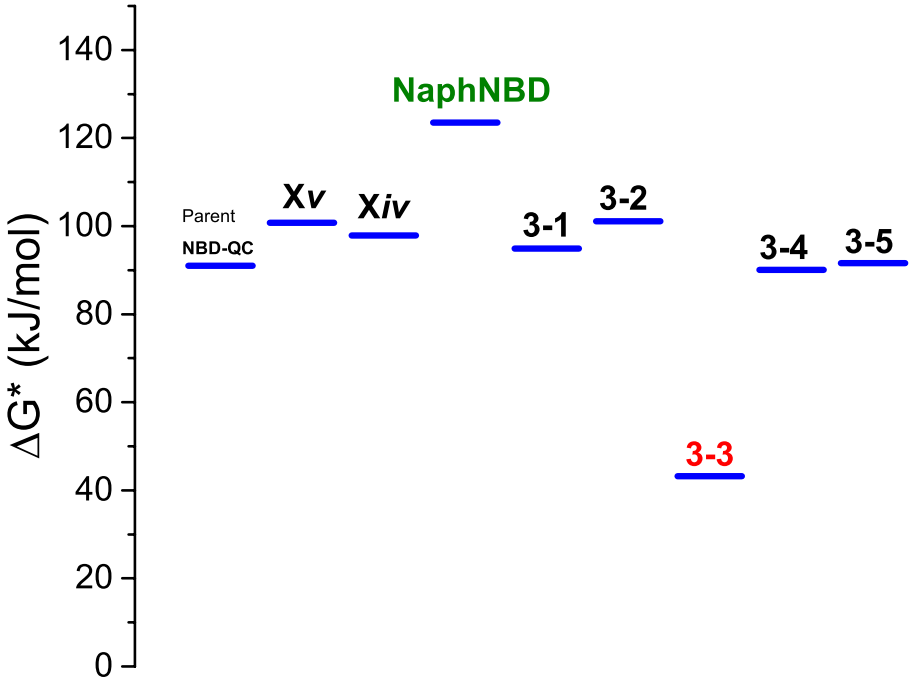

*Figure 3-3: ΔG^* values for various dimer NBD derivatives, as well as a monomer NBD derivative **D** with very long half-life (over 18 years) for comparison from ref. 167. Compound 3-3 with the shortest half-life (43.8 s) has the lowest ΔG^*.*

In summary, compared to the parent NBD/QC system, in Paper III, we succeeded in synthesizing significantly redshifted (by over 200 nm) NBD dimers based on thiophene and carbazole bridges with good quantum yields and very high molar absorptivity, which are

responsible for efficient light absorption. However, the compounds featured short half-lives. In particular the carbazole-bridged dimers **3-4** and **3-5**, and thiophene bridge dimer **3-3**, without ethynyl linker, were found to have very short half-lives, in the order of minutes and seconds, respectively (Scheme 3-5, Table 3-1). Similar to previous reports,[153,177] for the majority of D-A based dimers, a longer conjugation result in a significant redshift in absorption spectra, at the expense of shorter half-lives. On the contrary, for the cross-conjugated dimers, the half-lives are slightly longer, but their absorption is not as redshifted. Unfortunately, we did not measure the energy storage densities of the dimers, using differential scanning calorimeter (DSC), due to their short half-lives. This demonstrates how challenging it is to find a molecule that maintains a balance to fulfil all the parameters outlined in Section 3-2.

Of course, the ideal molecule has been stated to have preferably the following features: An absorption onset ≥ 590 nm, a high molar absorptivity and a quantum yield close to unity for efficient light absorption and photoisomerization, respectively. Furthermore, long half-lives in the range of a few days, if not years, for day-to-day solar energy storage applications, as low molecular weight as possible for higher energy density, storage and of course, high fatigue resistance i.e. the ability to withstand many switching cycles with no degradation. Despite the challenges, the DA approach offered an opportunity for redshifting the onset of absorption in NBD above 450 nm, while maintaining the quantum yield of photoisomerization above 80%. Recently, the issue of short half-lives was addressed by using ortho substituents on the aromatic unit in close proximity to the NBD unit, without compromising the other properties.[174] Moreover, the dimer approach also led to a high energy storage density, well over 500 kJ/kg. With such advancement in the synthesis to obtain multigram scale products, the next challenge will be finding the right catalyst for a controlled back-isomerization reaction. In fact, Wang et al., from our research group, have reported an efficient catalyst based on cobalt phthalocyanine in a flow reactor with a record setting temperature gradient up to 63.4 °C.[175] Thus, in the coming few years, it looks like that with the right type of molecule, an efficient catalytic system and a prudently optimized device, the MOST system can perhaps one day be applied in commercial settings as an alternative solar energy storage technology.

Chapter 4 NBD-QC for molecular electronics applications

In Chapter 3, we have introduced NBD-QC photochromic molecules and explored their utility for solar energy storage. In this chapter, emphasis will be given to exploring the use of NBD-QC for molecular electronics applications and emission tuning capabilities. Paper I and Paper II are the outcome of our study in the area of molecular conductance and emission properties in NBD-QC. Before we delve into Papers I and II, a brief introduction concerning past efforts to utilize the NBD-QC system is in order.

4.1. Charge transport in NBD-QC

The NBD-QC pair undergoes photoisomerization from the unsaturated NBD form to the saturated QC-isomer, hence it is bistable, an important criteria for any molecule to serve as a switch. In addition to bistability there are additional criteria that photochromic molecules are required to meet, in order to be used as molecular switches.[85,186] These are:

i. Fast response times (high molar absorptivity) to be able to perform many switching cycles
ii. High photoisomerization quantum yields, which allows efficient switching processes in short time.
iii. Fatigue resistance against thermal degradation or photodegradation
iv. Both forms needs to be photochemically distinct from each other, making them easier to detect.
v. Non-destructive write/read-out procedure to perform logic operations.
vi. Thermal stability for certain applications.

The last parameter is important, depending on what type application is sought after. If it is for long term data storage, it is a critical parameter. However, for short term data storage such as random access memory (RAM), this criteria may not be as significant.

The first attempt to use the NBD-QC photochromic system as a switch was reported by Bonfantini and Officer.[187] With the aim of controlling energy transport in a conjugated polyene system, they synthesized polyene chain molecules with an NBD-QC unit incorporated in the chain and the chain terminated by an anthracene and a porphyrin unit. Upon selective excitation of the anthracene unit, they anticipated enhanced porphyrin emission. The NBD-QC unit is then expected to serve as a switch to control the energy transport. Regrettably, the predicted emission switching property was not disclosed afterwards. Two years later, Lainé et al. utilized a similar strategy to synthesize a binuclear ruthenium-based 2,3-dicyanonorbornadiene complex to study

intramolecular electron transfer using UV-vis spectroscopy.[188] In the NBD form, upon oxidation, the UV-vis spectra showed a progressively disappearing metal-to-ligand charge transfer band due to the formation of mixed valence Ru(II)-Ru(III) species but not in the QC form. This spectroscopic observation was attributed to the NBD form being turned off to the QC form upon photoisomerization at 532 nm, blocking electronic interactions between the two appended metal centres. Despite the promising results, the NBD-QC system was deemed "not suitable" for further development due to alleged lack of back reaction,[189] and lack of photoisomerization altogether in certain NBD derivatives, e.g., compound **4-1** shown in Figure 4-1.[190] More recently, however, NBD-QC systems have received a renewed interest for molecular applications. The small structural change during photoisomerization in NBD-QC made it an ideal candidate to tether between metal electrodes for switching studies as well as solid state devices. As a result, Löfås et al. conducted a DFT study to investigate the potential of compound **4-2** as a molecular switch between metal (Au) electrodes, calculating a switching ratio[†] of around 50.[191]

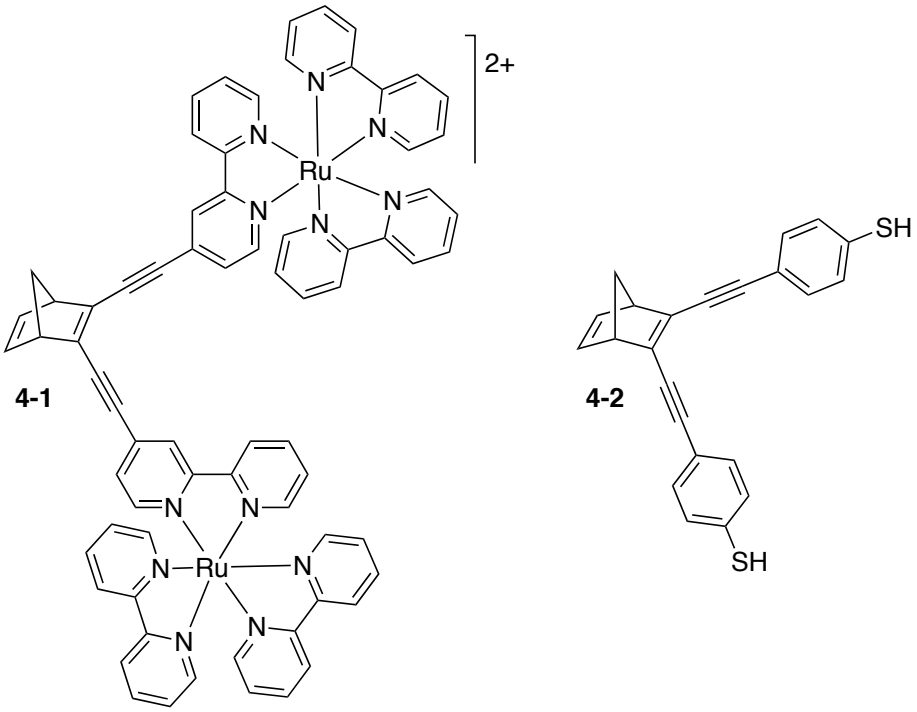

*Scheme 4-1: Examples of previously studied NBD-QC systems for electron transfer studies. Compound **4-1** was used by Fraysse et al.[190] to study metal-to-ligand charge transfer whereas compound **4-2** was proposed by Löfås et al.[191] as a potential photoswitch molecule between metal electrodes using a DFT calculation.*

Due to its potential for usage in solid state devices, we designed a strategy to utilize a NBD-QC photoswitch for molecular switching applications, by addressing some of the shortcomings

[†] Switching ratio is defined as the conductance ratio between the higher conducting and lower conducting forms of a molecule under study.

reported previously. Our design strategy has the following three components: a photoactive unit, a spacer unit and an anchoring unit. The central part is the NBD-QC photoswitch, which is a photoactive unit. In addition, we have introduced a spacer unit that provides a buffer zone between the photoactive unit and the metal electrodes so that electron transport occurs without quenching, upon photoisomerization. A thiol group, protected as a thioacetate, was used as anchoring group in order to make it possible to tie the molecule between two metal (gold) electrodes. The target molecules can be synthesized starting from 2,3-dibromonorbornadiene using C-C cross coupling reactions.

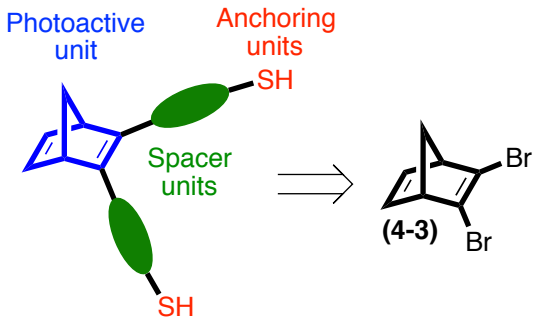

Scheme 4-2: Design strategy of a NBD-QC based photoswitch for charge transport studies.

4.2. The synthesis of 2,3-dibromonorbornadiene

Symmetrical di-substitution at the C2 and C3 positions has been achieved in the past using Sonogashira cross-coupling reactions, starting from the 2,3-dichloronorbornadienes,[192] 2,3-diiodonorbornadienes[193] or from the corresponding triflate analogues.[194] However, 2,3-dibromonorbornadiene (**4-3**) has proven to be more robust and reactive under Sonogashira conditions. The synthesis of compound **4-3** through the bromination of the cheap and commercially available NBD, has been reported by Tranmer et al. In our case, the synthesis of compound **4-3** was performed by following an improved procedure described by Lennartson et al. The synthesis was started by treating norbornadiene with n-butyl lithium and potassium *tert*-butoxide in a THF solution (Schlosser conditions) at -78 °C. Under these conditions, the vinylic proton of NBD is deprotonated, affording a norbornadienyl anion, which is subsequently trapped by a half equivalent of tosyl bromide to yield the intermediate 2-bromonorbornadiene. As a result of the mono bromo-substitution at the C2 position, the proton on the adjacent C3 carbon becomes acidic enough to be deprotonated in situ by the excess norbornadienyl anion. Eventually, another half equivalent of tosyl bromide is added to yield compound **4-3** in a moderate yield (37%).

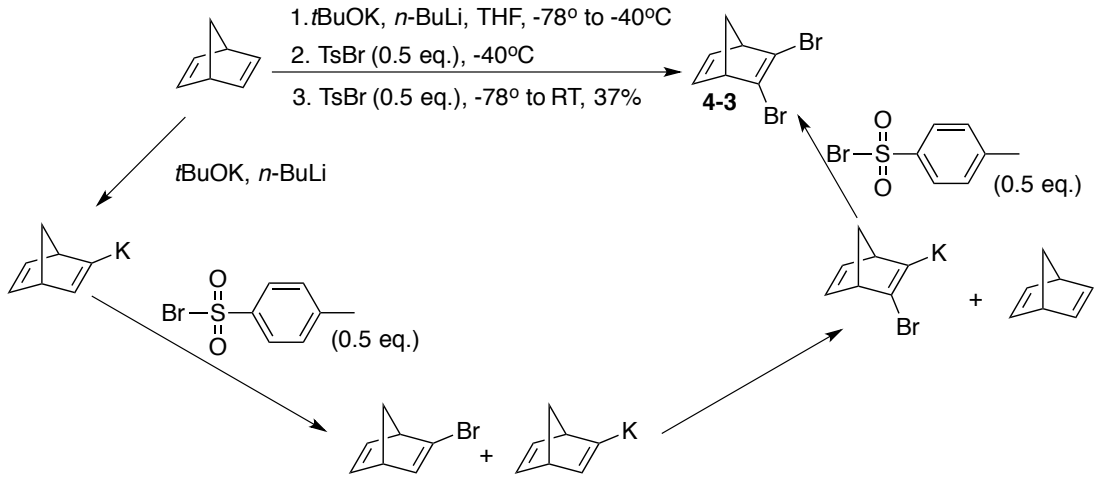

*Scheme 4-3: The synthetic route to 2,3-dibromonorbornadiene (**4-3**) using tosyl bromide as a brominating agent.*

4.3. 2,3-Disubstituted NBD derivatives via the Sonogashira reaction

With 2,3-dibromonorbornadiene at hand, further elaboration to form symmetrically substituted products is imminent, for instance, via a Sonogashira reaction in the presence of terminal alkynes (the mechanism for the Sonogashira reaction is described in Chapter 7, Section 7.1). This reaction strategy leads to an NBD with an oligophenylene ethynylene substituents, such groups being known for their high molecular conductance.[195] A typical Sonogashira C-C coupling reaction involves the reaction between an aryl or vinyl halide with a terminal alkyne in the presence of a palladium catalyst (e.g. 5 mol% $Pd(PPh_3)Cl_2$), and CuI (10 mol%) in basic media. Often, amine bases such as diisopropylamine, triethylamine or *N*,*N*-diisopropylethylamine (Hünigs base) are used. Sometimes, co-solvents such as toluene or tetrahydrofuran are added along with the base. However, co-solvents can be avoided if the substrates are sufficiently soluble in the base of choice.[196,197]

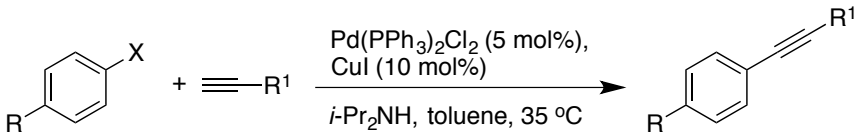

Scheme 4-4: Typical Sonogashira reaction conditions used in this thesis.

In terms of reactivity, vinyl halides are more reactive than aryl halides in Sonogashira reactions.[196] Since, 2,3-dibromonorbornadiene is a vinyl halide, it is a suitable substrate for a Sonogashira reaction. Terminal alkynes with a sulphur moiety or substrates that can be elaborated to include a thiol functionality were employed in our case. Sulphur atoms as anchoring groups were chosen for their ability to form a robust molecule-electrode binding,[50] as well as a uniform self-assembled monolayer (SAM) with gold.[198] Thus, aiming for a thiophene anchoring group, 2,3-NBD was reacted with 2- or 3-ethynylthiophene under the typical

Sonogashira reaction conditions given in Scheme 4-5, affording symmetrically substituted compounds 4-4 and 4-5 in good yields (~ 60%). The difference in the connectivity of the two isomers will help us understand the role of structural isomers on the spectrochemical data and conductance measurements.

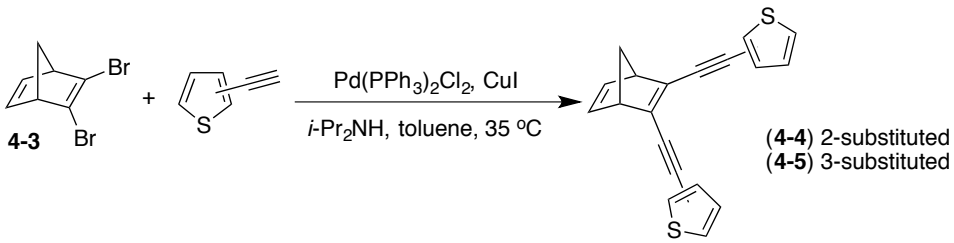

Scheme 4-5: The synthesis of 2- or 3-thiophene terminated NBD via the Sonogashira reaction.

We also targeted NBD derivatives with a longer OPE arm, decorated with a thioacetate or thiol anchoring groups. The longer OPEs arms that we used in the design are present in order to minimize the risk of quenching of the chromophore excited states by the gold electrodes.[97] The synthesis was started by preparing compounds **4-6** and **4-7** from the corresponding commercially available *p*- or *m*-bromoiodobenzene with triisopropylsilyl acetylene (TIPS acetylene) and trimethylsilyl acetylene (TMS acetylene) in one pot, via a double Sonogashira reaction (Scheme 4-6). Deprotection of the TMS group furnished the terminal alkynes **4-8** or **4-9** in excellent yield (> 90%). The terminal alkynes **4-8** or **4-9** were subsequently reacted with 2,3-dibromonorbornadiene (**4-3**) to yield compounds **4-10** or **4-11**. In the penultimate reaction, the TIPS groups were deprotected using tetrabutylammonium fluoride (TBAF) to furnish air-sensitive terminal alkyne intermediates. Eventually, the terminal alkyne intermediates were reacted with 4-iodophenylthioacetate, which was prepared following a literature procedure,[199] affording the target products in yields ranging from 20 to 40 % for the respective para (**4-12**) and meta (**4-13**) products.

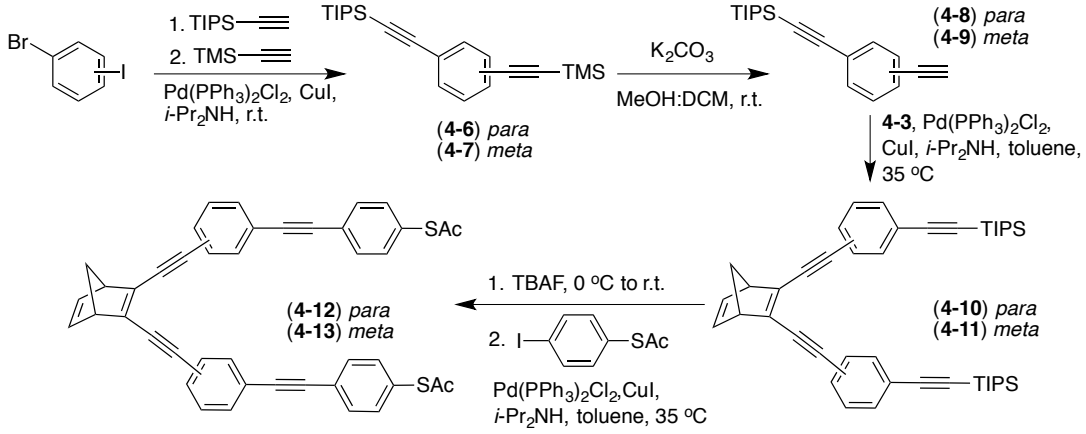

*Scheme 4-6: The synthesis of NBD derivatives **4-12** and **4-13** with oligophenylene ethynylene (OPE) arms.*

4.3.1. Spectroscopic and photoisomerization study of the NBD derivatives (Paper II)

The UV-vis absorption spectra of the final target compounds (**4-4**, **4-5**, **4-12** and **4-13**) were measured in toluene and presented in Figure 4-1A. The recorded absorption bands are attributed to the $\pi \rightarrow \pi^*$ transitions. Compounds **4-4** and **4-12**, that have the longest conjugation showed redshifted onsets of absorption at 440 nm and 461 nm, in comparison to the corresponding structural isomers **4-5** (λ_{onset} = 410 nm) and **4-13** (λ_{onset} = 420 nm), respectively. The observed differences in the absorption spectra between compound **4-4** and compound **4-5** are attributed to the extended conjugation resulting from 2-substitution compared to 3-substitution on the thiophene.

For para-substituted compound **4-12**, the conjugation is extended throughout the molecule, but this is not the case for the meta compound **4-13**. Due to the extended conjugation and the presence of an alkyne spacer unit,[154] compound **4-12** not only has a redshifted absorption spectra, but also a high molar absorptivity compared to the meta isomer. For comparison, the molar absorptivity at the first absorption maxima for compound **4-12** (ε = 43000 $M^{-1}cm^{-1}$) is almost three times higher than for the meta compound **4-13** (15000 $M^{-1}cm^{-1}$). High molar absorptivity corresponds to how strong a light is absorbed, resulting in higher probability for an electronic transition. From the onsets of absorption, the optical HOMO-LUMO band gaps were estimated to be 2.82 eV, 3.02 eV, 2.69 eV and 2.95 eV for each compounds, **4-4**, **4-5**, **4-12** and **4-13**, respectively.

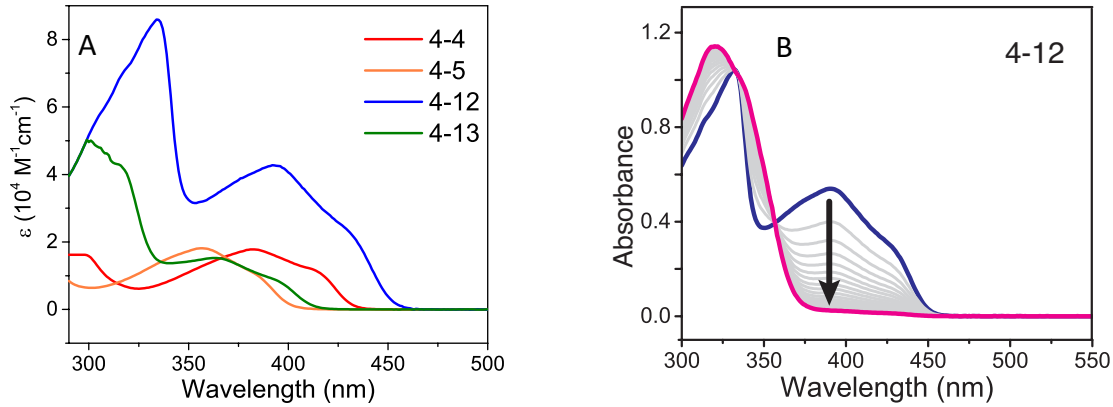

*Figure 4-1: A, Steady state UV-Vis absorption spectra of compounds **4-4**, **4-5**, **4-12** and **4-13** in toluene. B, Photoisomerization of compound **4-12** in toluene using a 405 nm LED lamp.*

In Chapter 3, light-induced isomerization of NBD to the QC form is explained. This process can occur either under direct[159] or sensitized excitation.[142] However, due to unwanted side reactions with sensitized excitation that leads to sample deterioration,[161] direct excitation is preferred. Thus, the corresponding parent NBD forms in $CDCl_3$ and toluene were irradiated under UV light to study the photoisomerization process. The first direct evidence comes from an NMR

study (*vide infra* Figure 4-2). The NBD form has characteristic peaks for the vinylic protons around 6.9 ppm, for the bridgehead protons around 3.7 ppm, and for the bridging protons between 2.3 and 2.1 ppm, highlighted by the yellow boxes. Upon photoisomerization, the characteristic NBD protons gradually disappear and new peaks between 2.1-2.5 ppm appear. Compared to the unsubstituted cyclopropane (0.2 ppm) with aromatic type ring current that shields the proton coupling,[200] the QC proton values are downshifted. This shift is explained by the formation of two cyclopropyl units in the adjacent planes, counteracting the magnetic anisotropy and hence deshielding the cyclopropyl protons.[159]

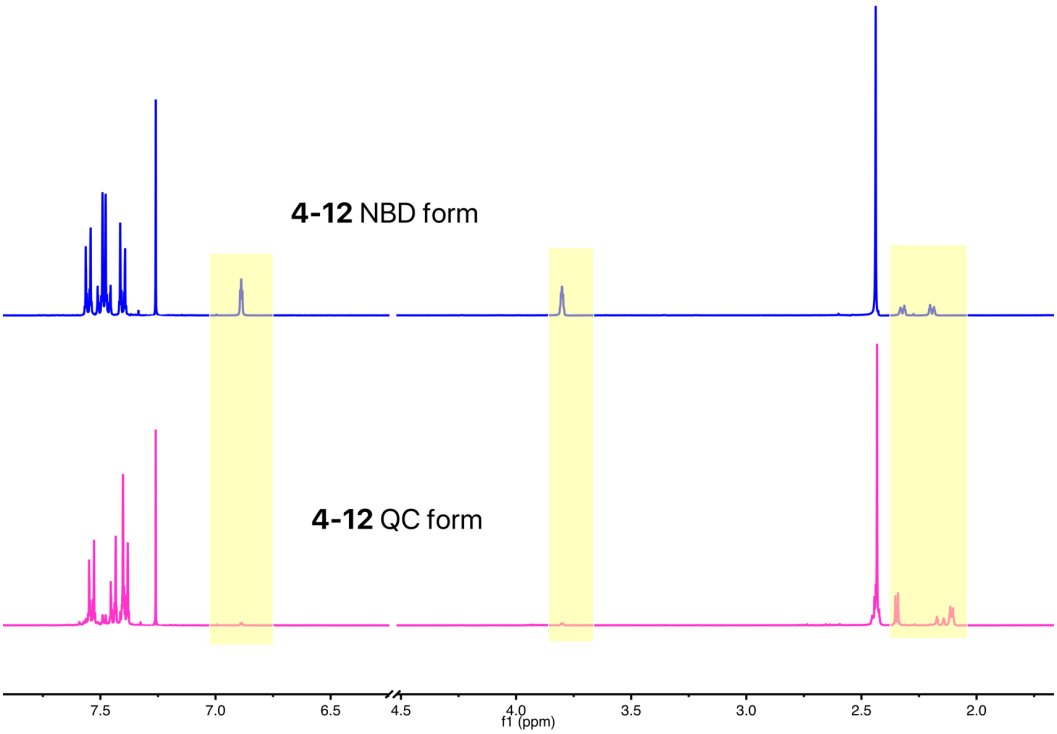

*Figure 4-2: ^{1}H-NMR spectra of compound **4-12** NBD form, in $CDCl_3$ (top). Upon photoisomerization using a 365 nm UV light for 5 minutes, chemical shift for the protons of the central NBD unit changed to that of QC (bottom), highlighted by the yellow boxes.*

Additional evidence for the photoisomerization from NBD to QC comes from a UV-vis study. Upon photoisomerization, the onsets of absorption for QC exhibited a significant blueshift compared to the NBD form (*vide infra* Figure 4-3), paralleling the expected structural change from the unsaturated NBD to a saturated QC and hence breaking the conjugation. The photoisomerization process was also closely followed upon irradiation with a 405 nm and 365 nm LED lamps for compounds **4-4** and **4-12**, as well as compounds **4-5** and **4-13**, respectively. The conversion from NBD to QC was quantitatively complete in less than a minute, with no observable photostationary state. Moreover, the spectra has isosbestic points, indicating stoichiometric conversion with no side reactions. (Figure 4-1B) The quantum yield for the photoisomerization processes were determined using the ferrioxalate actinometer.[185] The

detailed procedure is described in Chapter 7, Section 7.3. The summarized results are shown in Table 4-1. The trend for the photoisomerization quantum yield is as follows: lower values are observed for the compounds with extended conjugation compared to their less conjugated counterparts. The highest photoisomerization quantum yield (Φ = 77%) is recorded for compound **4-13** with the meta connectivity, while the lowest (Φ = 15%) was for compound **4-12**, with the para connectivity.

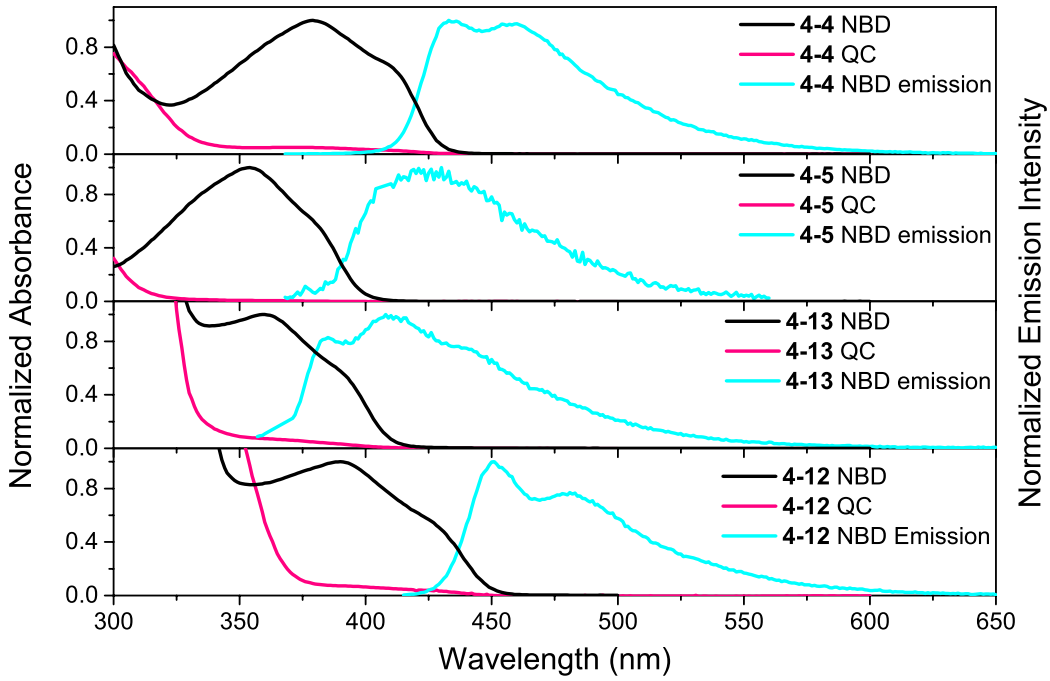

*Figure 4-3: Normalized absorption spectra for the NBD and QC forms of **4-4**, **4-5**, **4-12** and , as well as the corresponding emission spectra in toluene (λ_{ex} = 364, 362, 330 and 407 nm). Adapted from Paper II, Published by the PCCP Owner Societies.*

4.3.2 Fluorescence in the NBD derivatives (Paper II)

Interestingly, the compound with the lowest photoisomerization quantum yield was found to be fluorescent. Hence, we wanted to understand if the low quantum yield for compound **4-12** could be a result of its competing fluorescence. In collaboration with Albinsson and co-workers, we studied the emissive properties of all the compounds and, indeed, they were found to be emissive. The time-corelated single photon counting (TCSPC) and fluorescence measurements were carried out by Edhborg. The fluorescence quantum yield for each compound was determined by using Coumarin 102 as a reference (Φ_F = 80%). As anticipated, compound **4-12**, in particular, was found to be highly emissive (Φ_F = 49%), compared to the rest of the compounds, which had fluorescence quantum yields of less than 5%. In fact, emission in NBD compounds has been reported in the past. The first example was presented by Maffi et al.[201] Babudri et al. have also disclosed emission in NBD-based polymers with a fluorescence quantum yield of 24%.[202]

To account for the high emission measured for compound **4-12**, the excited state lifetimes of all the four compounds were measured using time-correlated single photon counting (TCSPC) and compared to each other. The measured lifetimes, τ_F, are summarized in Table 4-1. It is known that compounds with long, linearly conjugated chains are found to show emission.[203] Analogously, compound **4-12** with the longest linear conjugation of the four compounds was found to have the highest emission as well as a significantly long-lived excited state (τ_F = 1.28 ns). Furthermore, under direct excitation, substituted NBDs are reported to undergo photoisomerization to the QC-form on the singlet surface.[204] For such types of systems, photoisomerization quantum yields and fluorescence quantum yields are reported to be complementary,[205] i.e. high photoisomerization quantum yields leads to lower fluorescence quantum yields and *vice versa*. Indeed, this was observed for each pair of the compounds studied herein. The longer conjugated compounds **4-4** and **4-12** have higher fluorescence compared to their structural isomers, compounds **4-5** and **4-13**, while their photoisomerization quantum yields are lower.

Upon light induced photoisomerization of the NBD form to the QC form, the fluorescence emission was also found to disappear completely for all compounds (see the example shown for compound **4-12** in Figure 4-4). Recently, emission from a polymer containing NBD units in the backbone was reported to have higher emission in the NBD form and lower emission in the QC form, similar to our observation. In our case, since the whole molecule seems to be the reason for the emission, we explained our observation in the following way. Upon photoisomerization, the long conjugation pathway, which is responsible for emission, become interrupted by the newly formed saturated QC unit. Hence the emission becomes essentially switched "off" due to photoisomerization. This result is shown in Figure 4-4A.

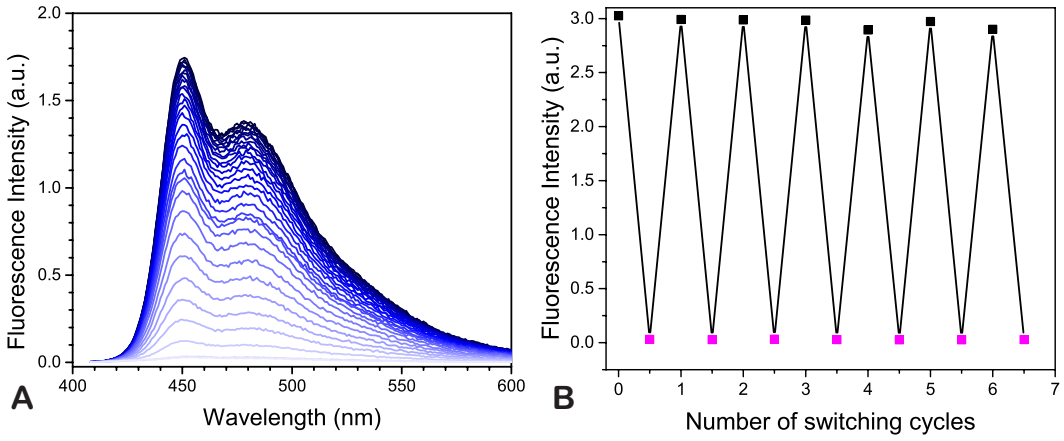

*Figure 4-4: A, Emission turn-off and turn-on for compound **4-12** at 50 °C and B, its emission switching cyclability at 6 °C, in toluene. The fluorescence switching ratio between the NBD form and QC form is about 100. Reprinted from Paper II, Published by the PCCP Owner Societies.*

The QC-form can be back converted to the NBD form using various methods.[71,106,160] One of the most common method is via heat-induced back isomerization.[175] The kinetics for the thermal back conversion was studied at different temperatures for all compounds and found to follow first order kinetics (for experimental details, see Chapter 7, Section 7.3). The rate constants for the thermal back reactions at each different temperatures for all the four NBD derivatives were extracted, using single exponential fitting. The extracted rate constants were then plotted against temperature based on the Arrhenius equation, yielding a straight line. The half-lives were determined from the rate constants at room temperature, and the activation energies were determined from the slopes in the Arrhenius plots. The results are summarized in Table 4-1. The half-life and the activation energy are found to follow similar trends. The longer conjugated compounds **4-4** and **4-12** have lower activation barriers as well as lower half-lives than their less-conjugated counterparts.

During the thermal back conversion of QC to the NBD form, the emission has also increased progressively until full recovery. In particular, we showed the result for compound **4-12** in Figure 4-4B. The photo-thermal emission switching cycle was repeated for several times and the emission was found to be turned "off" and "on" accordingly. A more extensive cyclability experiment was conducted for compound **4-12** at higher temperature, 50 °C. The photoisomerization was carried out using a 405 nm LED UV light for 2 minutes followed by thermal relaxation for 28 minutes in air and under nitrogen, respectively.

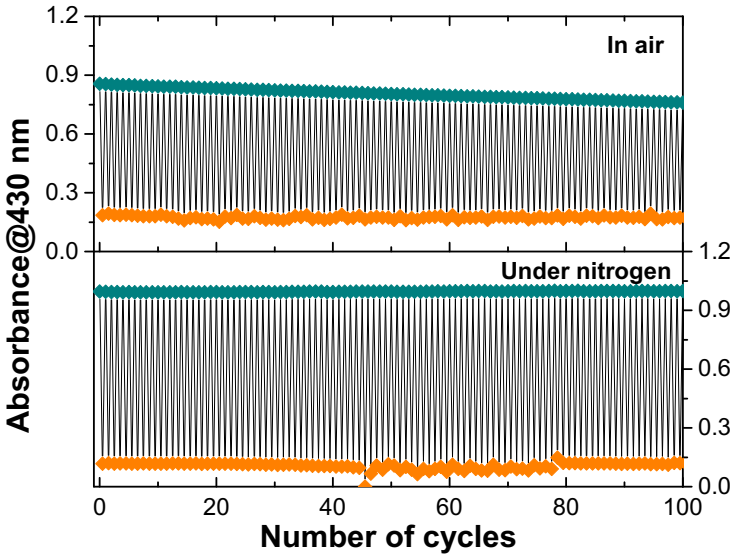

*Figure 4-5: Cyclability test in air (top) and under nitrogen (bottom) for compound **4-12** at 50 °C, in toluene. Under nitrogen almost no degradation was observed compared to the sample run in air.*

Under nitrogen no apparent degradation was observed demonstrating the robustness of compound **4-12**. However, in air, about 16% loss for over 100 switching cycles i.e. 99.84% yield per cycle was estimated using Equation 4-2.

$$y = (1 - x)^n \qquad 4\text{-}1$$

y is the non-degraded molecule, with a degree of degradation, x, after n number of cycles. For large n, and small x, the above equation can be approximated to be:

$$y = 1 - nx \qquad 4\text{-}2$$

In addition to the thermal back reaction process, we also investigated light induced QC to NBD back isomerization. The light-induced back-conversion of QC is expected to be facile since it is allowed by the Woodward-Hoffmann rules.[143] In fact, in the past, that has been shown that to be the case.[71] This process can make the NBD-QC system an all-light controlled system. Hence, a QC solution of compound **4-12** was irradiated at 340 nm (close to the **4-12** QC isomer absorption maximum), yielding the parent compound readily in less than a minute (Figure 4-6). Even though this process has been described in the past,[71] we have in Paper II, demonstrated the utility of low energy near-UV light to trigger the back isomerization from QC to NBD. This feature makes our system attractive for biological applications, where low energy light is required. The cyclability was also tested by performing multiple cycles, demonstrating the robustness and versatility, despite the lower fatigue resistance compared to photo-thermoswitching. Very recently, this feature has been utilized to demonstrate a molecular keypad lock for the first time using an NBD-QC system.[206]

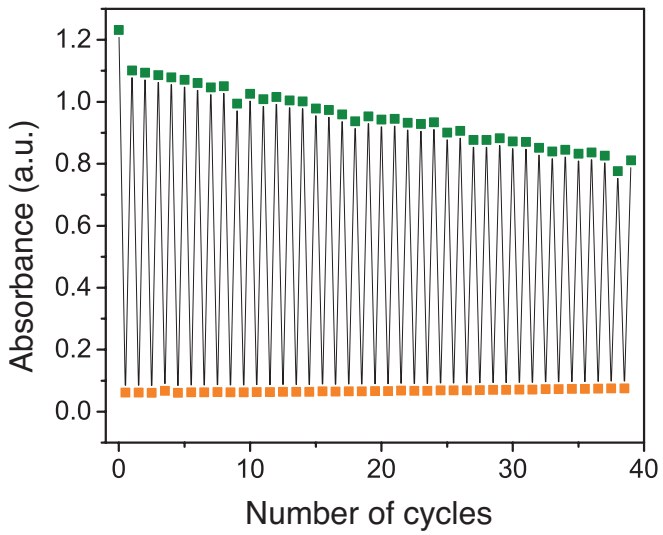

*Figure 4-6: All optical switching of compound **4-12**, in toluene. The green squares are the NBD form, which upon photoisomerization using a 405 nm light converts to QC form (orange squares) in about a minute. Similarly, the QC form isomerizes back to the NBD form with a 340 nm light in less than a minute. Adapted from Paper II, Published by the PCCP Owner Societies.*

*Table 4-1: Summary of photophysical properties for compounds **4-4**, **4-5**, **4-12** and **4-13** in toluene.*

Compound	λ_{max} (nm) [ε ($M^{-1}cm^{-1}$)]	λ_{onset} (nm)	$\Phi_{NBD \rightarrow QC}$ (%)	E_a (kJ/mol)	$t_{1/2,\ 25\ ^oC}$ (min)	Φ_F (%)	τ_F (ns)
4-4	381[18000]	443	30	93.8	49	4	0.21
4-5	357[18000]	415	54	103.7	201	0. 2	0.02
4-12	391[43000]	461	15	100.7	78.6	49	1.28
4-13	364[15000]	424	77	135.6	130	1	0.02

4.3.3. Charge transport in the NBD derivatives (Paper I)

Having effectively demonstrated that the physical properties as well as structural forms of NBD-QC pair can be switched by using light, we wanted to gain insights into how charge transport properties behave in this system upon photoisomerization. For this purpose, an STM-break junction experiment, which is introduced in Chapter 2, Section 2.4., was conducted, in collaboration with the Hihath research group at UC Davis. The STM-BJ experiments were conducted by Li. Due to its versatility, the STM-BJ technique provides a unique opportunity to study charge transport through molecules in solution or in SAMs.[51]

In STM-BJ, as described in Chapter 2, the STM tip is brought into close contact to the bottom electrode and the current is measured continuously as the tip is retracted at a certain applied bias voltage (*vide infra* Figure 4-7A). Depending on the number of molecules trapped between the top and bottom electrode, steps on the decaying conductance are observed until the junction breaks. One of the advantages with STM-BJ is that thousands of conductance vs distance curves can be collected in a short time. The data can then be analysed statistically to determine the most probable conductance value. Based on the procedure described above, the conductance of the NBD form of compound **4-12** was measured from a mesitylene solution (~1μM) at 50 mV bias voltage between the electrodes. From statistical analysis, a conductance value of 1.2×10^{-4} G_o was measured for the NBD form. A lower conductance of 1.9×10^{-5} G_o was determined for the QC form (Figure 4-7B). The measurement was carried out, first by irradiating the NBD solution using a 405 nm LED to induce photoisomerization, followed by current measurements under constant irradiation, to hinder thermal relaxation during the measurement. As inferred from solution switching measurements, higher conductance values were measured for the linearly conjugated NBD form of compound **4-12** relative to its QC form. However, the conductance switching ON/OFF ratio between the two forms were found to be only 6.6, which is low compared to predicted values by Löfås et al.[191]

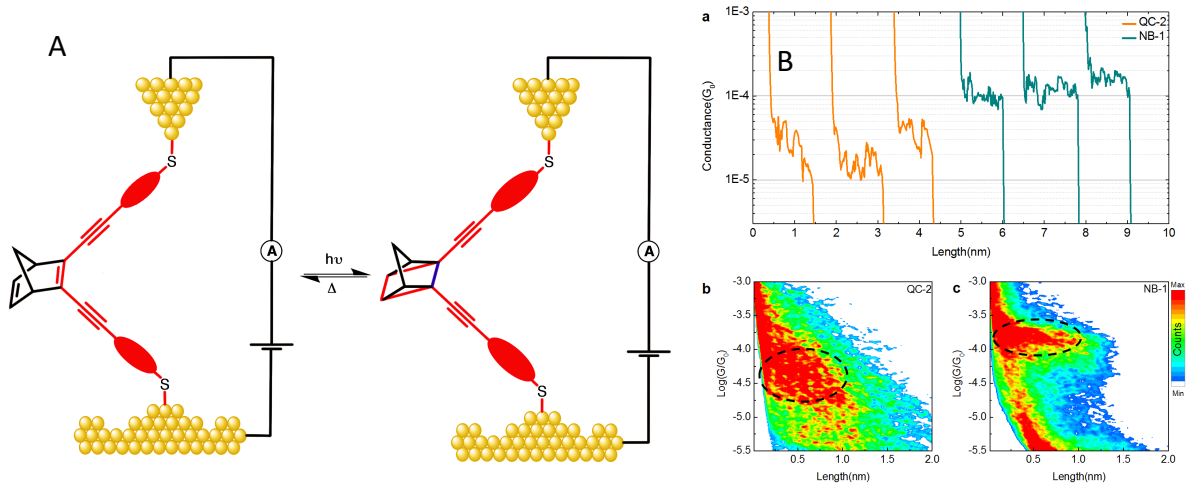

*Figure 4-7: A, Illustration of the STM-BJ measurement using compound 4-12. B, many conductance traces (top) and histograms (bottom) obtained for the NBD and QC forms of compound **4-12**. Adapted from Paper I, published under a Creative Common attribution (CC-BY) © American Chemical Society.*

The conductance measurements for the rest of the compounds are tabulated in Table 4-2. From the conductance measurements, it was clear to observe that the longer molecules, compound **4-12** and **4-13** have lower molecular conductance values. In comparison to the shorter thiophene terminated compounds compound **4-4** and **4-5**, their conductance value is at least one order of magnitude lower. This is in line with previous reports showing higher conductance for shorter molecules.[207] The slight difference in conductance, for the two thiophene terminated compounds, **4-4** and **4-5** was anticipated. Since compound **4-4** has a longer conjugation pathway than compound **4-5**, it has a slightly lower conductance. Moreover, the binding geometry and availability of the thiophene anchoring groups in the two isomers is different. For compound **4-5**, besides the conjugation being shorter, the sulphur is more available than for the compound **4-4** resulting in a better binding geometry between the electrodes, and hence a better conductance.[208] Similarly, the lower conductance for compound **4-13** can be explained in terms of the meta connectivity on the aromatic ring, which is known to reduce conductance values.[24]

Table 4-2: Conductance values of NBD derivatives

Compounds	Molecular conductance (G_o)		Switching ratio	
	NBD form	QC form	Experimental	Theoretical
4-4	2.3×10^{-3}	-	-	-
4-5	2.6×10^{-3}	-	-	-
4-12	1.2×10^{-4}	1.9×10^{-5}	6.6	12
4-13	6.8×10^{-5}	2.1×10^{-5}	3.2	-

The measured conductance values for compound **4-12** were further confirmed by measuring conductance switching in situ, specifically when the QC form is back converted the NBD form. However, conductance measurement during in situ photoisomerization from NBD form to QC form resulted in no apparent change in molecular conductance between the two forms. This is attributed to the rapid quenching of the excited state to the ground NBD form before it gets the chance to isomerize, due to the strong electronic coupling between the molecule and the gold electrode. This phenomena has been reported by other researchers as well.[97,109] So, it looks like having long para-OPE arms as buffers, as in compound **4-12**, does not seem to help circumvent the issues with quenching. However, we are testing further bidirectional switching using compound **4-13**, with the meta-OPE arms. Otherwise, a saturated spacer unit could be placed between the anchoring group and the aromatic unit to be able in order to alleviate issues with quenching.[23]

One of the advantages of the NBD-QC pair is that upon photoisomerization only little structural change can occur due to the rigidity of the structure. This makes it an ideal candidate for placement between two static metal electrodes. However, the structural rigidity comes at a cost, a modest switching ratio of 6.6. For molecular electronics applications, however, a large switching ratio seems to be preferred.[23,191]

To better understand why the switching ratio is low, we collaborated with the Solomon research group at the University of Copenhagen. The DFT calculation and local current analysis for compound **4-12** were done by Pirrotta. DFT calculation for the transmission of the NBD form and the QC form was found to be through the HOMO energy level as obtained for other thiolated systems.[191] The calculated switching ratio of the NBD form to the QC form was found to be 12, almost twice the experimental measurement. To closely examine the cause for the observed switching ratios, the transport pathways were probed using local current analysis. For the NBD form of compound **4-12**, the local current analysis for the NBD form indicated current going through the double bond at C2-C3, as anticipated. For the QC form, however, the majority of the current flow through the longer pathway on the cyclobutene unit following C2-C1-C6-C5-C4-C3 compared to the shorter pathway C2-C3. The smaller current flow through the shorter pathway can be understood in terms of sigma quantum interference, which has been observed in the past in σ-*cis* defects.[209] However, the longer pathway is also a σ-*cis* defect and could not explain fully our observations.

Therefore more systematic local current analysis in a series of compounds containing varying cyclopropane unit was conducted. The results are presented in Figure 4-8. From the analysis, the location of the straining cyclopropane unit on the cyclobutene unit is found to play an important

role in guiding the current flow. For the cyclobutane derivative the current flow was found in either direction, via shorter or longer pathways, with equal probabilities. However, for the strained cyclobutane with a cyclopropane unit on both sides, the current flow prefers to go the longer route similar to QC. This recalls the great scientific debate on the π-like structure of the cyclopropyl unit.[210,211] Now, after rigorous study the consensus among scientists is that cyclopropane does indeed have indeed a π-character.[212] This means, the OPE arm in compound **4-12** can maintain some sort of conjugation in the QC form, by following the longer pathway. This may explain why the switching ratio is small.

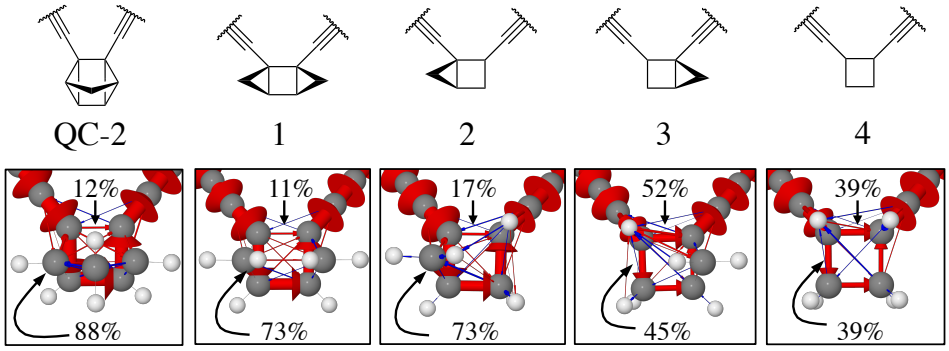

Figure 4-8: Local currents analyses for a series of strained cyclic alkanes resembling QC, starting from cyclobutane. Reprinted from Paper I, published under a Creative Common attribution (CC-BY) © American Chemical Society.

In summary, in Papers I and II, we have synthesized symmetrically substituted NBD derivatives with sulphur anchoring groups for tethering between metal electrodes. A total of four compounds, two shorter thiophene terminated compounds **4-4** and **4-5,** and two longer compounds **4-12** and **4-13** with thioacetate as anchoring groups, were prepared and characterized using UV-vis spectroscopy. The thiophene-terminated NBD compounds are different in the way the NBDs are connected to the thiophene unit, i.e., 2- or 3-positions. Similarly, the compounds with the thiol anchoring groups, **4-12** and **4-13,** have a longer OPE arm arranged in a meta and para fashion, on the aromatic moiety. Both NMR and UV vis study showed the photo conversion from the NBD form to the QC form and vice versa. The compounds with longer conjugation **4-4** and **4-12** were found to have redshifted absorption spectra in comparison to their counterparts **4-5** and **4-13**, respectively, whereas the photoisomerization quantum yields as well as half-lives, for these derivatives, were relatively lower.

Moreover, all the NBD derivatives were found to be emissive, particularly, compound **4-12** with the longest conjugation was found to be highly emissive (Φ_F = 49%). The emission can be switched off and switched on upon photoisomerization, which can serve as an output for application in optical memory devices.[33,75] To test the fatigue resistance of the NBD derivatives, we performed cyclability studies using light and heat in that sequence, and the NBD-QC

photochromic pair demonstrated excellent stability over one hundred switching cycles, particularly under nitrogen. Furthermore, the back conversion reaction was demonstrated to be stimulated using light, making the NBD-QC system an all photonic controlled system, which opens a host of applications e.g. molecular keypad locks.[206]

Molecular conductance measurement were conducted using the STM-BJ method and generally, higher conductance for the NBD form and lower conductance for the QC form were determined. Although the switching ratio is not very high, the little structural change that occurs upon photoisomerization makes the NBD-QC system an ideal candidate for tethering between static metal electrodes.

Chapter 5 Photocleavable protection towards parallel fabrication

This chapter presents our vision for using photocleavable protecting groups (PPG) to protect terminal alkynes and carry out selective chemical transformation based on the idea presented in Chapter 1, Figure 1-4. Thus, 2-nitrobenzyl based PPG from our original work reported in Paper IV, for use in such applications, is summarized. Furthermore, the effect of substituents on the benzylic position, next to the 2-nitrobenzyl group on the rate of photodeprotection and a tandem photodeprotection-decarboxylation-click reaction, to make a molecular wire, is discussed.

5.1. Brief introduction to Photocleavable Protecting Groups (PPG)

Protecting groups are groups that are attached temporarily to a reactive part of a molecule so that other reactions or processes takes place.[213] When the desired task has been achieved, the protecting groups can be removed by different means such as acids, bases or heat. In this context, photocleavable protection groups are very attractive since their deprotection can be triggered by light, without the need to use harsh chemical reagents. This method is mild and provides orthogonal protection while allowing spatial and temporal control, which makes it attractive to use in controlled drug release,[214] and for surface modification in nanoscale objects.[215] The following criteria should be met for a molecule to be a good PPG.[216]

a. Easy to synthesize and soluble in the target media.
b. Clean photodeprotection reaction with a high quantum yield
c. Ideally, the photochemical by-product shall be inert and transparent at the irradiation wavelength.
d. Stable prior to the photodeprotection process.

There are many photoactive molecules that fulfil the requirements, and are used as a PPGs. The most common ones are 2-nitrobenzyl and its derivatives, benzoin-derivatives, phenacyl derivatives and coumaryl derivatives (Scheme 5-1).[216,217] In this thesis, we focus on 2-nitrobezyl PPGs, which are by far the most widely used.[65,218–220]

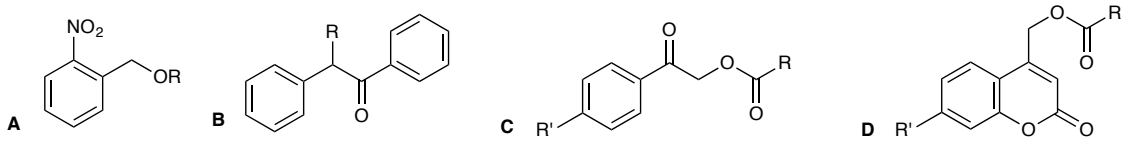

Scheme 5-1: Typical examples of photolabile protecting groups. A, Nitrobenzyl, B. benzoin, C. phenacyl and D. coumaryl derivatives.

5.2. The 2-nitrobenzyl PPG

Since the first report by Barltrop et al.[65] to protect carboxylic acids, 2-nitrobenzyl group has been used in biology, chemistry and materials science. The photochemistry involves an excitation of the nitro group as shown in Scheme 5-2. An intramolecular hydrogen abstraction from the benzylic position results in the intermediate **5-1a**. **5-1a** undergoes rapid tautomerization to the corresponding aci-nitro form, **5-1b**, which subsequently undergoes irresversible cyclization to **5-1d**. A final ring opening reaction then takes place in order to release the protected group, along with o-nitrosobenzaldehyde by product **5-2**.[221] The byproduct **5-2**, however, brings an unwanted complication when using this PPG. It is reactive and dimerizes into azobenzene-2,2'-dicarboxylic acid, which competes to absorb the incident light and reduces the photodeprotection efficiency. To overcome the unwanted issues due to the nitroso by product, many researchers have come up with different strategies, the most common being benzylic substitution.[65,220,222]

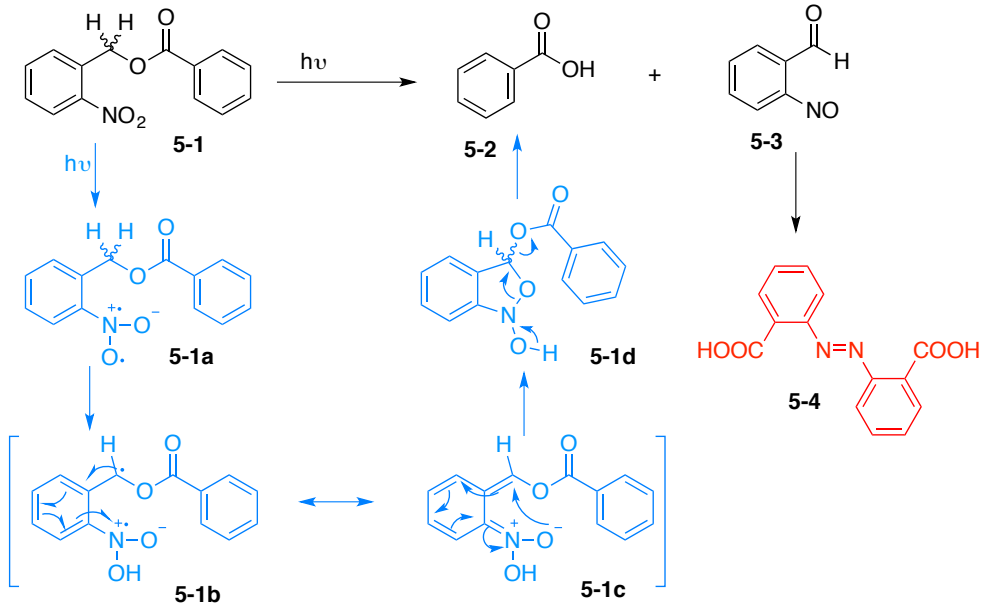

Scheme 5-2: Mechanistic details for the photodeprotection of a typical 2-nitrobenzyl PPG.

Substituting the benzylic position with a phenyl moiety was reported to increase the yield for the released product up to 95%, compared to only 17% for the unsubstituted.[65] Similarly, methyl substitution has also been reported to improve the yield of the photodeprotected product from 25% to 95%.[220] Other researchers have also used various substituents to improve the quantum yields of photodeprotection.[222,223] Particularly, electron withdrawing groups, such as trifluoromethyl, at the benzylic carbon are reported to increase the quantum yield up to 70%.[224]

5.3. Terminal alkyne protection strategy

Terminal alkynes are versatile synthetic building blocks used in organic synthesis laboratories to make drugs,[225] natural products[226] as well as components for molecular electronics applications.[21] Their linear structure make them suitable to prepare molecular wires via the Sonogashira reaction,[17] copper-catalysed alkyne azide cycloaddition (CUAAC) reaction[227] and Glaser coupling.[228] They can also undergo Diels-Alder reactions with cyclopentadiene to afford various substituted norbornadienes.[174] However, low molecular weight terminal alkynes are extremely volatile and most terminal alkynes are prone to oxidation due to their acidic proton. Consequently, they are often protected by silylating agents such as trimethylsilyl and triisopropylsilyl groups.[213] However, these appraoches require chemical methods to release the terminal alkyne.

Recently, Mihovilovic and co-workers proposed alkynoic acids as a source of terminal alkyne since they have higher boiling points compared to their counter parts making them easier to handle.[229] Even the smallest alkynoic acid, propiolic acid, is a liquid with a boiling point of 144 ^{o}C, almost similar to the boiling point of phenylacetylene. When needed, they can be decarboxylated in situ quantitatively in the presence of a copper salt or heat. This method has been exploited to demonstrate decarboxylative coupling reactions with aryl halides.[230] However, the carboxylic acid functional group may present compatibility issues as well as limits the range of reaction conditions used.

Another unique terminal alkyne protection strategy is to use a PPG. Moth-Poulsen and co-workers reported the release of terminal alkyne via photodeprotection of tertiary propargylic ethers protected with 2-nitrobenzyl PPG under alkaline reflux conditions.[64] The released terminal alkynes range from orthogonally protected to those with a thiol anchoring group, which makes it attractive for self-assembly on plasmonic structures such as gold nanoparticles. The only disadvantage of the reported method is that after photodeprotection of the PPG, the terminal alkyne is released under harsh conditions, which may limit the range of applications.

With the aim of releasing terminal alkynes at milder conditions, in Paper IV we reported 2-nitrobenzyl PPG protected arylpropiolic acids. The idea is that after photodeprotection of the 2-nitrobenzyl PPG, copper-assisted decarboxylation will release a terminal alkyne, which can further be reacted e.g. with azides selectively under CuAAC reaction conditions, utilizing the copper salt used for the decarboxylation. Moreover, by incorporating substituents on the benzylic carbon, we envisaged to improve the photocleavage efficiency of the 2-nitrobenzyl PPG. To this end, we synthesised five compounds and characterized them fully by NMR, IR,

thermogravimetric analysis (TGA), and UV-vis spectroscopy. Furthermore, the compounds were investigated for their potential in releasing terminal alkynes efficiently under milder conditions. Ultimately, a proof-of-principle tandem photodeprotection-decarboxylation-CuAAC demonstration is disclosed.

The arylpropiolic acids, **5-5a-c**, were prepared starting from the corresponding aryl iodides and propiolic acid, using the Sonogashira reaction in satisfactory yields (Scheme 5-3). Benzylic substituted 2-nitrobenzyl alcohols, **5-6b-e**, were synthesized from 2-nitrobenzaldehyde with the corresponding Grignard reagents, while 2-nitrobenzyl alcohol (**5-6a**) was obtained from a commercial source (Scheme 5-4).

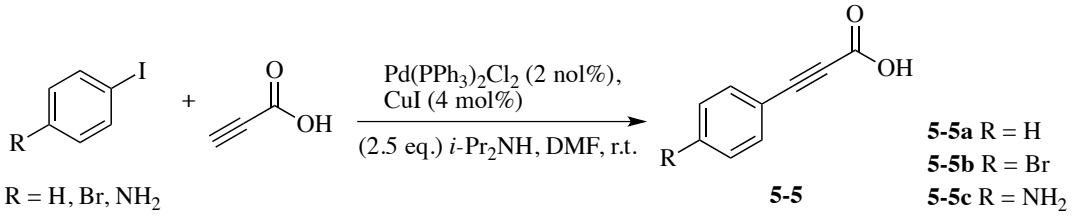

Scheme 5-3: The synthesis of phenylpropiolic acid and its derivatives via the Sonogashira coupling of aryl halides and propiolic acid.

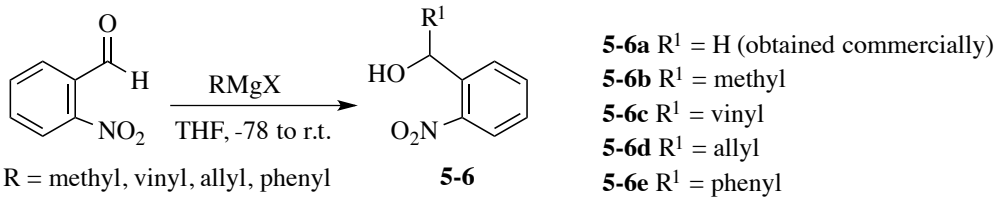

Scheme 5-4: The synthesis of 2-nitrobenzyl derivatives via the Grignard reaction starting from 2-nitrobenzaldehyde.

To couple the alcohols and phenylpropiolic acid, a microwave-assisted Steglich esterification reaction was employed (see Chapter 7, Section 7.1.2), furnishing the desired 2-nitrobenzyl PPG-protected phenylpropiolic products, **5-7a-e**, in good yields in a relatively short time (Scheme 5-5). Moreover, the esterification reaction of the Boc-protected *p*-aminophenylpropiolic acid (**5-5c**) with 2-nitrobenzyl alcohol (**5-6a**) was conducted to yield the desired ester product, as well. To be able to obtain the amino product that can be immobilized on surfaces, we aimed at deprotecting the Boc group. However, upon deprotection either in acidic or basic conditions, the reaction failed to afford the desired amino product, instead the ester linkage was found to be broken.

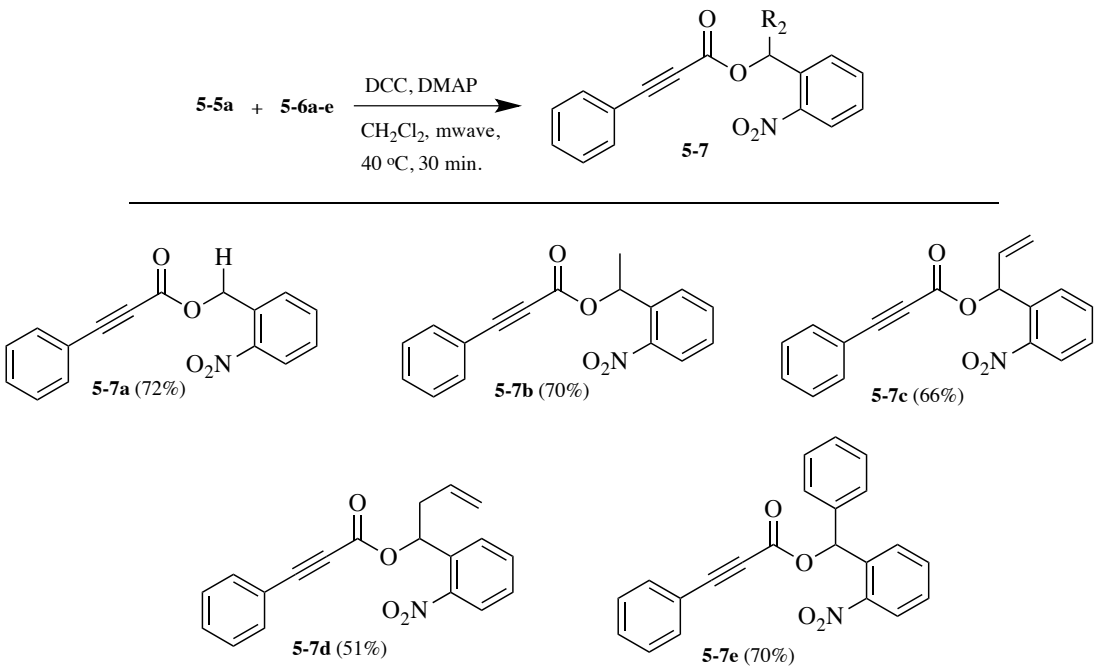

Scheme 5-5: 2-Nitrobenzyl PPG-protected phenylpropiolic esters via the microwave-assisted Steglich esterification reaction.

Initially, we measured the thermal stability of the PPG esters using TGA to determine the effect protecting the acid with the PPG. The result showed the thermal stability of the PPG esters (**5-7a-e**) compared to the reference acid, **5-5a**. At 210 °C, more than 90 wt% of the acid was lost while less than 5 wt% was lost for the PPG esters. Satisfied with the thermal stability, we shifted our attention to the UV-vis absorption study. Despite the benzylic substitution, the absorption spectra of all the PPG esters (**5-7a-e**) looked nearly identical, with a slight hyperchromic as well as bathochromic shift compared to the acid, **5-5a**.

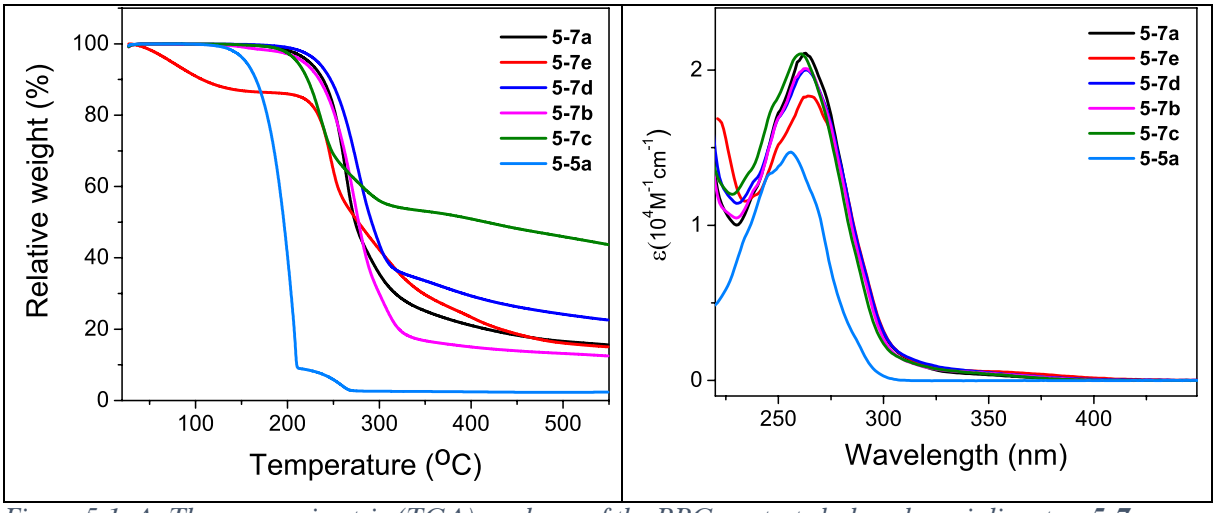

*Figure 5-1: A, Thermogravimetric (TGA) analyses of the PPG-protected phenylpropiolic esters **5-7a-e** as well as B, the corresponding UV-vis spectra. For comparison phenylpropiolic acid (**5-5a**) is shown. Adapted from Paper IV, published under a Creative Common attribution (CC-BY) © American Chemical Society.*

Subsequently, the photodeprotection efficiency of the PPG due to the benzylic substitution was investigated by irradiating acetonitrile solution of all the PPG esters at multiple periods of time using a 254 nm UV lamp. The absorption spectra of each PPG esters showed little change while the acid showed faster evolution over time (*vide infra* Figure 5-2). Intrigued by the result, we investigated the quantum yield of photodeprotection. With the exception of the unsubstituted PPG ester (8%), all the benzylic substituted PPG esters were determined to have high quantum efficiencies, in the range between 41 - 45%.

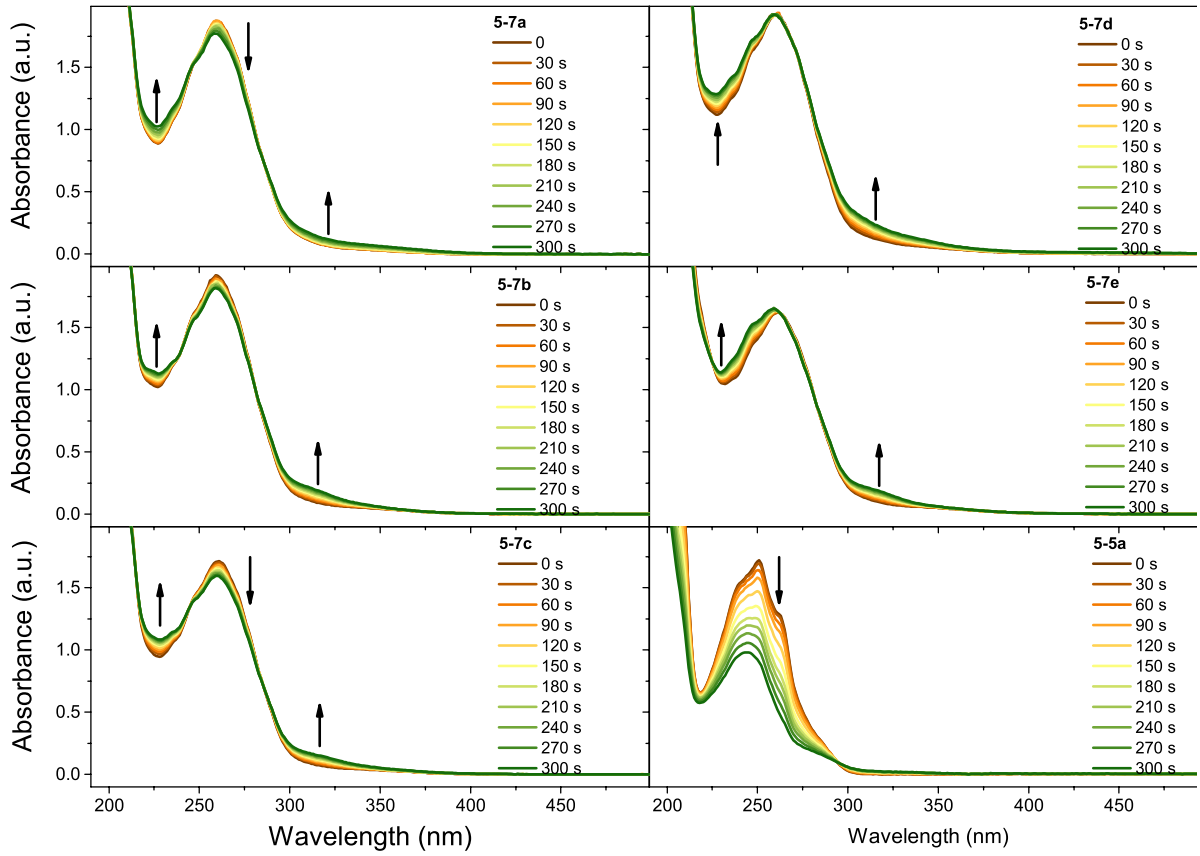

*Figure 5-2: The UV-vis spectra of the 2-nitrobenzyl PPG-protected esters (**5-7a-e**) as well as phenylpropiolic acid (**5-5a**) upon irradiation with a 254 nm. The arrow indicates the evolution direction of the absorption spectra with time. Reproduced from Paper IV, published under a Creative Common attribution (CC-BY) © American Chemical Society*

In the past, photodeprotection of PPGs has often been carried out by exposing a solution that contains a PPG for a longer period of time using a high intensity UV lamp.[231] Recently, however, microchannel flow reactors are reported to increase the efficiency of photoreactions since the solution passing through the channel will be under uniform irradiation.[232,233] One can also control the exposure time precisely by adjusting the flow rate. Henceforth, we investigated the utility of a microchannel flow reactor along with a low intensity handheld UV lamps for such purpose. The photodeprotection process was then followed by ^{1}H-NMR. A 5 mM $CDCl_3$ was injected through the reactor chip at different flow rates, 2.0, 1.2, and 0.4 mL/h, with residence times 100,

167, and 500 s, respectively while the sample was irradiated using a hand held 254 nm UV lamp. From proton NMR studies, 41, 74 and 100% photodeprotection were calculated for the corresponding flow rates. As an example, the proton NMR result for the photodeprotection of ester **5-7b** is shown in Figure 5-3.

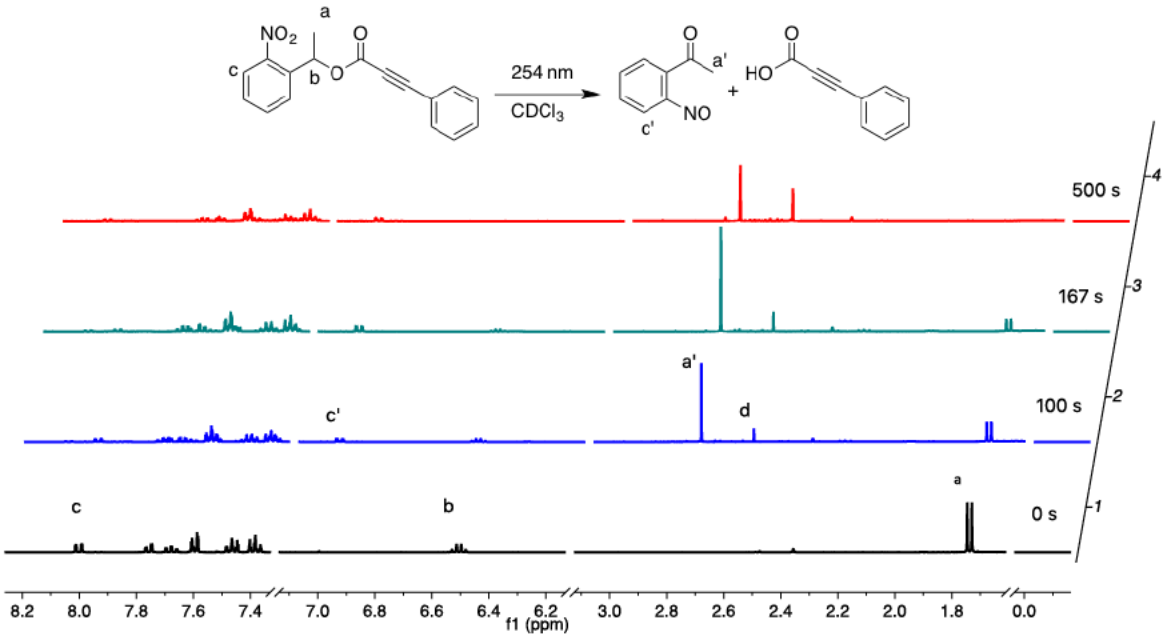

Figure 5-3: 1H-NMR for the photodeprotection of compound 5-7b in a flow reactor chip at different flow rates, using a 254 nm handheld UV lamp. Upon photoirradiation new peaks a', c' and d started to emerge, while peaks a and c disappear gradually. Reproduced from Paper IV, published under a Creative Common attribution (CC-BY) ©American Chemical Society

Then, we turn our attention towards demonstrating the photodeprotection of the PPG, in tandem with decarboxylation of the released acid in the presence of a copper salt to release the terminal alkyne. Once the terminal alkyne is released, it can undergo 1,3-dipolar cycloaddition reaction to yield a 1,2,3-triazole. In a typical tandem sequence, each solution of the esters (in dichloromethane) was injected through the microchannel flow reactor at different flow rates. The irradiated solution was then collected in a vial containing CuI, diisopropylethylamine (DIPEA) and acetic acid (HOAc), since it was found to be an efficient combination for decarboxylation and CuAAC reaction at a mild temperature.[234,235] Then, an azido solution was added, and the content was allowed to react at 60 °C, affording the anticipated 1,2,3-triazole product, **5-8**.

In summary, we have synthesized 2-nitrobenzyl PPG-protected esters that can be photocleaved at a milder temperature (60 °C) than reported in the literature.[64] Moreover, an improved photodeprotection strategy, using a microchannel flow reactor, was demonstrated. In tandem with CuI assisted decarboxylation followed by CuAAC with an azido compound, it was possible to show a triazole product that has a potential to be used as a molecular wire.[236] However, to be

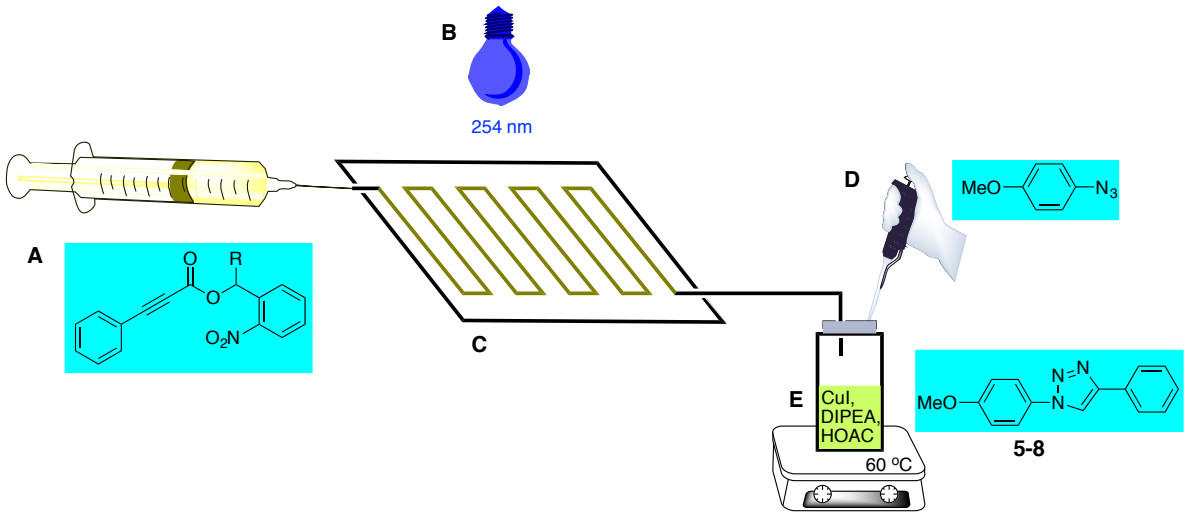

*Figure 5-4: Illustration of the in-flow tandem photodeprotection-decarboxylation-CuAAC reaction. **A**, The 2-nitrobenzyl PPG-protected esters were dissolved in dichloromethane and injected through a microchannel flow reactor (**C**). A 254 nm UV light (**B**) is irradiated upon the reactor chip, which was then collected in a vial (**E**) containing CuI, DIPEA and HOAC. Azidoanisole (**D**) is added into the vial via a syringe and stirred at 60 °C for 15 minutes, at which point the solvent has evaporated. The ^{1}H-NMR of the crude product indicated the formation of the 1,2,3-triazole product, **5-8**.*

able to tether between gold electrodes or immobilize on gold nanoparticles to create a dimer as presented in Chapter 1, Section 1.3, anchoring groups are essential. Even though our plan with the amino group failed to give us the desired product, replacing the amino group with, for example a hydroxyl unit, may lead to a thioacetate anchoring group in reaction with a thioacetate bearing alkyl halides (e.g. *S*-(4-bromobutyl) thioacetate).

Therefore, with the right type of anchoring group on the PPG esters to be able to attach on surfaces, we envisage selective photodeprotection followed by selective decarboxylation to release "single" terminal alkyne with high precision. This can potentially be achieved by using localized surface plasmon resonance (LSPR) effect.[237] Briefly, LSPR is an optical phenomena that occurs when light causes the collective motion of electrons, in conductive nanoparticles that are smaller than the wavelength of the incident light. In this process the energy absorbed from light is converted into heat.[238] The heating effect, in particular, is the highest between two nanoparticles, sometimes called "hot spots".[239] The released terminal alkyne using LSPR can be used as a plasmonic sensor or it can further be reacted with nanoparticles that bear complementary functional groups e.g. azido compounds, to create a dimer connected by a "single" molecule. With the proof-of-principle demonstrated in Paper IV and with the combined knowledge in self-assembly[66] and parallel fabrication[240] at our disposal in our lab, the construction of a "single" molecule electronics device is not a matter of how but rather a matter of when.

Chapter 6 Conclusions and outlooks

Molecular electronics is a relatively young field in the interface between chemistry, physics, nanoscience and nanotechnology. It aims at overcoming fundamental physics limitations that threaten to halt Moore´s law. The field envisions to utilize organic molecules as components for future electronic devices. This stems from the fact that molecules are the smallest functional components that can serve as wires or transistors. So far, ingeniously designed molecules that function as diodes, switches and transistors have been reported. However, except some niche applications such as the guitar auto tuner demonstrated by the McCreery group,[241] the field is struggling to materialize the promised commercial molecular electronics-based device due to various reasons, one of them being stability issues.

To be able to create a stable metal-molecule-metal junction, we have exploited the norbornadiene-quadricyclane (NBD-QC) photoswitch pair, which has been extensively studied for solar energy storage applications. In Paper III, we have disclosed our contribution by synthesizing dimers of NBD derivatives connected by a thiophene or a carbazole unit. The idea was to redshift the absorption spectra to the visible region to maximize the solar energy harvest as well as increase the energy storage density. We have demonstrated that it is possible to redshift the absorption spectra by up to 60 nm for certain NBD derivatives compared to previous reports, that are connected by a phenyl unit. However, except for certain derivatives, their short half-lives (a few minutes or even seconds) have limited their potential to be used in solar energy storage applications. Perhaps, such derivatives could find applications as instant light to heat converting devices.

Towards molecular electronics applications, we prepared thiophene- and thioacetate-terminated NBDs to be able to tether them between metal electrodes and studied their charge transport properties, which is reported in Paper I. Initially, we have investigated their potential in solution using ^{1}H-NMR, UV-Vis and fluorescence spectroscopy. The results indicated that the NBD-QC system can be photoswitched between two forms i.e. the conjugated NBD form and the less-conjugated QC form using light and heat. One of the main advantages with the NBD-QC system is only little structural change occurs upon photoisomerization, which make them ideal candidates to tie them between metal junctions. This property was demonstrated by tethering them between metal junctions. STM-BJ studies showed higher conductance for the NBD form and lower conductance for the QC form. We have also achieved strong coupling between the molecule and the gold electrodes. However, this strong coupling led to switching only in one direction. For practical applications, we are working with our collaborators to address issues related to switching irreversibility between the junction using bias switching.

In Paper II, we have also reported our observation that some of the long and conjugated NBD derivatives emit efficiently in the NBD form, with a fluorescence quantum yield of 49%. To our knowledge, this is the highest value reported for an NBD-QC system. In the QC form, no emission was measured. Such type of emission switching using light may potentially find application in optical memory devices. Furthermore, we reported our findings that demonstrated the possibility of back isomerization of QC to NBD using light, instead of heat. This allowed our molecules to be opened up for all light switching operations, which occurs in a short time-scale compared to the photothermal reversible switching. Moreover, molecules that are designed for electronics applications are expected to work for long periods of time, without fatigue. Therefore, the fatigue resistance of our molecules was also tested over many switching cycles. The results indicated that the NBD-QC compounds studied in this thesis are very stable for over 100 switching cycles, with little or no sign of degradation upon photothermal reversible switching, in particular under inert conditions. The fatigue test further demonstrated the robustness of the NBD-QC-based photoswitch systems.

In Paper IV, we have pursued a 2-nitrobenzyl-based photocleavable protection group (PPG) strategy to protect terminal alkynes. The idea was put forward in Chapter 1 as a way to release terminal alkynes, after selective photodeprotection of the PPG, which can further be elaborated to a molecular wire. First we synthesized various PPG-protected phenylpropiolic esters. The 2-nitrobenzyl PPG was derivatized on the benzylic position to enhance the photodeprotection efficiency. This thesis demonstrated a significant improvement on the rate of photodeprotection of these PPG-protected phenylpropiolic esters compared to the ester without benzylic substitution. Furthermore, in this thesis, we have shown a proof-of-principle and efficient tandem photodeprotection-decarboxylation-CuAAC reaction to afford a 1,2,3-triazole based molecular wire using a microchannel reactor. Even though our initial attempt to synthesize PPG protected terminal alkynes failed to afford the desired product, in the next step, we aim to use a different strategy to be able to make a PPG ester with an anchoring unit. With an anchoring group bearing a PPG protected phenylpropiolic ester, immobilizing onto gold nanoparticles is straightforward. Then, by applying the tandem photodeprotection-decarboxylation-CuAAC protocol developed in Paper IV, nanoparticle dimers that are conjoined by a “single” molecule can be made for “single” molecule electronic device.[240]

Finally, looking back at the research question, yes, we have partially shown that it is possible to synthesize a molecule that can lead to a stable junction using the NBD-QC system, in Paper I. However, additional work has to be done on the direction of Paper IV, to create a protoype “single” molecule electronic device that can lead to logic operations.

Chapter 7 Methods

This chapter gives a general overview of the synthetic methodologies used throughout the thesis, as well as methods used for spectroscopic characterization and analysis. Initially, palladium-catalysed C-C cross coupling reactions based on the Sonogashira reaction, as well as Stille coupling, will be discussed, followed by esterification reactions based on the microwave-assisted Steglich reaction. Then, the basics of UV-visible absorption and emission measurement techniques will be described. Next, the determination of photoisomerization quantum yield using UV-vis absorption spectroscopy will be elaborated. Eventually, the thermal back reaction kinetic analysis for the determination of reaction rates, half-life, Arrhenius parameters and Eyring parameters will be presented.

7.1. Synthetic methodologies

7.1.1. Cross-coupling reactions

Palladium-catalysed reactions have played an immense role in revolutionizing how molecules are constructed. In particular, palladium-catalyzed cross-coupling reactions have shaped basic research in organic synthesis as well as in materials science and technology.[242] There are a many different types of carbon-carbon cross-coupling reactions, however.[243] In this thesis, two of these coupling methods, i.e. the Sonogashira reaction and the Stille reaction, will be highlighted.

The Sonogashira reaction

There are multiple ways of coupling an sp^2 carbon of an alkenyl halide or aryl halide with an sp carbon of a terminal alkyne to afford arylalkynes. One way is to react aryl or vinyl halides with copper acetylides, under reflux conditions, known as the Stephens-Castro reaction.[244] The second method is by using a palladium catalyst and copper(I)iodide in the presence of an amine base, as reported by Sonogashira and Hagihara.[197] The latter method is most widely used, since it enables alkynylation of aryl or vinyl halides at room temperature. However, it also has its own limitations. In the Sonogashira protocol, the copper acetylide is formed in situ from the alkyne in the presence of a copper salt. However, the C-C bond formation occurs in the presence of a palladium complex. Sometimes, homocoupling of the terminal alkynes via the Glaser coupling[228] may happen if the reaction solution is not deoxygenated well. Besides affecting the yield, the homocoupling can be a critical problem if the terminal alkyne is expensive or difficult to synthesize. However, this problem can be overcome by slow addition of the terminal alkyne. Although the exact mechanism is debated, the generally accepted mechanism for the

Sonogashira reaction involves the following key steps in the main palladium cycle (Scheme 7-1): oxidative addition, transmetallation, trans/cis isomerization and reductive elimination.

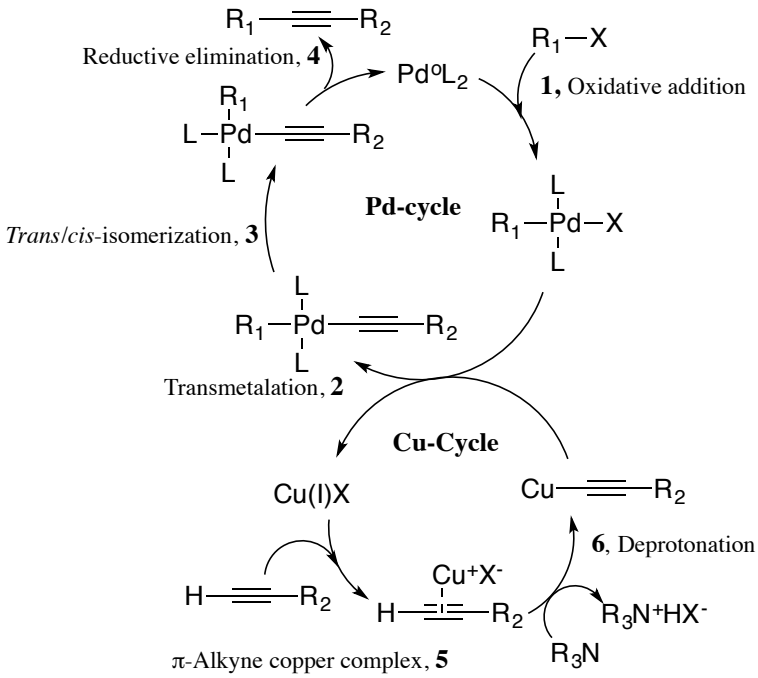

Scheme 7-1: The generally accepted mechanism for the Sonogashira reaction with two independent catalytic cycles.[197]

The general reactivity order of the substrates in Sonogashira reaction is vinyl iodide > vinyl triflate > vinyl bromide > vinyl chloride > aryl iodide > aryl triflate ≥ aryl bromide >> aryl chloride. Moreover, electron poor substrates are more reactive in the Sonogashira reaction. Since, 2,3-dibromonorbornadiene is a vinyl halide, it is relatively reactive under these conditions. As a palladium source, in general, we have often used the more stable and soluble dichlorobis(triphenylphosphine)palladium(II) ($Pd(PPh_3)_2Cl_2$, 5 – 10 mol%). In certain cases, we have also used the more active tetrakis(triphenylphosphine)palladium ($Pd(PPh_3)_4$). Except in copper-free Sonogashira reactions, copper(I)iodide is used as a cocatalyst with a catalytic load of 10 mol%. As a base, triethylamine and diisopropylamine are used. Sometimes, the latter is preferred because the reaction turns viscous when the reaction proceeds as expected. For substrates that are not soluble enough in the base, co-solvents such as toluene and THF have been used.

General Sonogashira reaction procedure

In an oven dried two-necked reaction flask provided with a magnetic stirring bar, $Pd(PPh_3)_2Cl_2$ (5 mol%), CuI (10 mol%), aryl or vinyl halide (1 eq.) were dissolved in a mixture of toluene and amine base (e.g. diisopropylamine). The mixture was purged with nitrogen or argon for

approximately 30 min. Then, the alkyne (1.1 eq. per halide) was added dropwise, at which point the colour turned to dark red. The reaction was allowed to proceed at room temperature until the starting materials were consumed, as indicated by thin layer chromatography (TLC). The solution was then diluted with dichloromethane and filtered through a short plug of silica gel. The volatiles were removed using a rotary evaporator and the crude product was submitted to flash chromatography, using an eluent gradient of 0-10% dichloromethane in hexane. The solvents were evaporated to afford the final product.

The Stille reaction

In a Stille reaction, an aryl or vinyl halide is coupled with an organotin compound. The reaction mechanism is believed to follow a similar catalytic pathway to the Sonogashira reaction (*vid supra* Scheme 7-1), the only difference being at the transmetalation step, where tin instead of copper is involved. Moreover, the use of a base is not required, which makes this method versatile with broad substrate scope and functional group tolerance. Adding cocatalysts, for example copper(I)iodide and Caesium fluoride, found to boost the reaction.[245] As a result, during our synthetic work with the Stille protocol, we have used cocatalysts to yield the desired product in a satisfactory yield. The main disadvantage with the Stille coupling is the high toxicity of organotin compounds, which makes the workup cumbersome. The general reaction procedure for the Stille reaction is very similar to the Sonogashira procedure. However, before purification by flash chromatography, the crude product was further treated with potassium fluoride to extract the tin side products.

7.1.2. Microwave-assisted Steglich Esterification

The Steglich esterification is a variation of an esterification reactions with 4-dimethylaminopyridine (DMAP) used as a catalyst and dicyclohexylcarbodiimide (DCC) as a coupling reagent. This method has been used in the synthesis of amides.[246] The reaction is mild and suitably carried out in dichloromethane at room temperature. The by-product is dicyclohexylurea (DCU), which is insoluble in most organic solvents and can easily be filtered off. Adding 3-10 mol% DMAP is important for the reaction to work efficiently, with DMAP acting as an acyl transfer reagent.[247] The reaction mechanism is depicted in Scheme 7-2. Under normal reaction conditions, the reaction takes a few hours. However, under microwave conditions, the reaction was complete within 30 min. in our hands. The effect of microwave heating in accelerating reactions has been discussed previously.[248]

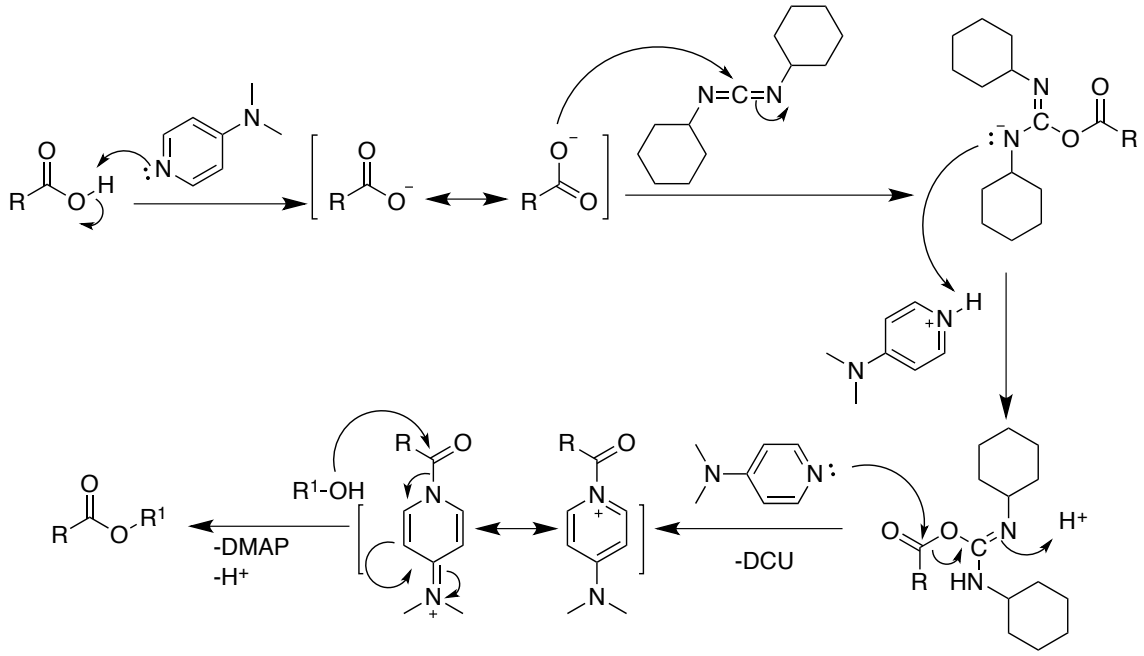

Scheme 7-2: The Steglich esterification reaction using DCC in the presence of a catalytic amount of DMAP.[249]

7.2. UV-visible absorption and emission

To verify the presence of a molecule in a solution as well as to determine the amount can often be accomplished using an absorption spectroscopy. The typical instrumentation design is shown in Figure 7-1. In absorption spectroscopy, an incident light with an intensity (I_o) is partly absorbed by a sample solution containing certain molecules, causing a transition from the ground singlet state (S_o) to an excited state (S_1, S_2 or higher states). Then, the transmitted light (I) through the solution is compared against the incident light to determine how much light has been absorbed in the process. This quantity is commonly called the absorbance (A) of the compound. Absorbance is usually plotted against the wavelength of the absorbed light in nanometre. A numerical value for absorbance is obtained using the Lambert-Beer's law (or Bouguer-Lambert-Beer law) shown in the following Equation 7-1.

$$A = -logT = log\frac{I_o}{I} = \varepsilon(\lambda)cl \qquad 7\text{-}1$$

where T is the light transmitted through the sample. ε is molar absorption coefficient, also known as molar absorptivity, which is related to how well a light is absorbed by the molecule in the solution. It has the unit $M^{-1}cm^{-1}$. c is the sample concertation in mol/liter (M) and l is the length the incident light travels through the solution measured in cm. In our measurements, a quartz cuvette with dimensions 1 cm by 1 cm was used. Note that the absorbance is dimensionless. Absorbance unit (AU) is often used on UV-vis plots, even though it is discouraged by spectroscopists.[250]

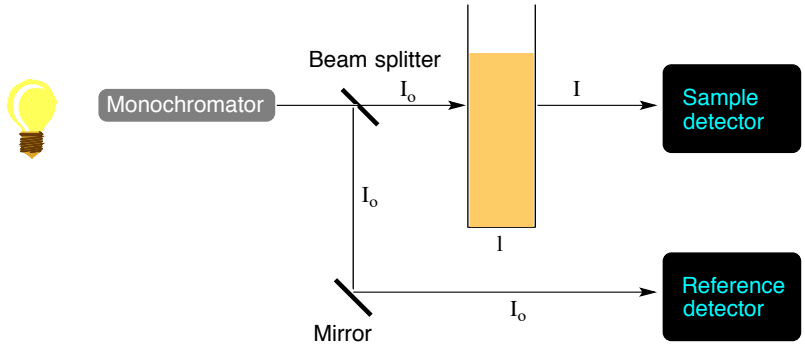

Figure 7-1: A typical layout for a UV-vis absorption spectrophotometer.

In a typical UV-vis measurement, a toluene solution of a compound is prepared in a volumetric flask. It is then transferred to a cuvette and placed in the cuvette holder inside the spectrophotometer. The wavelength range to be scanned is set between 280 and 700 nm. Similarly, a blank toluene absorption is also measured in the same wavelength range in order to the contribution from the background absorption.

To measure emission (fluorescence), a sample is irradiated at a certain wavelength while the emission is collected, by a detector, often located at a right angle to the excitation light source, over a range of wavelengths.[251] A device that is used to measure emission is called a spectrofluorimeter. In a typical emission measurement, a toluene solution of the sample under study, with an absorbance around 0.5, is excited at one wavelength and the emission is recorded over a range of wavelengths.

7.3. Quantum yield measurements and kinetics analysis

Light is a considered to be the "greenest" reagent to bring about chemical transformations.[252] Upon photoirradiation, a molecule (A) is promoted to an excited state (A^*), which is reactive and undergoes a chemical transformation before relaxing back to the ground state, yielding a new product (B) (Equation 7-2).

$$A + h\nu \rightarrow A^* \rightarrow B \qquad (7\text{-}2)$$

The rate at which a photochemical transformation occurs by absorbing light at a given time is called the quantum yield (Φ) and is expressed by the following equation (Equation 7-3):

$$\Phi = \frac{number\ of\ molecules\ reacted}{number\ of\ photons\ absorbed} \qquad (7\text{-}3)$$

For a typical of photochemical reaction, such as A to B, shown in Equation 7-2, the change in concentration of A is proportional to the quantum yield (Φ_A), the photon flux (I) and the fractions of photons absorbed by A (β) given in Equation 7-4.

$$\frac{d[A]}{dt} \propto -\Phi_A . I . \beta_A \tag{7-4}$$

For a reaction carried out at a higher concentration, where the absorption is above 2, Equation 7-3 can be integrated and simplified to Equation 7-5.[253] At a higher concentration, it is assumed that more than 99% of the photons are absorbed by the reactant, A and the product, B, does not absorb at all. Since the amount of B formed is too small, a thermal back reaction is absent when the photochemical reaction is carried out. Hence, change in the concentration of A is given by:

$$[A] = [A_o] - \frac{\Phi_A . I . t_{irr}}{N_A . V} \tag{7-5}$$

Subsequently, to determine the quantum yield, we have used samples with an absorption value above 2. The photon flux (I, s^{-1}) is most often determined using chemical actinometry. In this thesis, all the photon fluxes are determined using the well-known ferrioxalate actinometer.[185]

In a typical photon flux measurement, ferrioxalate solution (3mL, V_1) was pipetted into a cuvette and irradiated with a monochromatic light source, close enough (max. 5 cm) to the cuvette. 2 mL (V_2) of the irradiated solution was then transferred to a volumetric flask (25 mL, V_3) containing a buffer (1 mL) and a phenanthroline solution (2 mL). Three to five solutions, which are irradiated for different times, were prepared. The mixture was mixed by hand-shaking, covered with aluminium foil and left undisturbed for 1 hour prior to the UV-vis measurement. As a reference, non-irradiated ferrioxalate was prepared following the same procedure. Then the absorption spectra of the solutions were measured. The absorbance value at 510 nm was plotted against the time of irradiation, which should give a straight line through the zero point. If the ferrioxalate solution was irradiated for too long, the line becomes flat due to bleaching. Note that all measurements were conducted in a dark room. The slope of the line was then used to calculate the quantum flow according to the following Equation 7-6.

$$\mathrm{I}\left(\frac{\text{quanta}}{\text{s}}\right) = slope . \frac{V_1 . V_3}{V_2 . \varepsilon_{510\ nm} . l . \Phi_{Fe}} \tag{7-6}$$

where, ε_{510} is the molar absorptivity of the complex at 510 nm (11100 $M^{-1}cm^{-1}$), l is the thickness of the cuvette and ΦFe is the quantum yield for decomposition of ferrioxalate at the irradiation wavelength.

Then the sample, whose quantum yield was to be determined, was pipetted into a cuvette with a known weight, and irradiated using the same light that was used for the ferrioxalate solution. The sample was then irradiated for different periods of time, and its absorption was measured each time using a UV-vis spectrophotometer. The weight of the cuvette with the solution was measured after the experiment, and the concentration of the solution was then determined from the corresponding absorbance. It is important to remember that the molar absorptivity of the sample is known or measured beforehand. Eventually, the concentration at a given wavelength was plotted against the different irradiation times used. For linear lines, the slopes were used to determine the quantum yield based on Equation 7-5.

7.4. Kinetics study of thermal back reactions

For T-type photochromic molecules, such as NBD-QC, the photoisomer relaxes back to the parent isomer thermally. Often, this process is followed by UV-vis spectroscopy and for first order kinetics, the thermal reaction rate (k) can be determined by exponential fitting. The half-life ($t_{1/2}$) at a given temperature can in turn be determined from the reaction rate at that temperature, based on the following equation (Equation 7-7).

$$t_{\frac{1}{2}} = \frac{\ln(2)}{k} \tag{7-7}$$

If the thermal relaxation is conducted at multiple temperatures, the activation barrier (E_a) and enthalpy ($\Delta H_{storage}$) can be determined based on the empirical Arrhenius equation (Equation 7-8) and the Eyring equation (Equation 7-9), which is based on the transition state theory, respectively.

$$\ln(k) = \ln(A) - \frac{E_a}{RT} \tag{7-8}$$

$$ln\left(\frac{k}{T}\right) = -\frac{\Delta H^{\ddagger}}{RT} + ln\left(\frac{k_B}{h}\right) + \frac{\Delta S^{\ddagger}}{R} \tag{7-9}$$

Acknowledgments

Since I set foot in Sweden over four years ago to start my journey as a PhD student, I met many incredibly nice people who made my life easier. First, it all starts with Professor Kasper Moth-Poulsen, thank you for choosing me to work in this collaborative ERC project. I am also very grateful for helping me navigate throughout my PhD research. Whenever there seems to be challenges, you suggest solutions that most of the time works. Moreover, your gift to my family, when we welcome Joseph and Christmas presents through the years makes me happy to work with a person who not only cares about results but also people. My special thanks goes to Professor Nina Kann. You are such a nice person and a role model to work under. You have always been there to discuss my challenges as well as opportunities. Your guidance and commitment has helped me to stay focused. I am very lucky to have you as my co-supervisor. I would also like to thank my former supervisor Professor Wendimagegn Mammo, whose help and mentoring has been unreserved. I would like to acknowledge my examiner and collaborator professor Bo Albinsson. I am very glad to see our collaboration come to fruition on the second trial. I like to acknowledge Professor Björn Åkerman for the informative discussion about enthalpy and entropy as well as Associate Professor Karl Börjesson, for our collaboration and for your guidance while I started working with UV-Vis spectroscopy.

Our collaborators, Professor Joshua Hihath and Haipeng Billie Li at UC Davis are duly acknowledged. Our collaboration has been fruitful and I hope the best is yet to come. Professor, Gemma Solomon and Dr. Alessandro Pirrotta, It has been a pleasure to work with you, as well. I thank professor Mogens and Mads for our nice collaboration on the solar energy storage. I thank associate professor Timur Shegai and his group for our collaborative efforts. Even though, it did not work out as planned, it was a pleasure to know you and some of your group members, with whom I have had an interesting discussion about plasmonic materials.

I also thank the present and former group members of our research group, whom I cannot list them all here. In particular, I like to thank Dr. Yuri. I appreciate the items that you gave me for my daughter. Dr. Christian Rohner for welcoming me while I was travelling via Berlin. Dr Sarah, Ambra and Fredrik for reviewing my thesis thoroughly. Your feedbacks have really been invaluable to me. Johnas, thank you! I am happy to know you. You always see positive sides of things. I wish you all the best finishing your thesis. Dr. Tina, your friendship and pep talks as well as insights in suggesting and taking projects forwards is commendable. The awesome nano-team, are duly acknowledged. With such talented group of people, I am sure the team will be

productive soon. I also like to thank Mariza, for the nice illustration for the cover of my thesis, Liyang for the fika room evening-time conversation as well as giving me a feedback on my thesis.

Thank you Dr. Desta! I remember fondly, my first day scrambled egg in Sweden. It was yummy. I also remember our “Mekses” chat with you and Associate professor Ergang. It, indeed, was memorable time. I also thank Dr. Desalegn, Dr. Zewdneh and Birhan, for our unforgettable past times! Victor, Renee, and Elham for being a great lab mates and Maria, for being the nicest officemate. Our conversations during challenging times have helped me move forward. I wish you the best with your maternity leave and of course, finishing your studies. I extend my acknowledgment to all former and current colleagues on floor 8, with whom I enjoyed many fikas and enlightening discussions.

At the beginning Frida and now Lotta, you guys have made my life easier with the paper works and keeping the floor in a good mood. In particular, Lotta your insistence to teach me Swedish has kind of worked. Nu jag kan säga, jag förstår Svenska! Tack så jätte mycket! I also do not forget the work of Roger and Sara for making sure we have the chemicals and materials we need for our research. I also thank Dr. Bijan and Dr. Patrik for helping me with NMR issues.

I would like to sincerely thank my parents and siblings, who have been supportive throughout my studies. Birhanu, thank you so much for your unwavering brotherly support and encouragement. Your calls have been immensely helpful and yeah finally, I am almost there! I also thank my in-laws, you have been very understanding and encouraging!

My Special acknowledgment is reserved for my beautiful wife and children. Selamawit, Elnatha and Joseph. I love you so much!!! Seli, thank you for being besides me through thick and thin. I love you and I know, I owe you bigtime!

Chapter 9 References

(1) Garrett, A. B. The Discovery of the Transistor: W. Shockley, J. Bardeen, and W. Brattain. *J. Chem. Educ.* **1963**, *40* (6), 302.

(2) Lehovec, K. Multiple Semiconducor Assembly. 3029366, 1962.

(3) Moore, G. E. Cramming More Components onto Integrated Circuits (Reprinted from Electronics, Pg 114-117, April 19, 1965). *Proc. Ieee* **1965**, *86* (1), 82–85.

(4) Kersting, K.; Meyer, U. From Big Data to Artificial Intelligence? *Künstel Intell* **2018**, *32*, 3–8.

(5) Sreenivasan, S. V. Nanoimprint Lithography Steppers for Volume Fabrication of Leading-Edge Semiconductor Integrated Circuits. *Microsystems Nanoeng.* **2017**, *3* (April), 17075.

(6) Keyes, R. W. Physical Limits of Silicon Transistors and Circuits. *Rep. Prog. Phy.* **2005**, *68* (12), 2701–2746.

(7) Deleonibus, S. Physical and Technological Limitations of NanoCMOS Devices to the End of the Roadmap and Beyond. *Eur. Phys. J. Appl. Phys.* **2007**, *36*, 197–214.

(8) Moore, A. L.; Shi, L. Emerging Challenges and Materials for Thermal Management of Electronics. *Mater. Today* **2014**, *17* (4), 163–174.

(9) Iqbal, M. A.; Rahman, M. New Thermal Management Approach for Transistor-Level 3-D Integtration. *2017 IEEE SOI-3D-Subthreshold Microelectron. Unified Conf. S3S 2017* **2018**, *2018–March*, 1–3.

(10) Thompson, S. E.; Parthasarathy, S. Moore's Law: The Future of Si Microelectronics. *Mater. Today* **2006**, *9* (6), 20–25.

(11) Feynman, R. P. Simulating Physics with Computers. *Int. J. Theor. Phys.* **1982**, *21* (6–7), 467–488.

(12) Benioff, P. Quantum Robots and Quantum Computers. *Quantum* **1997**, 18.

(13) Yang, H.; Khayrudinov, V.; Dhaka, V.; Jiang, H.; Autere, A.; Lipsanen, H.; Sun, Z.; Jussila, H. Nanowire Network – Based Multifunctional All-Optical Logic Gates. *Sci. Adv.* **2018**, *4*.

(14) Aviram, A.; Ratner, M. A. Molecular Rectifiers. *Chem. Phys. Lett.* **1974**, *29* (2), 277–283.

(15) Metzger, R. M. Unimolecular Electronics. *Chem. Rev.* **2015**, 150507090420005.

(16) Tour, J. M. Conjugated Macromolecules of Precise Length and Constitution. Organic Synthesis for the Construction of Nanoarchitectures. *Chem. Rev.* **1996**, *96* (1), 537–554.

(17) Tour, J. M. Molecular Electronics. Synthesis and Testing of Components. *Acc. Chem. Res.* **2000**, *33* (11), 791–804.

(18) Collier, C. P., Wong, E. W., Belohradsky, M., Raymo, F. M., Stoddart, J. F., Kuekes, P. J., Williams, R. S., Heath, J. R. Electronically Configurable Molecular-Based Logic Gates. *Science (80-.).* **1999**, *285* (5426), 391–394.

(19) McCreery, R. Molecular Electronics. *Electrochem. Soc. Interface* **2004**, *Spring*, 2.

(20) Xiang, D.; Wang, X.; Jia, C.; Lee, T.; Guo, X. Molecular-Scale Electronics: From Concept to Function. *Chem. Rev.* **2016**, *116* (7), 4318–4440.

(21) James, D. K.; Tour, J. M. Molecular Wires. *Top. Curr. Chem.* **2005**, *257*, 33–62.

(22) Matsuda, K.; Irie, M. Diarylethene as a Photoswitching Unit. *J. Photochem. Photobiol. C Photochem. Rev.* **2004**, *5* (2), 169–182.

(23) Jia, C.; Migliore, A.; Xin, N.; Huang, S.; Wang, J.; Yang, Q.; Wang, S.; Chen, H.; Wang, D.; Feng, B.; et al. Covalently Bonded Single-Molecule Junctions with Stable and Reversible Photoswitched Conductivity. *Science (80-.).* **2016**, *352* (6292), 1443–1445.

(24) van der Molen, S. J.; Liao, J.; Kudernac, T.; Agustsson, J. S.; Bernard, L.; Calame, M.; van Wees, B. J.; Feringa, B. L.; Schönenberger, C. Light-Controlled Conductance Switching of Ordered Metal–Molecule–Metal Devices. *Nano Lett.* **2009**, *9* (1), 76–80.

(25) van der Molen, S. J.; Liljeroth, P. Conductance Properties of Switchable Molecules. *Mol. Switch. Second Ed.* **2011**, *1*, 719–777.

(26) Metzger, R. M. Unimolecular Electrical Rectifiers. *Chem. Rev.* **2003**, *103* (9), 3803–3834.

(27) Kornilovitch, P.; Bratkovsky, A.; Williams, S. Single-Molecule Designs for Electric Switches and Rectifiers. *Ann. N. Y. Acad. Sci.* **2003**, *1006* (2003), 198–211.

(28) Yuan, L.; Breuer, R.; Jiang, L.; Schmittel, M.; Nijhuis, C. A. A Molecular Diode with a Statistically Robust Rectification Ratio of Three Orders of Magnitude. *Nano Lett.* **2015**, *15* (8).

(29) Capozzi, B.; Xia, J.; Adak, O.; Dell, E. J.; Liu, Z.-F.; Taylor, J. C.; Neaton, J. B.; Campos, L. M.; Venkataraman, L. Single-Molecule Diodes with High Rectification Ratios through Environmental Control. *Nat. Nanotechnol.* **2015**, No. May, 1–7.

(30) Díez-Pérez, I.; Hihath, J.; Lee, Y.; Yu, L.; Adamska, L.; Kozhushner, M. A.; Oleynik, I. I.; Tao, N. Rectification and Stability of a Single Molecular Diode with Controlled

Orientation. *Nat. Chem.* **2009**, *1* (8), 635–641.

(31) Browne, W. R.; Feringa, B. L. Light Switching of Molecules on Surfaces. *Annu. Rev. Phys. Chem.* **2009**, *60* (1), 407–428.

(32) El Gemayel, M.; Börjesson, K.; Herder, M.; Duong, D. T.; Hutchison, J. A.; Ruzié, C.; Schweicher, G.; Salleo, A.; Geerts, Y.; Hecht, S.; et al. Optically Switchable Transistors by Simple Incorporation of Photochromic Systems into Small-Molecule Semiconducting Matrices. *Nat. Commun.* **2015**, *6*, 1–8.

(33) Irie, M. Diarylethenes for Memories and Switches. *Chem. Rev.* **2000**, *100* (5), 1685–1716.

(34) Guédon, C. M.; Valkenier, H.; Markussen, T.; Thygesen, K. S.; Hummelen, J. C.; van der Molen, S. J. Observation of Quantum Interference in Molecular Charge Transport. *Nat. Nanotechnol.* **2012**, *7*, 305–309.

(35) Tsuji, Y.; Hoffmann, R.; Strange, M.; Solomon, G. C. Close Relation between Quantum Interference in Molecular Conductance and Diradical Existence. *Proc. Natl. Acad. Sci.* **2016**, *113* (4), E413–E419.

(36) Lambert, C. J. Basic Concepts of Quantum Interference and Electron Transport in Single-Molecule Electronics. *Chem. Soc. Rev.* **2015**, *44* (4).

(37) Sanvito, S. Part of the Molecule-Based Magnets Themed Issue. *Chem. Soc. Rev.* **2011**, *40* (6), 3336–3355.

(38) von Hippel, A. Molecular Engineering. *Science (80-.).* **1956**, *123* (3191), 315–317.

(39) Metzger, R. M.; Chen, B.; Höpfner, U.; Lakshmikantham, M. V.; Vuillaume, D.; Kawai, T.; Wu, X.; Tachibana, H.; Hughes, T. V.; Sakurai, H.; et al. Unimolecular Electrical Rectification in Hexadecylquinolinium Tricyanoquinodimethanide. *J. Am. Chem. Soc.* **1997**, *119* (43), 10455–10466.

(40) Chen, X.; Roemer, M.; Yuan, L.; Du, W.; Thompson, D.; Del Barco, E.; Nijhuis, C. A. Molecular Diodes with Rectification Ratios Exceeding 105driven by Electrostatic Interactions. *Nat. Nanotechnol.* **2017**, *12* (8), 797–803.

(41) Wohltjen, H. *Molecular Electronics: Biosensors and Biocom*, 1st ed.; Hong, F. T., Ed.; A Division of Plenum Publishing Corporation: New York, 1989.

(42) Carter, F. L. Molecular Level Fabrication Techniques and Molecular Electronics Devices. *Microelectron. Eng.* **1984**, 11–24.

(43) Batra, A.; Darancet, P.; Chen, Q.; Meisner, J. S.; Widawsky, J. R.; Neaton, J. B.; Nuckolls, C.; Venkataraman, L. Tuning Rectification in Single-Molecular Diodes. *Nano*

Lett. **2013**.

(44) Janes, D. Rectifying Current Behaviours. *Nat. Chem.* **2009**, *1* (8), 601–603.

(45) Hwang, J. J.; Tour, J. M. Combinatorial Synthesis of Oligo(Phenylene Ethynylene)S. *Tetrahedron* **2002**, *58* (52), 10387–10405.

(46) Reed, M. A.; Zhou, C.; Muller, C. J.; Burgin, T. P.; Tour, J. M. Conductance of a Molecular Junction. *Science* **1997**, *278* (5336), 252–254.

(47) Xu, B.; Tao, N. J. Measurement of Single-Molecule Resistance by Repeated Formation of Molecular Junctions. *Science (80-.).* **2003**, *301* (5637), 1221–1223.

(48) Cui, X. D.; Primak, A.; Zarate, X.; Tomfohr, J.; Sankey, O. F.; Moore, A. L.; Moore, T. A.; Gust, D.; Harris, G.; Lindsay, S. M. Reproducible Measurement of Single-Molecule Conductivity. *Science (80-.).* **2001**, *294* (5542), 571–574.

(49) Lather, A.; Lamba, V. K.; Malik, H.; Ratner, M. A. Molecular Switches : A Review. *Eng. Sci. Technol. An Int. J.* **2012**, *2* (3), 460–466.

(50) Su, T. A.; Neupane, M.; Steigerwald, M. L.; Venkataraman, L.; Nuckolls, C. Chemical Principles of Single-Molecule Electronics. *Nat. Rev. Mater.* **2016**, *1*, 1–15.

(51) Chen, F.; Hihath, J.; Huang, Z.; Li, X.; Tao, N. J. Measurement of Single-Molecule Conductance. *Annu. Rev. Phys. Chem.* **2007**, *58* (1), 535–564.

(52) Coskun, A.; Spruell, J. M.; Barin, G.; Dichtel, W. R.; Flood, A. H.; Botros, Y. Y.; Stoddart, J. F. High Hopes: Can Molecular Electronics Realise Its Potential? *Chem. Soc. Rev.* **2012**, *41* (14), 4827.

(53) Jia, C.; Guo, X. Molecule-Electrode Interfaces in Molecular Electronic Devices. *Chem. Soc. Rev.* **2013**, *42* (13).

(54) Sun, L.; Diaz-Fernandez, Y. a; Gschneidtner, T. a; Westerlund, F.; Lara-Avila, S.; Moth-Poulsen, K. Single-Molecule Electronics: From Chemical Design to Functional Devices. *Chem. Soc. Rev.* **2014**, *43*, 7378–7411.

(55) Mativetsky, J. M.; Pace, G.; Elbing, M.; Rampi, M. A.; Mayor, M.; Samorì, P. Azobenzenes as Light-Controlled Molecular Electronic Switches in Nanoscale Metal−molecule−metal Junctions. *J. Am. Chem. Soc.* **2008**, *130* (29), 9192–9193.

(56) Irie, M.; Fukaminato, T.; Matsuda, K.; Kobatake, S. Photochromism of Diarylethene Molecules and Crystals: Memories, Switches, and Actuators. *Chem. Rev.* **2014**, *114* (24), 12174–12277.

(57) Kim, Y. H.; Jang, S. S.; Goddard, W. A. Possible Performance Improvement in

[2]Catenane Molecular Electronic Switches. *Appl. Phys. Lett.* **2006**, *88* (16).

(58) McCreery, A. J. B. and L. Z.-W. and M. S. and N. P. and B. S. and R. L. Musical Molecules: The Molecular Junction as an Active Component in Audio Distortion Circuits. *J. Phys. Condens. Matter* **2016**, *28* (9), 94011.

(59) Chen, J., Reed, M. A., Rawlett, A. M., Tour, J. M. Large On-Off Ratios and Negative Differential Resistance in a Molecular Electronic Device. *Science (80-.).* **1999**, *286* (5444), 1550–1552.

(60) Park, J.; Pasupathy, A. N.; Goldsmith, J. I.; Chang, C.; Yaish, Y.; Petta, J. R.; Rinkoski, M.; Sethna, J. P.; Abruña, H. D.; McEuen, P. L.; et al. Coulomb Blockade and the Kondo Effect in Single-Atom Transistors. *Nature* **2002**, *417* (6890), 722–725.

(61) Garner, M. H.; Li, H.; Chen, Y.; Su, T. A.; Shangguan, Z.; Paley, D. W.; Liu, T.; Ng, F.; Li, H.; Xiao, S.; et al. Comprehensive Suppression of Single-Molecule Conductance Using Destructive σ-Interference. *Nature* **2018**, *558* (7710), 416–419.

(62) Zang, Y.; Ray, S.; Fung, E.-D.; Borges, A.; Garner, M. H.; Steigerwald, M. L.; Solomon, G. C.; Patil, S.; Venkataraman, L. Resonant Transport in Single Diketopyrrolopyrrole Junctions. *J. Am. Chem. Soc.* **2018**, *140* (Cv), jacs.8b06964.

(63) Dubonosov, A. D.; Bren, V. A.; Chernoivanov, V. A. Norbornadiene–Quadricyclane as an Abiotic System for the Storage of Solar Energy. *Russ. Chem. Rev.* **2002**, *71* (11), 917–927.

(64) Gschneidtner, T. a.; Moth-Poulsen, K. A Photolabile Protection Strategy for Terminal Alkynes. *Tetrahedron Lett.* **2013**, *54* (40), 5426–5429.

(65) Barltrop, J. A.; Plant, P. J.; Schofield, P. Photosensitive Protective Groups. *Chem. Commun.* **1966**, No. 22, 822–823.

(66) Gschneidtner, T. a.; Diaz Fernandez, Y. a.; Moth-Poulsen, K. Progress in Self-Assembled Single-Molecule Electronic Devices. *J. Mater. Chem. C* **2013**, *1* (43), 7127.

(67) Keicher, T.; Löbbecke, S. *Organic Azides: Synthesis and Applications*, 1st ed.; Bräse, S., Banert, K., Eds.; John Wiley and Sons: West Sussex, 2010.

(68) Bouas-Laurent, H.; Dürr, H. Organic Photochromism (IUPAC Technical Report). *Pure and Applied Chemistry*. 2001, p 639.

(69) Hirshberg, Y. Photochromie Dans La Serie de La Bianthrone. *Comp. Rend. Acad. Sci.* **1950**, *231*, 903–904.

(70) Sheepwash, M. A. L.; Ward, T. R.; Wang, Y.; Bandyopadhyay, S.; Mitchell, R. H.;

Bohne, C. Mechanistic Studies on the Photochromism of [e]-Annelated Dimethyldihydropyrenes. *Photochem. Photobiol. Sci.* **2003**, *2* (2), 104–112.

(71) Kamogawa, H.; Yamada, M. Photoresponsive Vinyl Polymer Bearing Norbornadiene as a Pendant Group. *Macromolecules* **1988**, *21*, 918–923.

(72) Pardo, R.; Zayat, M.; Levy, D. Photochromic Organic-Inorganic Hybrid Materials. *Chem. Soc. Rev.* **2011**, *40* (2), 672–687.

(73) Vsevolodov, N.; Amiel, D. Photosensitive Materials for Use as Optical Memory. In *Biomolecular Electronics: An Introduction via Photosensitive Proteins*; Vsevolodov, N., Ed.; Birkhäuser Boston: Boston, MA, 1998; pp 131–175.

(74) Crano, J. C.; Flood, T.; Knowles, D.; Kumar, A.; Van Gemert, B. Photochromic Compounds: Chemistry and Application in Ophthalmic Lenses. *Pure Appl. Chem.* **1996**, *68* (7), 1395–1398.

(75) Kawata, S.; Kawata, Y. Three-Dimensional Optical Data Storage Using Photochromic Materials. *Chem. Rev.* **2000**, *100* (5), 1777–1788.

(76) Roubinet, B.; Weber, M.; Shojaei, H.; Bates, M.; Bossi, M. L.; Belov, V. N.; Irie, M.; Hell, S. W. Fluorescent Photoswitchable Diarylethenes for Biolabeling and Single-Molecule Localization Microscopies with Optical Superresolution. *J. Am. Chem. Soc.* **2017**, *139* (19), 6611–6620.

(77) Qin, M.; Huang, Y.; Li, F.; Song, Y. Photochromic Sensors: A Versatile Approach for Recognition and Discrimination. *J. Mater. Chem. C* **2015**, *3* (36), 9265–9275.

(78) Wang, Z.; Udmark, J.; Börjesson, K.; Rodrigues, R.; Roffey, A.; Abrahamsson, M.; Nielsen, M. B.; Moth-Poulsen, K. Evaluating Dihydroazulene/Vinylheptafulvene Photoswitches for Solar Energy Storage Applications. *ChemSusChem* **2017**, *10* (15), 3049–3055.

(79) Aiken, S.; Edgar, R. J. L.; Gabbutt, C. D.; Heron, B. M.; Hobson, P. A. Negatively Photochromic Organic Compounds: Exploring the Dark Side. *Dye. Pigment.* **2018**, *149*, 92–121.

(80) Barachevsky, V. A. Negative Photochromism in Organic Systems. *Rev. J. Chem.* **2017**, *7* (3), 334–371.

(81) Minkin, V. I. Photoswitchable Molecular Systems Based on Spiropyrans and Spirooxazines. *Mol. Switch. Second Ed.* **2011**, *1*, 37–80.

(82) Mitchell, R. H.; Ward, T. R.; Chen, Y.; Wang, Y.; Weerawarna, S. A.; Dibble, P. W.; Marsella, M. J.; Almutairi, A.; Wang, Z. Q. Synthesis and Photochromic Properties of

Molecules Containing [e]-Annelated Dihydropyrenes. Two and Three Way π-Switches Based on the Dimethyldihydropyrene-Metacyclophanediene Valence Isomerization. *J. Am. Chem. Soc.* **2003**, *125* (10), 2974–2988.

(83) Lennartson, A.; Roffey, A.; Moth-Poulsen, K. Designing Photoswitches for Molecular Solar Thermal Energy Storage. *Tetrahedron Lett.* **2015**, *56* (12), 1457–1465.

(84) *Photochromism: Molecules and Systems*, 1st ed.; Dürr, H., Bouas-Laurent, H., Eds.; Elsevier B.V: Amsterdam, 2003.

(85) Feringa, B. L.; Jager, W. F.; de LAnge, B. Organic Materials for Reversible Optical Data Storage. *Tetrahedron* **1993**, *49*, 8267–8310.

(86) Rau, H. Azo Compounds. In *Photochromism: Molecules and systems*; Dürr, H., Bouas-Laurent, H., Eds.; Amsterdam, 2003; pp 165–192.

(87) Merino, E.; Ribagorda, M. Control over Molecular Motion Using the Cis–Trans Photoisomerization of the Azo Group. *Beilstein J. Org. Chem.* **2012**, *8*, 1071–1090.

(88) Schweighauser, L.; Wegner, H. A. Chemical Talking with Living Systems: Molecular Switches Steer Quorum Sensing in Bacteria. *ChemBioChem* **2015**, *16* (12), 1709–1711.

(89) Klajn, R. Immobilized Azobenzenes for the Construction of Photoresponsive Materials. *Pure Appl. Chem.* **2010**, *82* (12), 2247–2279.

(90) Yu, B.-C.; Shirai, Y.; Tour, J. M. Syntheses of New Functionalized Azobenzenes for Potential Molecular Electronic Devices. *Tetrahedron* **2006**, *62* (44), 10303–10310.

(91) García-Amorós, J.; Velasco, D. Recent Advances towards Azobenzene-Based Light-Driven Real-Time Information-Transmitting Materials. *Beilstein J. Org. Chem.* **2012**, *8*, 1003–1017.

(92) Yokoyama, Y.; Gushiken, T.; Ubukata, T. Fulgides and Related Compounds. *Mol. Switch. Second Ed.* **2011**, *1* (i), 81–95.

(93) Yokoyama, Y. Fulgides for Memories and Switches. *Chem. Rev.* **2000**, *100* (5), 1717–1740.

(94) Irie, M.; Mohri, M. Thermally Irreversible Photochromic Systems. Reversible Photocyclization of Diarylethene Derivatives. *J Org Chem* **1988**, *53*, 803–808.

(95) Jia, C.; Wang, J.; Yao, C.; Cao, Y.; Zhong, Y.; Liu, Z.; Liu, Z.; Guo, X. Conductance Switching and Mechanisms in Single-Molecule Junctions. *Angew. Chemie - Int. Ed.* **2013**, *52* (33).

(96) Jan van der Molen, S.; Liljeroth, P. Charge Transport through Molecular Switches. *J.*

Phys. Condens. Matter **2010**, *22* (13), 133001–133030.

(97) Sendler, T.; Luka-Guth, K.; Wieser, M.; Lokamani; Wolf, J.; Helm, M.; Gemming, S.; Kerbusch, J.; Scheer, E.; Huhn, T.; et al. Light-Induced Switching of Tunable Single-Molecule Junctions. *Adv. Sci.* **2015**, *2* (5), 1–7.

(98) Guglielmetti. 4n+2 Systems: Spiropyrans. In *Photochromism: Molecules and systems*; Dürr, H., Bouas-laurent, H., Eds.; Elsevier B.V: Amsterdam, 2003; pp 314–466.

(99) Klajn, R. Spiropyran-Based Dynamic Materials. *Chem. Soc. Rev.* **2014**, *43* (1), 148–184.

(100) Hirshberg, Y. Reversible Formation and Eradication of Colors by Irradiation at Low Temperatures. A Photochemical Memory Model. *J. Am. Chem. Soc.* **1956**, *78* (10), 2304–2312.

(101) Görner, H.; Fischer, C.; Gierisch, S.; Daub, J. Vinylheptafulvene Photochromism: Effects of Substituents, Solvent, and Temperature in the Photorearrangement of Dihydroazulenes to Vinylheptafulvenes. *J. Phys. Chem.* **1993**, *97*, 4110–4117.

(102) Broman, S. L.; Nielsen, M. B. Dihydroazulene: From Controlling Photochromism to Molecular Electronics Devices. *Phys. Chem. Chem. Phys.* **2014**, *16* (39), 21172–21182.

(103) Broman, S. L.; Lara-Avila, S.; Thisted, C. L.; Bond, A. D.; Kubatkin, S.; Danilov, A.; Nielsen, M. B. Dihydroazulene Photoswitch Operating in Sequential Tunneling Regime: Synthesis and Single-Molecule Junction Studies. *Adv. Funct. Mater.* **2012**, *22* (20), 4249–4258.

(104) Shirakawa, H. The Discovery of Polyacetylene Film: The Dawning of an Era of Conducting Polymers (Nobel Lecture). *Angew. Chemie - Int. Ed.* **2001**, *40*, 2574–2580.

(105) Landge, S. M.; Tkatchouk, E.; Benítez, D.; Lanfranchi, D. A.; Elhabiri, M.; Goddard, W. A.; Aprahamian, I. Isomerization Mechanism in Hydrazone-Based Rotary Switches: Lateral Shift, Rotation, or Tautomerization? *J. Am. Chem. Soc.* **2011**, *133* (25), 9812–9823.

(106) Brummel, O.; Waidhas, F.; Bauer, U.; Wu, Y.; Bochmann, S.; Steinrück, H. P.; Papp, C.; Bachmann, J.; Libuda, J. Photochemical Energy Storage and Electrochemically Triggered Energy Release in the Norbornadiene-Quadricyclane System: UV Photochemistry and IR Spectroelectrochemistry in a Combined Experiment. *J. Phys. Chem. Lett.* **2017**, *8* (13), 2819–2825.

(107) Krupička, M.; Sander, W.; Marx, D. Mechanical Manipulation of Chemical Reactions: Reactivity Switching of Bergman Cyclizations. *J. Phys. Chem. Lett.* **2014**, *5* (5), 905–909.

(108) Lara-Avila, S.; Danilov, A. V.; Kubatkin, S. E.; Broman, S. L.; Parker, C. R.; Nielsen, M.

B. Light-Triggered Conductance Switching in Single-Molecule Dihydroazulene/Vinylheptafulvene Junctions. *J. Phys. Chem. C* **2011**, *115* (37), 18372–18377.

(109) Dulić, D.; van der Molen, S. J.; Kudernac, T.; Jonkman, H. T.; de Jong, J. J. D.; Bowden, T. N.; van Esch, J.; Feringa, B. L.; van Wees, B. J. One-Way Optoelectronic Switching of Photochromic Molecules on Gold. *Phys. Rev. Lett.* **2003**, *91* (20), 1–4.

(110) Whalley, A. C.; Steigerwald, M. L.; Guo, X.; Nuckolls, C. Reversible Switching in Molecular Electronic Devices. **2007**, *42* (129), 12590–12591.

(111) Kim, T.; Vazquez, H.; Hybertsen, M. S.; Venkataraman, L. Conductance of Molecular Junctions Formed with Silver Electrodes. *Nano Lett.* **2013**, *13* (7), 3358–3364.

(112) Chang, S.; Sen, S.; Zhang, P.; Gyarfas, B.; Ashcroft, B.; Lefkowitz, S.; Peng, H.; Lindsay, S. Palladium Electrodes for Molecular Tunnel Junctions. *Nanotechnology* **2012**, *23* (42), 425202.

(113) Kiguchi, M.; Tal, O.; Wohlthat, S.; Pauly, F.; Krieger, M.; Djukic, D.; Cuevas, J. C.; Van Ruitenbeek, J. M. Highly Conductive Molecular Junctions Based on Direct Binding of Benzene to Platinum Electrodes. *Phys. Rev. Lett.* **2008**, *101* (4), 1–4.

(114) Guo, X.; Small, J. P.; Klare, J. E.; Wang, Y.; Purewal, M. S.; Tam, I. W.; Hong, B. H.; Caldwell, R.; Huang, L.; Brien, S. O.; et al. Covalently Bridging Gaps in Single Wall CNT with Conducting Molecules. *Science (80-.).* **2008**, *311* (2006), 356–358.

(115) Jia, C.; Guo, X. Molecule–Electrode Interfaces in Molecular Electronic Devices. *Chem. Soc. Rev.* **2013**, *42* (13), 5642–5660.

(116) Moth-Poulsen, K.; Bjørnholm, T. Molecular Electronics with Single Molecules in Solid-State Devices. *Nat. Nanotechnol.* **2009**, *4* (9), 551–556.

(117) Hihath, J. Controlling the Molecule-Electrode Contact in Single-Molecule Devices. In *Handbook of single-molecule electronics*; Moth-Poulsen, K., Ed.; Pan Stanford Publishing Pte. Ltd.: Singapore, 2016; pp 117–154.

(118) Hybertsen, M. S.; Venkataraman, L. Structure-Property Relationships in Atomic-Scale Junctions: Histograms and Beyond. *Acc. Chem. Res.* **2016**.

(119) Li, X.; He, J.; Hihath, J.; Xu, B.; Lindsay, S. M.; Tao, N. Conductance of Single Alkanedithiols : Conduction Mechanism and Effect of Molecule - Electrode Contacts. *J. Am. Chem. Soc.* **2006**, *128* (6), 2135–2141.

(120) Venkataraman, L.; Park, Y. S.; Whalley, A. C.; Nuckolls, C.; Hybertsen, M. S.; Steigerwald, M. L. Electronics and Chemistry: Varying Single-Molecule Junction

Conductance Using Chemical Substituents. *Nano Lett.* **2007**, *7* (2), 502–506.

(121) French, W. R.; Iacovella, C. R.; Rungger, I.; Souza, A. M.; Sanvito, S.; Cummings, P. T. Structural Origins of Conductance Fluctuations in Gold-Thiolate Molecular Transport Junctions. *J. Phys. Chem. Lett.* **2013**, *4* (6), 887–891.

(122) Hybertsen, M. S.; Venkataraman, L.; Klare, J. E.; Whalley, A. C.; Steigerwald, M. L.; Nuckolls, C. Amine-Linked Single-Molecule Circuits: Systematic Trends across Molecular Families. *J. Phys. Condens. Matter* **2008**, *20* (37).

(123) Venkataraman, L.; Klare, J. E.; Tam, I. W.; Nuckolls, C.; Hybertsen, M. S.; Steigerwald, M. L. Single-Molecule Circuits with Well-Defined Molecular Conductance. *Nano Lett.* **2006**, *6* (3), 458–462.

(124) Kamenetska, M.; Quek, S. Y.; Whalley, A. C.; Steigerwald, M. L.; Choi, H. J.; Louie, S. G.; Nuckolls, C.; Hybertsen, M. S.; Neaton, J. B.; Venkataraman, L. Conductance and Geometry of Pyridine-Linked Single-Molecule Junctions. *J. Am. Chem. Soc.* **2010**, *132* (19), 6817–6821.

(125) Chen, W.; Widawsky, J. R.; Vázquez, H.; Schneebeli, S. T.; Hybertsen, M. S.; Breslow, R.; Venkataraman, L. Highly Conducting π-Conjugated Molecular Junctions Covalently Bonded to Gold Electrodes. *J. Am. Chem. Soc.* **2011**, *133* (43), 17160–17163.

(126) Hong, W.; Li, H.; Liu, S. X.; Fu, Y.; Li, J.; Kaliginedi, V.; Decurtins, S.; Wandlowski, T. Trimethylsilyl-Terminated Oligo(Phenylene Ethynylene)s: An Approach to Single-Molecule Junctions with Covalent Au-C σ-Bonds. *J. Am. Chem. Soc.* **2012**, *134* (47), 19425–19431.

(127) Hines, T.; Diez-Perez, I.; Hihath, J.; Liu, H.; Wang, Z. S.; Zhao, J.; Zhou, G.; M??llen, K.; Tao, N. Transition from Tunneling to Hopping in Single Molecular Junctions by Measuring Length and Temperature Dependence. *J. Am. Chem. Soc.* **2010**, *132* (33), 11658–11664.

(128) Moreland, J.; Ekin, J. Electron Tunneling Experiments Using Nb-Sn "Break" Junctions. *J. Appl. Phys.* **1985**, *58*, 3888–3895.

(129) Huber, R.; González, M. T.; Wu, S.; Langer, M.; Grunder, S.; Horhoiu, V.; Mayor, M.; Bryce, M. R.; Wang, C.; Jitchati, R.; et al. Electrical Conductance of Conjugated Oligomers at the Single Molecule Level. *J. Am. Chem. Soc.* **2008**, *130* (3), 1080–1084.

(130) Huang, C.; Rudnev, A. V.; Hong, W.; Wandlowski, T. Break Junction under Electrochemical Gating: Testbed for Single-Molecule Electronics. *Chem. Soc. Rev.* **2015**, *44* (4), 889–901.

(131) Xiang, D.; Jeong, H.; Lee, T.; Mayer, D. Mechanically Controllable Break Junctions for Molecular Electronics. *Adv. Mater.* **2013**, *25*, 4845–4867.

(132) Yasuda, S.; Yoshida, S.; Sasaki, J.; Okutsu, Y.; Nakamura, T.; Taninaka, A.; Takeuchi, O.; Shigekawa, H. Bond Fluctuation of S/Se Anchoring Observed in Single-Molecule Conductance Measurements Using the Point Contact Method with Scanning Tunneling Microscopy. *J. Am. Chem. Soc.* **2006**, *128* (24), 7746–7747.

(133) Darwish, N.; Aragonès, A. C.; Darwish, T.; Ciampi, S.; Díez-Pérez, I. Multi-Responsive Photo- and Chemo-Electrical Single-Molecule Switches. *Nano Lett.* **2014**, *14* (12), 7064–7070.

(134) Kaliginedi, V.; V. Rudnev, A.; Moreno-García, P.; Baghernejad, M.; Huang, C.; Hong, W.; Wandlowski, T. Promising Anchoring Groups for Single-Molecule Conductance Measurements. *Phys. Chem. Chem. Phys.* **2014**, *16* (43).

(135) Park, Y. S.; Whalley, A. C.; Kamenetska, M.; Steigerwald, M. L.; Hybertsen, M. S.; Nuckolls, C.; Venkataraman, L. Contact Chemistry and Single-Molecule Conductance: A Comparison of Phosphines, Methyl Sulfides, and Amines. *J. Am. Chem. Soc.* **2007**, *129* (51), 15768–15769.

(136) Dell, E. J.; Capozzi, B.; Xia, J.; Venkataraman, L.; Campos, L. M. Molecular Length Dictates the Nature of Charge Carriers in Single-Molecule Junctions of Oxidized Oligothiophenes. *Nat. Chem.* **2015**, *7* (3), 209–214.

(137) Aradhya, S. V; Frei, M.; Hybertsen, M. S.; Venkataraman, L. Van Der Waals Interactions at Metal/Organic Interfaces at the Single-Molecule Level. *Nat. Mater.* **2012**, *11*, 872.

(138) Schleyer, P. V. R.; Wiliiams, J. E.; Blanchard, K. R. The Evaluation of Strain in Hydrocarbons. The Strain in Adamantane and Its Origin. *J. Am. Chem. Soc.* **1970**, *92* (8), 2377–2386.

(139) Khoury, P. R.; Goddard, J. D.; Tam, W. Ring Strain Energies: Substituted Rings, Norbornanes, Norbornenes and Norbornadienes. *Tetrahedron* **2004**, *60* (37), 8103–8112.

(140) Kabakoff, D. S.; Bünzli, J. claude G.; Oth, J. F. M.; Hammond, W. B.; Berson, J. A. Enthalpy and Kinetics of Isomerization of Quadricyclane to Norbornadiene. Strain Energy of Quadricyclane. *J. Am. Chem. Soc.* **1975**, *97* (6), 1510–1512.

(141) Wilcox, C. F.; Winstein, S.; McMillan, W. G. Neighboring Carbon and Hydrogen. XXXIV. Interaction of Non-Conjugated Chromophores. *J. Am. Chem. Soc.* **1960**, *82* (20), 5450–5454.

(142) Hammond, G. S.; Turro, N.; Fischer, A. Photosensitized Cycloaddition Reactions. *J. Am. Chem. Soc.* **1961**, *83* (22), 4674–4675.

(143) Woodward, R. B.; Hoffmann, R. The Conservation of Orbital Symmetry. *Angew. Chemie - Int. Ed.* **1969**, *8*, 781–932.

(144) Jack, K.; Machin, B.; Tigchelaar, A.; Tam, W. Synthesis of Substituted Norbornadienes. **2013**, *10* (c), 584–630.

(145) Philippopouios, C.; Economou, D.; Economou, C.; Marangozis, J. Norbornadiene-Quadricyclane System in the Photochemical Conversion and Storage of Solar Energy. *Ind. Eng. Chem. Prod. Res. Dev.* **1983**, *22* (4), 627–633.

(146) Yoshida, Z. ichi. New Molecular Energy Storage Systems. *J. Photochem.* **1985**, *29* (1–2), 27–40.

(147) An, X.; Xie, Y. Enthalpy of Isomerization of Quadricyclane to Norbornadiene. *Thermochim. Acta* **1993**, *220* (C), 17–25.

(148) Doman, L. EIA projects 28% increase in world energy use by 2040 https://www.eia.gov/todayinenergy/detail.php?id=32912# (accessed Oct 21, 2018).

(149) Ibrahim, H.; Ilinca, A.; Perron, J. Energy Storage Systems—Characteristics and Comparisons. *Renew. Sustain. Energy Rev.* **2008**, *12* (5), 1221–1250.

(150) Lanzafame, P.; Abate, S.; Ampelli, C.; Genovese, C.; Passalacqua, R.; Centi, G.; Perathoner, S. Beyond Solar Fuels: Renewable Energy-Driven Chemistry. *ChemSusChem* **2017**, *10* (22), 4409–4419.

(151) Kuisma, M. J.; Lundin, A. M.; Moth-Poulsen, K.; Hyldgaard, P.; Erhart, P. A Comparative Ab-Initio Study of Substituted Norbornadiene-Quadricyclane Compounds for Solar Thermal Storage. *J. Phys. Chem. C* **2016**, acs.jpcc.5b11489.

(152) Kolpak, A. M.; Grossman, J. C. Azobenzene-Functionalized Carbon Nanotubes As High-Energy Density Solar Thermal Fuels. *Nano Lett.* **2011**, *11* (8), 3156–3162.

(153) Mansø, M.; Petersen, A. U.; Wang, Z.; Erhart, P.; Nielsen, M. B.; Moth-Poulsen, K. Molecular Solar Thermal Energy Storage in Photoswitch Oligomers Increases Energy Densities and Storage Times. *Nat. Commun.* **2018**, *9* (1), 1945.

(154) Quant, M.; Lennartson, A.; Dreos, A.; Kuisma, M.; Erhart, P.; Börjesson, K.; Moth-Poulsen, K. Low Molecular Weight Norbornadiene Derivatives for Molecular Solar-Thermal Energy Storage. *Chem. Eur. J.* **2016**, *22* (37), 13265–13274.

(155) Dreos, A.; Borjesson, K.; Wang, Z.; Roffey, A.; Norwood, Z.; Kushnir, D.; Moth-

Poulsen, K. Exploring the Potential of a Hybrid Device Combining Solar Water Heating and Molecular Solar Thermal Energy Storage. *Energy Environ. Sci.* **2017**.

(156) Moth-Poulsen, K.; Ćoso, D.; Börjesson, K.; Vinokurov, N.; Meier, S. K.; Majumdar, A.; Vollhardt, K. P. C.; Segalman, R. A. Molecular Solar Thermal (MOST) Energy Storage and Release System. *Energy Environ. Sci.* **2012**, *5* (9), 8534–8537.

(157) Scharf, H. -D; Fleischhauer, J.; Leismann, H.; Ressler, I.; Schleker, W. -g; Weitz, R. Criteria for the Efficiency, Stability, and Capacity of Abiotic Photochemical Solar Energy Storage Systems. *Angew. Chemie Int. Ed. English* **1979**, *18* (9), 652–662.

(158) Bren ', V. A.; Dubonosov, A. D.; Minkin, V. I.; Chernoivanov, V. A. Norbornadiene–Quadricyclane — an Effective Molecular System for the Storage of Solar Energy Norbornadiene-Quadricyclane — an Effective Molecular System for the Storage of Solar Energy. *Russ. Chem. Rev. Uspekhi Khimii* **1991**, *60* (5), 913–9behabi48.

(159) Dauben, W. G.; Cargill, R. L. Photochemical Transformations—VIII The Isomerization of Bicyclo[2.2.1]Heptadiene to Quadricyclo[2.2.1.0.0]Heptane (Quadricyclane). *Tetrahedron* **1961**, *15*, 197–201.

(160) Cristol, S.; Snell, R. Bridged Polycyclic Compounds. VI. The Photoisomerization of Bicyclo Hepta-2, 5-Diene-2, 3-Dicarboxylic Acid to Quadricyclo[2,2,1,0] Heptane-2, 3-Dicarboxylic Acid. *J. Am. Chem. Soc.* **1958**, *80* (8), 1950–1952.

(161) Card, R. J.; Neckers, D. C. [Poly(Styryl)Bipyridine]Palladium(0)-Catalyzed Isomerization of Quadricyclene. *J. Org. Chem.* **1978**, *43* (15), 2958–2960.

(162) Cerdas, F.; Titscher, P.; Bognar, N.; Schmuch, R.; Winter, M.; Kwade, A.; Herrmann, C. Exploring the Effect of Increased Energy Density on the Environmental Impacts of Traction Batteries: A Comparison of Energy Optimized Lithium-Ion and Lithium-Sulfur Batteries for Mobility Applications. *Energies* **2018**, *11* (1).

(163) Hautala, R. R.; Little, J.; Sweet, E. The Use of Functionlaized Polymers as Photosensitizers in an Energy Storage Reaction. *Sol. Energy* **1977**, *19*, 503–508.

(164) Edman, J. R. 2,3-Dicyanoquadricyclane. Synthesis and Isomerization. **1966**, *32* (10), 1966–1967.

(165) Behr, A.; Keim, W.; Thelen, G.; Scharf, H.; Ressler, I. Solar-Energy Storage with Quadricyclane Systems. *Synthesis (Stuttg).* **1982**, 627–630.

(166) Kaupp, G.; Prinzbach, H. Photochemische Umwandlungen. 30. Mitteilung [1]. Zur Kinetik Der Norbornadien-Quadricyclan-Photocycloaddition. *Helv. Chim. Acta* **1969**, *52* (4), 956–966.

(167) Maruyama, K.; Terada, K.; Yamamoto, Y. HIGHLY EFFICIENT VALENCE ISOMERIZATION BETWEEN NORBORNADIENE AND QUADRICYCLANE DERIVATIVES UNDER SUNLIGHT. *Chem. Lett.* **1981**, *10* (7), 839–842.

(168) Toda, T.; Hasegawa, E.; Mukai, T.; Tsuruta, H.; Hagiwara, T.; Yoshida, T. Photochemical Valence Isomerization between Norbornadiene and Quadricyclane Has Been Investigated Extensively from the Mechanistic Point of View . 2) In Addi- Tion , Much Attention Has Been Focussed Recently on This Isomerization as a Solar Energy Conver. *Chemstry Lett.* **1982**, 1551–1554.

(169) Domelsmith, L. N.; Mollere, P. D.; Houk, K. N.; Hahn, R. C.; Johnson, R. P. Photoelectron and Charge-Transfer Spectra of Benzobicycloalkenes. Relationships between through-Space Interactions and Reactivity. *J. Am. Chem. Soc.* **1978**, *100* (10), 2959–2965.

(170) Jorner, K.; Dreos, A.; Emanuelsson, R.; El Bakouri, O.; Fdez. Galván, I.; Börjesson, K.; Feixas, F.; Lindh, R.; Zietz, B.; Moth-Poulsen, K.; et al. Unraveling Factors Leading to Efficient Norbornadiene–Quadricyclane Molecular Solar-Thermal Energy Storage Systems. *J. Mater. Chem. A* **2017**, *5* (24), 12369–12378.

(171) Hirao, K.; Ando, A.; Hamada, T.; Yonemitsu, O. Valence Isomerisation between Coloured Acylnorbornadienes and Quadricyclanes as a Promising Model for Visible (Solar)Light Energy Conversion. *J. Chem. Soc. Chem. Commun.* **1984**, No. 5, 300–302.

(172) Nagai, T.; Fujii, K.; Takahashi, I.; Shimada, M. Trifluoromethyl-Substituted Donor – Acceptor Norbornadiene , Useful. *Bull. Chem. Soc. Jpn* **2001**, *74*, 1673–1678.

(173) Miki, S.; Asako, Y.; Yoshida, Z. Photochromic Solid Films Prepared by Doping with Donor–Acceptor Norbornadienes. *Chem. Lett.* **1987**, *16* (1), 195–198.

(174) Jevric, M.; Petersen, A. U.; Mansø, M.; Kumar Singh, S.; Wang, Z.; Dreos, A.; Sumby, C.; Nielsen, M. B.; Börjesson, K.; Erhart, P.; et al. Norbornadiene-Based Photoswitches with Exceptional Combination of Solar Spectrum Match and Long-Term Energy Storage. *Chem. – A Eur. J.* **2018**, *24* (49), 12767–12772.

(175) Wang, Z.; Roffey, A.; Losantos, R.; Lennartson, A.; Jevric, M.; Petersen, A. U.; Quant, M.; Dreos, A.; Wen, X.; Sampedro, D.; et al. Macroscopic Heat Release in a Molecular Solar Thermal Energy Storage System. *Energy Environ. Sci.* **2018**.

(176) Dreos, A.; Wang, Z.; Udmark, J.; Ström, A.; Erhart, P.; Börjesson, K.; Nielsen, M. B.; Moth-Poulsen, K. Liquid Norbornadiene Photoswitches for Solar Energy Storage. *Adv. Energy Mater.* **2018**, *8* (18), 1–9.

(177) Maruyama, K.; Tamiaki, H.; Kawabata, S. Development of a Solar Energy Storage Process. Photoisomerization of a Norbornadiene Derivative to a Quadricyclane Derivative in an Aqueous Alkaline Solution. *J. org. Chem.* **1985**, *50*, 4742–4749.

(178) Bren, V. A.; Minkin, V. I.; Dubonosov, A. D.; Chernoivanov, V. A.; Rybalkin, V. P.; Borodkin, G. S. Biphotochromic Norbornadiene Systems. *Mol. Cryst. Liq. Cryst. Sci. Technol. Sect. A Mol. Cryst. Liq. Cryst.* **1997**, *297–298*, 247–253.

(179) Kucharski, T. J.; Tian, Y.; Akbulatov, S.; Boulatov, R. Chemical Solutions for the Closed-Cycle Storage of Solar Energy. *Energy Environ. Sci.* **2011**, *4* (11), 4449.

(180) Börjesson, K.; Lennartson, A.; Moth-Poulsen, K. Efficiency Limit of Molecular Solar Thermal Energy Collecting Devices. *ACS Sustain. Chem. Eng.* **2013**, *1* (6), 585–590.

(181) Lennartson, A.; Quant, M.; Moth-Poulsen, K. A Convenient Route to 2-Bromo-3-Chloronorbornadiene and 2,3-Dibromonorbornadiene. *Synlett* **2015**, *26* (11), 1501–1504.

(182) Seidler, A.; Svoboda, J.; Dekoj, V.; Chocholoušová, J. V.; Vacek, J.; Stará, I. G.; Starý, I. The Synthesis of π-Electron Molecular Rods with a Thiophene or Thieno[3,2-b]Thiophene Core Unit and Sulfur Alligator Clips. *Tetrahedron Lett.* **2013**, *54* (22), 2795–2798.

(183) Shanmugaraju, S.; Bar, A. K.; Chi, K. W.; Mukherjee, P. S. Coordination-Driven Self-Assembly of Metallamacrocycles via a New Pt II Organometallic Building Block with 90?? Geometry and Optical Sensing of Anions. *Organometallics* **2010**, *29* (13), 2971–2980.

(184) Balaban, A. T.; Oniciu, D. C.; Katritzky, A. R. Aromaticity as a Cornerstone of Heterocyclic Chemistry. *Chem. Rev.* **2004**, *104* (5), 2777–2812.

(185) Hatchard, C. G.; Parker, C. A. A New Sensitive Chemical Actinometer - II. Potassium Ferrioxalate as a Standard Chemical Actinometer. *Proc. R. Soc. London. Ser. A. Math. Phys. Sci.* **1956**, *235* (1203), 518–536.

(186) Haddon, R. C.; Lamola, A. A. The Molecular Electronic Device and the Biochip Computer: Present Status. *Proc. Natl. Acad. Sci. U. S. A.* **1985**, *82* (7), 1874–1878.

(187) Bonfantini, E. E.; Officer, D. L. The Synthesis of Norbornadienes Conjugatively Linked to Tetraphenylporphyrin and Anthracene: Towards a Norbornadiene-Derived Molecular Electronic Device. *J. Chem. Soc. Chem. Commun.* **1994**, No. 12, 1445–1446.

(188) Lainé, P.; Marvaud, V.; Gourdon, A.; Launay, J.-P.; Argazzi, R.; Bignozzi, C.-A. Electron Transfer through Norbornadiene and Quadricyclane Moieties as a Model for Molecular Switching. *Inorg. Chem.* **1996**, *35* (3), 711–714.

(189) LAUNAY, J. P.; COUDRET, C. Chemical Approaches of Molecular Switches. *Ann. N. Y. Acad. Sci.* **1998**, *852* (1 MOLECULAR ELE), 116–132.

(190) Fraysse, S.; Coudret, C.; Launay, J.-P. Synthesis and Properties of Dinuclear Complexes with a Photochromic Bridge: An Intervalence Electron Transfer Switching "On" and "Off." *Eur. J. Inorg. Chem.* **2000**, No. 7, 1581–1590.

(191) Löfås, H.; Jahn, B. O.; Wärnå, J.; Emanuelsson, R.; Ahuja, R.; Grigoriev, A.; Ottosson, H. A Computational Study of Potential Molecular Switches That Exploit Baird's Rule on Excited-State Aromaticity and Antiaromaticity. *Faraday Discuss.* **2014**, *174*, 105–124.

(192) Durr, R.; Cossu, S.; De Lucchi, O. 2,3-Dichlorobicyclo[2.2.1]Hepta-2,5-Diene: A Convenient Precursor of Norbornadiene-2,3-Diynes. *Synth. Commun.* **1997**, *27* (8), 1369–1372.

(193) Ryan, J. H.; Stang, P. J. Synthesis of Bicyclic Enediynes from Bis[Phenyl[(Trifluoromethanesulfonyl)Oxy]Iodo]Acetylene: A Tandem Diels-Alder/Palladium(II)- and Copper(I)-Cocatalyzed Cross-Coupling Approach. *J. Org. Chem.* **1996**, *61* (18), 6162–6165.

(194) Tsui, G. C.; Le Marquand, P.; Allen, A.; Tam, W. Synthesis of Anti-2,7-Disubstituted Norbornadienes. *Synthesis (Stuttg).* **2009**, *2009* (04), 609–619.

(195) Xiao, X.; Xu, B.; Tao, N. J. Measurement of Single Molecule Conductance: Benzenedithiol and Benzenedimethanethiol. *Nano Lett.* **2004**, *4* (2), 267–271.

(196) Chinchilla, R.; Nájera, C. The Sonogashira Reaction: A Booming Methodology in Synthetic Organic Chemistry. *Chem. Rev.* **2007**, *107* (3), 874–922.

(197) Chinchilla, R.; Nájera, C. Recent Advances in Sonogashira Reactions. *Chem. Soc. Rev.* **2011**, *40* (10), 5084–5121.

(198) Pensa, E.; Cortés, E.; Corthey, G.; Carro, P.; Vericat, C.; Fonticelli, M. H.; Benítez, G.; Rubert, A. A.; Salvarezza, R. C. The Chemistry of the Sulfur–Gold Interface: In Search of a Unified Model. *Acc. Chem. Res.* **2012**, *45* (8), 1183–1192.

(199) Jennum, K.; Vestergaard, M.; Pedersen, A. H.; Fock, J.; Jensen, J.; Santella, M.; Led, J. J.; Kilså, K.; Bjørnholm, T.; Nielsen, M. B. Synthesis of Oligo(Phenyleneethynylene)s with Vertically Disposed Tetrathiafulvalene Units. *Synthesis (Stuttg).* **2011**, No. 4, 539–548.

(200) Baranac-Stojanović, M.; Stojanović, M. 1H NMR Chemical Shifts of Cyclopropane and Cyclobutane: A Theoretical Study. *J. Org. Chem.* **2013**, *78* (4), 1504–1507.

(201) Maafi, Direct Valence Isomerization of Newly Synthesized Norbornadiene Aromatic

Derivatives. A Kinetics and Photophysical Study (1994) Chemistry Lett.Pdf.

(202) Babudri, F.; Bilancia, G.; Cardone, A.; Coppo, P.; De Cola, L.; Farinola, G. M.; Hofstraat, J. W.; Naso, F. Photochemical Tuning of Light Emission in a Conjugated Polymer Containing Norbornadiene Units in the Main Chain. *Photochem. Photobiol. Sci.* **2007**, *6* (4), 361–364.

(203) Yamaguchi, Y.; Matsubara, Y.; Ochi, T.; Wakamiya, T.; Yoshida, Z. How the π Conjugation Length Affects the Fluorescence Emission Efficiency. *J. Am. Chem. Soc.* **2008**, *130* (42), 13867–13869.

(204) Ikezawa, H.; Kutal, C.; Yasufuku, K.; Yamazaki, H. Direct and Sensitized Valence Photoisomerization of a Substituted Norbornadiene. Examination of the Disparity between Singlet- and Triplet-State Reactivities. *J. Am. Chem. Soc.* **1986**, *108* (7), 1589–1594.

(205) Malkin, S.; Fischer, E. Temperature Dependence of Photoisomerization. III. 1 Direct and Sensitized Photoisomerization of Stilbenes. *J. Phys. Chem.* **1964**, *68* (5), 1153–1163.

(206) Dreos, A.; Wang, Z.; Tebikachew, B. E.; Moth-Poulsen, K.; Andréasson, J. Three-Input Molecular Keypad Lock Based on a Norbornadiene–Quadricyclane Photoswitch. *J. Phys. Chem. Lett.* **2018**, 6174–6178.

(207) Khoo, K. H.; Chen, Y.; Li, S.; Quek, S. Y. Length Dependence of Electron Transport through Molecular Wires – a First Principles Perspective. *Phys. Chem. Chem. Phys.* **2015**, *17* (1), 77–96.

(208) Capitao, D.; Limoges, B.; Fave, C.; Schöllhorn, B. On the Decisive Role of the Sulfur-Based Anchoring Group in the Electro-Assisted Formation of Self-Assembled Monolayers on Gold. *Electrochim. Acta* **2017**, *257*, 165–171.

(209) Solomon, G. C.; Herrmann, C.; Hansen, T.; Mujica, V.; Ratner, M. a. Exploring Local Currents in Molecular Junctions. *Nat. Chem.* **2010**, *2* (3), 223–228.

(210) WALSH, A. D. Structures of Ethylene Oxide and Cyclopropane. *Nature* **1947**, *159*, 165.

(211) ROBINSON, R. Structures of Ethylene Oxide and Cyclopropane. *Nature* **1947**, *159*, 400.

(212) Bergman, R. Bonding Properties of Cyclopropane and Their Chemical Consequences. *Angew. Chemie - Int. Ed.* **1979**, *18*, 809–886.

(213) Wuts, P. G. M.; Greene, T. W. *Greene's Protective Groups in Organic Synthesis*; Wiley-Interscience: Hoboken, N.J., 2007.

(214) Dcona, M. M.; Mitra, D.; Goehe, R. W.; Gewirtz, D. A.; Lebman, D. A.; Hartman, M. C. T. Photocaged Permeability: A New Strategy for Controlled Drug Release. *Chem. Commun.* **2012**, *48* (39), 4755–4757.

(215) Fodor, S. P.; Read, J. L.; Pirrung, M. C.; Stryer, L.; Lu, A. T.; Solas, D. Light-Directed, Spatially Addressable Parallel Chemical Synthesis. *Science (80-.).* **1991**, *251* (4995), 767 LP-773.

(216) Klán, P.; Solomek, T.; Bochet, C. G.; Blanc, A.; Givens, R.; Rubina, M.; Popik, V.; Kostikov, A.; Wirz, J. Photoremovable Protecting Groups in Chemistry and Biology : Reaction Mechanisms and E Ffi Cacy. *Chem. Rev.* **2013**, *113*, 119–191.

(217) Wang, P. Photolabile Protecting Groups: Structure and Reactivity. *Asian J. Org. Chem.* **2013**, *2* (6), 452–464.

(218) Piloto, A. M.; Costa, S. P. G.; Gonçalves, M. S. T. Wavelength-Selective Cleavage of o-Nitrobenzyl and Polyheteroaromatic Benzyl Protecting Groups. *Tetrahedron* **2014**, *70* (3), 650–657.

(219) Kretschy, N.; Holik, A.-K.; Somoza, V.; Stengele, K.-P.; Somoza, M. M. Next-Generation o-Nitrobenzyl Photolabile Groups for Light-Directed Chemistry and Microarray Synthesis. *Angew. Chemie Int. Ed.* **2015**, *54* (29), 8555–8559.

(220) Kaplan, J. H.; Forbush, B.; Hoffman, J. F. Rapid Photolytic Release of Adenosine 5'-Triphosphate from a Protected Analog - Utilization by Na-K Pump of Human Red Blood-Cell Ghosts. *Biochemistry* **1978**, *17*, 1929–1935.

(221) Givens, R.; Kotala, M. B.; Lee, J.-I. Mechanistic Overview of Phototriggers and Cage Release. *Dynamic Studies in Biology*. October 27, 2005.

(222) Patchornik, A.; Amit, B.; Woodward, R. B. Photosensitive Protecting Groups. *J. Amer. Chem. Soc* **1970**, *92*, 6333–6335.

(223) Pirrung, M. C.; Pieper, W. H.; Kaliappan, K. P.; Dhananjeyan, M. R. Combinatorial Discovery of Two-Photon Photoremovable Protecting Groups. *Proc. Natl. Acad. Sci. U. S. A.* **2003**, *100* (22), 12548–12553.

(224) Specht, A.; Goeldner, M. 1-(O-Nitrophenyl)-2,2,2-Trifluoroethyl Ether Derivatives As Stable and Efficient Photoremovable Alcohol-Protecting Groups. *Angew. Chemie - Int. Ed.* **2004**, *43* (15), 2008–2012.

(225) Ekkebus, R.; van Kasteren, S. I.; Kulathu, Y.; Scholten, A.; Berlin, I.; Geurink, P. P.; de Jong, A.; Goerdayal, S.; Neefjes, J.; Heck, A. J. R.; et al. On Terminal Alkynes That Can React with Active-Site Cysteine Nucleophiles in Proteases. *J. Am. Chem. Soc.* **2013**,

135 (8), 2867–2870.

(226) Lehmann, J.; Wright, M. H.; Sieber, S. A. Making a Long Journey Short: Alkyne Functionalization of Natural Product Scaffolds. *Chem. - A Eur. J.* **2016**, *22* (14), 4666–4678.

(227) Kolb, H. C.; Finn, M. G.; Sharpless, K. B. Click Chemistry: Diverse Chemical Function from a Few Good Reactions. *Angewandte Chemie - International Edition*. 2001, pp 2004–2021.

(228) Siemsen, P.; Livingston, R. C.; Diederich, F. Acetylenic Coupling: A Powerful Tool in Molecular Construction. *Angew. Chemie - Int. Ed.* **2000**, *39* (15), 2632–2657.

(229) Kolarovič, A.; Schnürch, M.; Mihovilovic, M. D. Tandem Catalysis: From Alkynoic Acids and Aryl Iodides to 1,2,3-Triazoles in One Pot. *J. Org. Chem.* **2011**, *76* (8), 2613–2618.

(230) Park, J.; Park, E.; Kim, A.; Park, S. A.; Lee, Y.; Chi, K. W.; Jung, Y. H.; Kim, I. S. Pd-Catalyzed Decarboxylative Coupling of Propiolic Acids: One-Pot Synthesis of 1,4-Disubstituted 1,3-Diynes via Sonogashira-Homocoupling Sequence. *J. Org. Chem.* **2011**, *76* (7), 2214–2219.

(231) Suzuki, A. Z.; Watanabe, T.; Kawamoto, M.; Nishiyama, K.; Yamashita, H.; Ishii, M.; Iwamura, M.; Furuta, T. Coumarin-4-Ylmethoxycarbonyls as Phototriggers for Alcohols and Phenols. *Org. Lett.* **2003**, *5* (25), 4867–4870.

(232) Gilmore, K.; Seeberger, P. H. Continuous Flow Photochemistry. *Chem. Rec.* **2014**, *14* (3), 410–418.

(233) Plutschack, M. B.; Pieber, B.; Gilmore, K.; Seeberger, P. H. The Hitchhiker's Guide to Flow Chemistry. *Chem. Rev.* **2017**, *117* (18), 11796–11893.

(234) Park, K.; Palani, T.; Pyo, A.; Lee, S. Synthesis of Aryl Alkynyl Carboxylic Acids and Aryl Alkynes from Propiolic Acid and Aryl Halides by Site Selective Coupling and Decarboxylation. *Tetrahedron Lett.* **2012**, *53* (7), 733–737.

(235) Shao, C.; Wang, X.; Zhang, Q.; Luo, S.; Zhao, J.; Hu, Y. Acid–Base Jointly Promoted Copper(I)-Catalyzed Azide–Alkyne Cycloaddition. *J. Org. Chem.* **2011**, *76* (16), 6832–6836.

(236) Luo, L.; Frisbie, C. D. Length-Dependent Conductance of Conjugated Molecular Wires Synthesized by Stepwise "Click" Chemistry. *J. Am. Chem. Soc.* **2010**, *132* (26), 8854–8855.

(237) Murray, W. A.; Barnes, W. L. Plasmonic Materials. *Adv. Mater.* **2007**, *19* (22), 3771–

3782.

(238) Govorov, A. O.; Richardson, H. H. Generating Heat with Metal Nanoparticles. *Nano Today* **2007**, *2* (1), 30–38.

(239) Petryayeva, E.; Krull, U. J. Localized Surface Plasmon Resonance: Nanostructures, Bioassays and Biosensing—A Review. *Anal. Chim. Acta* **2011**, *706* (1), 8–24.

(240) Eklöf-Österberg, J.; Gschneidtner, T.; Tebikachew, B.; Lara-Avila, S.; Moth-Poulsen, K. Parallel Fabrication of Self-Assembled Nanogaps for Molecular Electronic Devices. *Small* **2018**, accepted.

(241) Bergren, A. J.; Zeer-Wanklyn, L.; Semple, M.; Pekas, N.; Szeto, B.; McCreery, R. L. Musical Molecules: The Molecular Junction as an Active Component in Audio Distortion Circuits. *J. Phys. Condens. Matter* **2016**, *28* (9), 94011.

(242) Corbet, J.-P.; Mignani, G. Selected Patented Cross-Coupling Reaction Technologies. *Chem. Rev.* **2006**, *106* (7), 2651–2710.

(243) *Metal-Catalyzed Cross-Coupling Reactions*, 2nd ed.; de Meijere, A., Diederich, F., Eds.; Wiley-VCH: Weinheim, 2004.

(244) Stephens, R. D.; Castro, C. E. The Substitution of Aryl Iodides with Cuprous Acetylides. A Synthesis of Tolanes and Heterocyclics1. *J. Org. Chem.* **1963**, *28* (12), 3313–3315.

(245) Mee, S. P. H.; Lee, V.; Baldwin, J. E. Significant Enhancement of the Stille Reaction with a New Combination of Reagents—Copper(I) Iodide with Cesium Fluoride. *Chem. – A Eur. J.* **2005**, *11* (11), 3294–3308.

(246) El-Faham, A.; Albericio, F. Peptide Coupling Reagents, More than a Letter Soup. *Chem. Rev.* **2011**, *111* (11), 6557–6602.

(247) Neises, B.; Steglich, W. Simple Method for the Esterification of Carboxylic Acids. *Angew. Chemie Int. Ed. English* **1978**, *17* (7), 522–524.

(248) Gawande, M. B.; Shelke, S. N.; Zboril, R.; Varma, R. S. Microwave-Assisted Chemistry: Synthetic Applications for Rapid Assembly of Nanomaterials and Organics. *Acc. Chem. Res.* **2014**, *47* (4), 1338–1348.

(249) Tsakos, M.; Schaffert, E. S.; Clement, L. L.; Villadsen, N. L.; Poulsen, T. B. Ester Coupling Reactions – an Enduring Challenge in the Chemical Synthesis of Bioactive Natural Products. *Nat. Prod. Rep.* **2015**, *32* (4), 605–632.

(250) Mäntele, W.; Deniz, E. UV–VIS Absorption Spectroscopy: Lambert-Beer Reloaded.

Spectrochim. Acta Part A Mol. Biomol. Spectrosc. **2017**, *173*, 965–968.

(251) Lakowicz, J. R. *Principles of Fluorescence Spectroscopy*, 3rd ed.; Springer Science+Business Media, LLC: New York, 2006.

(252) Albini, A.; Fagnoni, M. *The Greenest Reagent in Organic Synthesis: Light*; Tundo, P., Esposito, V., Eds.; Springer Netherlands: Dordrecht, 2008.

(253) Stranius, K.; Börjesson, K. Determining the Photoisomerization Quantum Yield of Photoswitchable Molecules in Solution and in the Solid State. *Sci. Rep.* **2017**, *7* (January), 41145.